*Year :* 2012

# Biomechanical analysis of alpine skiers performing giant slalom turns

## Meyer Frédéric

UNIL | Université de Lausanne

FACULTÉ DES SCIENCES SOCIALES ET POLITIQUES

INSTITUT DES SCIENCES DU SPORT

# Biomechanical analysis of alpine skiers performing giant slalom turns

**THÈSE DE DOCTORAT**

présentée à la

Faculté des sciences sociales et politiques
de l'Université de Lausanne

pour l'obtention du grade de

**Docteur ès sciences du sport**

par

**Frédéric Meyer**

Directeur de thèse
Dr. Fabio Borrani

LAUSANNE
2012

**UNIL** | Université de Lausanne

# Faculté des sciences sociales et politiques

## IMPRIMATUR

Le Conseil de la Faculté des sciences sociales et politiques de l'Université de Lausanne, sur proposition d'un jury formé des professeurs

- Fabio BORRANI, directeur de thèse, MER à l'Université de Lausanne

- Fabien OHL, Professeur à l'Université de Lausanne

- Grégoire MILLET, Professeur à l'Université de Lausanne

- Alberto MINETTI, Professeur à l'Université de Milan

- Robert C. REID, responsable de recherche à la Fédération norvégienne de ski, Baerums Verk

- Nicolas COULMY, Fédération française de ski, Annecy

autorise, sans se prononcer sur les opinions du candidat, l'impression de la thèse de Monsieur Frédéric MEYER, intitulée :

## «*Biomechanical analysis of alpine skiers performing giant slalom turns* »

Lausanne, le 16 avril 2012

*Le Doyen de la Faculté*
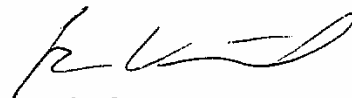
Professeur
René Knüsel

2

# Résumé

Le sport de compétition bénéficie depuis quelques années des progrès technologiques apportés par la science. Les techniques d'entraînement, le suivi des athlètes et les méthodes d'analyse deviennent plus pointus, induisant une nette amélioration des performances. Le ski alpin ne dérogeant pas à cette règle, l'objectif de ce travail était d'analyser la technique de skieurs de haut niveau en slalom géant afin de déterminer la quantité d'énergie fournie par les skieurs pour augmenter leur vitesse. Pour ce faire, il a été nécessaire de developer différents outils d'analyse adaptés aux contraintes inhérentes aux tests sur les pistes de skis; un système multi caméras, un système de synchronisation, un modèle aérodynamique et des plateformes de force ont notamment été développés. Les analyses effectuées grâce à ces différents outils ont montré qu'il était possible pour certains skieur d'augmenter leur énergie d'environ 1.5 % grâce au travail musculaire. Cependant, les athlètes n'ont en moyenne pas réussi à utiliser leur travail musculaire de manière efficace. Ce projet a également rendu possible des analyses adaptées aux conditions d'entraînement des skieurs en proposant des outils fonctionnels tels que l'analyse du drift grâce à des capteurs inertiels et GPS, ainsi que l'analyse simplifiée de trajectoires grâce au suivi de points morphologiques. L'auteur espère que ce travail servira de base pour approfondir les connaissances de la technique en ski alpin.

## Abstract

Over the past few years, technological breakthroughs have helped competitive sports to attain new levels. Training techniques, athletes' management and methods to analyse specific technique and performance have sharpened, leading to performance improvement. Alpine skiing is not different. The objective of the present work was to study the technique of highy skilled alpine skiers performing giant slalom, in order to determine the quantity of energy that can be produced by skiers to increase their speed. To reach this goal, several tools have been developed to allow field testing on ski slopes; a multi cameras system, a wireless synchronization system, an aerodynamic drag model and force plateforms have especially been designed and built. The analyses performed using the different tools highlighted the possibility for several athletes to increase their energy by approximately 1.5 % using muscular work. Nevertheless, the athletes were in average not able to use their muscular work in an efficient way. By offering functional tools such as drift analysis using combined data from GPS and inertial sensors, or trajectory analysis based on tracking morphological points, this research makes possible the analysis of alpine skiers technique and performance in real training conditions. The author wishes for this work to be used as a basis for continued knowledge and understanding of alpine skiing technique.

## Acknowledgements

I would like to thank the following people:

- Marie, my sweet half, my significant other, perhaps the person who contributes the most in this dissertation, spending hours in reading and correcting my articles, supporting me during all these years of labour and pushing me when necessary. I wouldn't have achieved this project without you and I'm looking forward to take on new challenges together!

- My parents Jean-Claude and Martine who supported me in all the challenges I went through, always pushing me to give my best in my studies and in my practice of sports. You teached me how to ski and accompanied me during all these years of competition. You gave me the curiosity and the taste of surpassing myself, necessary to achieve this project.

- Dr Fabio Borrani, my supervisor, for the trust he placed on me since the beginning, for giving me the opportunity to work on this wonderful subject, for the long hours spent on Skype to work on the encountered issues and for welcoming me in Auckland during my stay.

- My sister Sandrine, who contributed to this project with her master's final project and did an awesome work at digitalizing my images through long and boring hours of clicking.

- Dr Adrian Waegli and his colleagues from the TOPO lab at the EPFL, for the guidance on all the GPS aspects and the work done together.

- Dr Thomas Lochmatter and Dr Alexander Bahr for the development of the wireless synchronization system in a very shot period of time and the uncounted hours of welding.

- Dr Alain Shorderet, Dr Alain Prenleloup and the students of the LCSM lab of the EPFL, who developed a dedicated force platform, and more specifically Alain Prenleloup for his investment to have the material ready for the field tests and his active participation to the field tests.

# Table of content

# List of Figures

12

14

# List of Tables

# Abreviations and Symbols

**Acronyms**

| | |
|---|---|
| *2D* | *Two-dimensional* |
| *3D* | *Tridimensional* |
| *ANOVA* | *ANalysis Of VAriance* |
| *ATT* | *Actual Trigger Time* |
| *CoM* | *Centre of Mass* |
| *DGPS* | *Differential Global Positioning System* |
| *DLT* | *Direct Linear Transformation* |
| *DoF* | *Degree of Freedom* |
| *EMG* | *Electromyogram* |
| *EPFL* | *Swiss Federal School of Technology* |
| *FIS* | *International Ski Federation* |
| *GPS* | *Global Positioning System* |
| *GRF* | *Ground Reaction Force* |
| *GS* | *Giant slalom* |
| *IMU* | *Inertial Measurement Unit* |
| *INS* | *Inertial Navigation Systems* |
| *L1/L2* | *Civil/Military GPS frequencies* |
| *L5* | *Lumbar vertebra number five* |
| *LCSM* | *Mechanical System Design Laboratory* |
| *LED* | *Light Emitting Diode* |
| *LVDT* | *Linear Variable Displacement Transducer* |
| *LVTD* | *Linear Variable Displacement Transducer* |
| *MEMS* | *Micro-Electro-Mechanical System* |

| | |
|---|---|
| *P* | *Significance* |
| *PDA* | *Personal Digital Assistant* |
| *PPS* | *Pulse Per Second* |
| *R2* | *Coefficient of determination* |
| *RAM* | *Random Access Memory* |
| *RAM* | *Random Access Memory* |
| *RMS* | *Root Mean Square* |
| *S1* | *First Steering phase* |
| *S2* | *Second Steering phase* |
| *SD, σ* | *Standard deviation* |
| *SL* | *Special Slalom* |
| *SPE* | *Shear Panel Elements* |
| *T* | *Transition phase* |
| *TAI* | *International Atomic Time* |
| *UHF* | *Ultra High Frequency* |
| *WiTriSync* | *Wireless Trigger Synchronization* |
| *WiTriSync* | *Wireless Trigger Synchronization* |

**Variables**

| | |
|---|---|
| $a$ | acceleration |
| $A_F$ | Frontal Area |
| α | Angle between the *F* and the *V* vector |
| β | *S*lope angle |
| *BodyS* | Body Surface area |
| *Cste* | Constante |
| $C_D$ | Drag Coefficient |

18

| | |
|---|---|
| $C_DA$ | Drag area |
| $d$ | Error between the *PPS* signal and the *TAI* signal |
| $D$ | Drag Force |
| *dist* | Distance |
| $e$ | Error between the *PPS* signal and the *ATT* signal |
| $E$ | Error between the *TAI* signal and the *ATT* signal |
| *Eaero* | Energy dissipated due to aerodynamic drag |
| *Efrict* | Energy lost in ski-snow Friction |
| *Ekin* | Kinetic Energy |
| *Epot* | Potential Energy |
| *Eres* | Residual Energy |
| *Etot* | Total Energy |
| $F$ | Force |
| *Fcontact* | Contact Force between the skis and the snow |
| $g$ | Acceleration due to gravity |
| $\gamma$ | Skier heading angle |
| *GM1* to *GM4* | Generalized Models number one to four |
| $H$ | Distance between the feet and the head |
| *IM1* and *IM2* | Individualized Model number one and two |
| *M, m* | Mass |
| *MaxA* | Maximal Frontal Area |
| $\mu$ | Friction coefficient |
| $P$ | Power |
| $R$ | Radius |
| *rad_acc* | radial acceleration |
| $\rho$ | Air density |

| | |
|---|---|
| $t$ | Time |
| $T_{entry}$ | Turn entry |
| $T_{exit}$ | Turn exit |
| $T_{rad}$ | Turn radius |
| $UpH$ | Upright Height |
| $V$ | Velocity |
| $W$ | Distance between the two hands |
| $W_{Hum}$ | Human Work |
| $z$ | Vertical position of the CoM |

# 1. Introduction

## 1.1. Background

Like the majority of elite sport practices, alpine skiing competition becomes increasingly more professional with athletes enhancing their performances every year thanks to the improvement of training methods, the optimization of materials and the development of new insights in sport techniques. These developments are not only achieved by coaches and field-experienced practitioners, but also supported by detailed scientific analysis of various parameters involved in skiing performance. Indeed, alpine skiing is extremely complex as multi-disciplinary parameters like strength, coordination, explosiveness, technique, mental preparation, and season planning are involved in order to reach top international racing levels. Although slight differences may be observed between the world's best skiers, substantially larger differences may be noticed between a world cup winner and the 30th runner. Analysing elite athletes to understand these differences is thus primordial to improve skiing performance. This task is however known to be very challenging (Sands, 2008). Indeed, top athletes' coaches are reluctant to give access to their athletes unless scientific investigations prove to interfere as little as possible with precious training sessions and, most importantly, if they are capable to provide real-time and relevant feedbacks on athlete's skiing performances.

From a personal standpoint, as a skier, former competitor and instructor, I have always strived to understand and improve skiing techniques. Supported by biomechanical grounds, this work contributes to the understanding of alpine ski techniques and highlights some mechanisms that could lead to increased ski racing performance.

## 1.2. Research plan

This project has been separated in five phases which are briefly described here:

**Phase 1: Goals**

Based on a systematic literature review and a global understanding of the methods used in biomechanical research, the first part of this project consisted in determining the aim and direction to be given to this work.

**Phase 2: Tools development**

During this phase, an investigation method was selected and corresponding materials and equipments acquired. Contacts with laboratories of the Swiss Federal Institute of Technology in Lausanne (EPFL) and of the University of Auckland were established to develop dedicated tools and methods. At the EPFL, collaboration with the Geodetic Engineering Laboratory (TOPO) allowed us to analyse skidding using a tool they developed based on GPS and inertial sensors measurements. Collaboration with the Distributed Intelligent Systems and Algorithms Laboratory (DISAL) led to a versatile distributed system allowing the synchronisation of the different measurement devices. The Mechanical Systems Laboratory (LCSM) designed and machined an embedded force platform adapted to alpine skiing. Finally, an experimental aerodynamic drag model was established at the University of Auckland wind tunnel with the objective of estimating drag coefficients of skiers during giant slalom turns.

**Phase 3: Testing**

Material and methods in this study were validated by specific in situ measurements. The aerodynamic drag model was validated during a test session at the Snowplanet ski hall in Auckland, New Zealand. The panning camera system was experimented during a field test at the ski resort of St-Cergue (Switzerland) while the synchronization devices were tested at different outdoor locations. An experiment was also set up at Glacier 3000 in Les Diablerets (Switzerland) to investigate GPS-IMU functionalities and

the prototype of the embedded force platform was tested during ski days in Les Paccots and Saas-Fee (Switzerland). Finally, a four-day testing session was organized in the ski resort of Stoos (Switzerland) on a special slope closed to public to provide data for various analyses. Tests were conducted on elite athletes, in parallel to the Swiss national championships.

**Phase 4: Data Processing and Analysis**

Following field testing, 14 trials were chosen for digitalisation. 500 hours were necessary to process around 400'000 measurement points in total. Based on digitalisation, three-dimensional (*3D*) models were established and the following analyses were conducted. First, energy balance during slalom turns was calculated using the aerodynamic drag model and *3D* motion calculations of the centre of mass. Second, external work developed by the skier was calculated based on full body motion *3D* kinematics. Third, the *3D* models were used to determine the error induced on kinetic and potential energies estimations when using different morphological points instead of the centre of mass (*CoM*).

**Phase 5: Reporting**

The final phase of this project was to compile the results obtained during the analysis phase and to submit scientific articles to peer-reviewed journals. This thesis dissertation is thus a compilation of submitted articles and conference proceedings.

## 1.3. Structure of the dissertation

This dissertation details modern aspects of alpine skiing biomechanics including development and validation of dedicated measurement tools in order to analyse the kinematics and energies of alpine ski competitors performing giant slalom turns. **Chapter 1** introduces the background and the organization of the project. **Chapter 2** exposes the current state-of-the-art of methods used to acquire data to investigate snow sports biomechanics. **Chapter 3** presents the main results obtained so far in the analysis of alpine skiing technique. **Chapter 4** introduces the aims and

objectives of this research project, based on the results observed in the literature review. Individual goals for each proposed studies are described, as well as the relationships between the different studies. **Chapters 5 to 11** detail individual studies as stand alone articles; they are all built along the same structure including an introduction, methods, results and discussion sections, as required for scientific publications. **Chapter 12** is a final conclusion summarizing important results and discusses them in respect to previous literature. General limitations are also identified and discussed. Finally, **chapter 13** is dedicated to introducing ideas for further investigations based on the results and limitations of the current work.

# 2. Methodological advances in snow sports biomechanics

Japanese have been the first to investigate the mechanics of ski jumping and turning to prepare for the Sapporo 1972 Olympic Games. A review of the work that has been done in the seventies was presented by Watanabe (Watanabe, 1981). In Europe and the US, several books describing the technique of skiing were published at the same period (Joubert and Vuarnet, 1966; Sanders, 1976; Joubert, 1980; Howe, 1983).

Human locomotion analysis is distinguished into kinetic and kinematic analysis. Kinetic analysis as the most sophisticated method to describe movements focussing on the causes of the movements including forces is again differentiated into two methods: forward dynamics and inverse dynamics. Forward dynamics derives movement from direct measurements of the force developed by muscles. Inverse dynamics starts from kinematics measurements and the external forces to determine the force developed by muscles. Three types of data are necessary to perform inverse dynamics analysis: full body kinematics, segments inertial characteristics and external forces. The following subchapters will introduce these methods in the context of alpine skiing research. The evolution of investigation methods will be highlighted as well as the challenges encountered when aiming to perform outdoor field tests in winter.

## 2.1. Kinematics

Kinematics is the mechanical branch of physics that can be utilised to study body movements without considering the causes that generate the motion. Several methods exist to acquire kinematics data such as two-dimensional (*2D*) and *3D* video analysis, Global Positioning System (*GPS*), goniometer, accelerometer and Inertial Measurement Units (*IMU*).

## 2.1.1. Two-dimensional video analysis

The rationale for using video images to investigate kinematics is to determine joint and segment positions and trajectories based on a succession of recorded images. First, images need to be digitized, subsequently the field of view needs to be calibrated to be able to scale the pixels to metres. In 1970, Ikai (Ikai, 1970) used high speed cinematography (50 Hz) to determine ground reaction force (*GRF*) and speed of skiers performing turns. A panning camera was placed at the centre of the turn radius, assuming a circular trajectory of the skier. Ten reference poles were positioned along the turn trajectory to determine the speed. The distances between poles were measured and the time needed by the skier to travel from one pole to another was estimated by counting the number of elapsed frames. Read and Herzog (Read and Herzog, 1992) used *2D* video analysis to investigate jump landings .The optical axis of the camera was placed perpendicular to the plane of motion. Only one side of the skier was reconstructed as symmetrical arm and leg movements were assumed. In ski jumping, the speed at take-off was compared to the length of the jump using a single camera placed laterally to the jump (Watanabe et al., 1972). Subsequently, the body position was analysed during the in-run (Janura et al., 2006), at the take-off (Virmavirta and Komi, 1993a; Virmavirta and Komi, 1993b) and during the flight phases (Schmolzer and Muller, 2005; Ohgi et al., 2007). In ski jumping, the trajectory of the skier is on a single plane, allowing for accurate analysis using *2D* video techniques. Nevertheless, *2D* analysis are not adapted for movements that are not in the plane perpendicular to the optical axis of the camera. Förg-Rob and Nachbauer (Förg-Rob and Nachbauer, 1988) proposed a method using a single camera to determine the *2D* trajectory of the skis on the snow. The camera was placed on the side of the slope, slightly raised from the slope plane. As the optical axis of the camera was not perpendicular to the plane of motion, the distortion produced was rectified using quadratic polynomial equations. Reference markers were placed on the slope to allow a calibration of the *2D* space. The bindings' front parts were used to determine the skis' trajectories, and

were covered with black foil to help the digitization. Hraski and Hraski (Hraski and Hraski, 2009) present the only study placing the camera in the frontal plane at the gate to analyse side leaning, hips and knee angulations during giant slalom. This setup's main limitation is to provide only a single opportunity to have the skier facing the camera and record the desired parameters.

## 2.1.2. Three-dimensional video analysis

As most of the skiing disciplines involve complex movements in all directions, researchers have been focusing on capturing *3D* kinematics data. The method is more complex than *2D* analysis as the acquisition volume needs to be calibrated. Abdel-Aziz (Abdel-Aziz and Karara, 1971) proposed a solution using reference markers of known positions to determine the cameras internal (i.e. focal length, image format, and principal point) and external (i.e. the position of the camera centre and the camera's heading in world coordinates) parameters. Several studies have been using two fixed cameras to record *3D* movements. Goodwin (Goodwin, 1990) positioned the cameras on the side of the course to analyse slalom technique, but only one side of the skier was reconstructed. The same technique was used to investigate up-unweighting and down-unweighting turn transitions performed by experienced and novice skiers (Brierley and Bartlett, 1991). The starting phase in downhill was also analysed using two cameras filming from the front on both sides of the start track allowing for the whole body to be reconstructed (Pozzo et al., 2001). Supej et al. (Supej et al., 2003; Supej et al., 2005c) divided a slalom turn in two different acquisition subspaces using two fixed cameras for each subspace to reconstruct the whole turn. Three subspaces and six cameras were used to analyse one giant slalom gate (Supej et al., 2003, 2005b), and the same configuration was used to record two slalom gates (Lešnik and Žvan, 2007).

Other solutions have been developed for large acquisition volumes. Dapana (Dapena, 1978) introduced a method allowing horizontal panning of the cameras to increase the field of view. The method was improved by

Yeadon (Yeadon, 1989), allowing panning and tilting of the cameras to record ski jumping. Reference markers were placed in the desired acquisition volume and their positions were determined using geodetic surveying equipment. The direct linear regression was then used to calibrate the volume (Abdel-Aziz and Karara, 1971). Through this method, the authors reached both an accuracy of 0.05 m to estimate the CoM and an error of 1° in orientation angles. This approach was used in several studies. Landing phases of a jump during downhill racing were analysed (Gerritsen et al., 1996; Nachbauer et al., 1996). Frick et al. (Frick et al., 1997) analysed muscle actions of one elite and six up-and-coming ski racers in slalom. The same dataset was used to help design training equipment (Raschner et al., 1997). Moreover, other disciplines were analysed such as the double poling in cross-country skiing (Canclini et al., 2005), the early flight phase (Schwameder et al., 2005), the take-off (Virmavirta et al., 2007) and the landing in ski jumping (Greimel et al., 2009). Scheirman et al. (Scheirman et al., 1998) proposed a solution based on instrumented tripods measuring panning and tilting angles without the need for neither extensive reference markers on the slope nor a survey system. They reported a 4mm root mean square error (*RMSE*) for the length of calibration rods in a 15 m * 4 m * 2 m acquisition volume.

The utilisation of at least two cameras is needed to determine *3D* point positions. However, in that case only one part of the skier is visible. The utilisation of more cameras enhances the overall visibility and decreases the negative effect of markers occlusion. Additionnaly, redundancy is added and the same point is viewed from different angles, which further increases precision. (Nigg and Herzog, 1994). Schaff and Hauser (Schaff and Hauser, 1993) used three panning and tilting cameras to analyse skiers performing different techniques of turns. Later, an identical set-up was used to compare carving and traditional turns (Raschner et al., 2001). Klous (Klous, 2007) used five panning and tilting cameras to analyse both snowboard and ski turns and reported an average accuracy of 11 mm, 9 mm and 13 mm respectively in the x, y and z directions. Reid et al. (Reid et al., 2009; Reid, 2010) used four panning and tilting cameras to analyse

differences between 10 m and 13 m slalom courses with a resulting accuracy between 6 mm and 17 mm depending on the reconstructed points.

## 2.1.3. Technical considerations about video based measurements

In alpine skiing, only few studies used markers placed on the skier's suit to help the digitization (Schaff and Hauser, 1993; Müller et al., 1998; Lüthi et al., 2006; Klous, 2007; Kurpiers et al., 2009; Klous et al., 2010). Other studies used unspecified techniques or direct manual digitization, estimating joint centre position on the images. Nevertheless, the latter was found inappropriate to obtain correct accuracy (Bartlett et al., 2006).

The frame rate of the cameras is also a concern in biomechanics. The majority of the presented *3D* studies used 50 Hz video cameras. While this may be sufficient to record athletes body motion, this frequency is clearly insufficient to record vibration or impacts such as jump landings. Several studies used higher acquisition frequencies. Kurpiers et al. (Kurpiers et al., 2009) used four 100 Hz fixed cameras to analyse the effect of a mobile force platform in mogul skiing. Bohm et al. (Bohm et al., 2008) used a three cameras system running at 250 Hz to record full body motion of the take-off phase of big jumps in snowboard. Finally, a unique study in snow sport biomechanics has been presented by Lüthi et al. (Lüthi et al., 2006). In this study, 20 Vicon cameras (Vicon, Oxford, UK) were used to capture the movement of freestyle aerial jumps. Data was collected at 120 Hz with an average accuracy between 0.06 and 0.15 cm depending on the calibration quality. The comparison of different *3D* video based systems' accuracy has been investigated (Ehara et al., 1995; Ehara et al., 1997; Richards, 1999; Briggs et al., 2003).

A potential source of error when using multiple camera system is the incorrect positioning of the cameras around the desired acquisition volume. The angle between the optical axes of two cameras looking at the same point should be higher than 60° and less than 120° (Nigg and Herzog, 1994). Due to the slope configuration and limitation in cable

length, Nachbauer et al. (Nachbauer et al., 1996) were unable to position the cameras in a correct configuration, resulting in errors up to 20 cm in the *3D* reconstruction. Finally, even if solutions have been developed to increase the acquisition volume, camera systems offer recordings of only one or two consecutive turns in alpine skiing.

## 2.1.4. Goniometers

Researchers developed other kinematic methods allowing full run recording. First goniometers were used to estimate joint angles of the lower extremities. Fukuoka (Fukuoka, 1971) measured the changes in the knee angle of alpine skiers during turning, sending collected data via telemetry. Goniometers and Electromyogram (*EMG*) measurements were then used to determine lower extremity kinematics and muscle activity (Kuo et al., 1983; Louie et al., 1984). Quinn and Mote (Quinn and Mote, 1990) used potentiometers to determine ankle joint flexion and extension and Maxwell (Maxwell and Hull, 1989) measured both ankle and knee angles. Single axis goniometers were used to determine knee flexion and extension in telemark skiing (Nilsson and Haugen, 2004), cross country skiing (Stöggl et al., 2008), and alpine ski racing (Spitzenpfeil et al., 2009). Finally, muscles activity as well as hip and knee flexion and abduction during turns were studied using *EMG* and two axis goniometers (Yoneyama et al., 2001; Petrone et al., 2009). Usually, goniometers were used in addition to force platform measurements to determine loads on knee joints as described in chapter 2.3.

## 2.1.5. GPS

A new and simple method to estimate human motion is the *GPS*. The antenna is fixed on a body part, describing the motion of this particular point and representing the motion that is investigated. Different receptors exist, offering different accuracy at different costs. Two frequencies are available to determine the position. The civil frequency (*L1*) offers about 10 m position accuracy. The *L2* frequency, reserved for military purpose, is coded, but the phase of the frequency can be used to achieve accuracy around 10 cm. Differential GPS (*DGPS*) can be used with *L1* and *L2*

receivers to increase the accuracy. A second *GPS* receiver is placed at a fixed position next to the testing location, and variation of position from the fixed receiver are deducted for the moving receiver. This allows for an accuracy around 1 m for the *L1* frequency and less than 2 cm for the *L2* frequency (Waegli and Skaloud, 2009). Skaloud and Merminod (Skaloud and Merminod, 2000) and Skaloud and Limpach (Skaloud and Limpach, 2003) were the first to describe skier trajectories using *L2 DGPS*. More recently, low accuracy *GPSs* were used to analyse skier trajectories and performance (Waegli and Skaloud, 2009), skiing training sessions and athletes comparison (Gomez-Lopez et al., 2009), and to describe a course and to estimate radial accelerations (Huber et al., 2009).

## 2.1.6. Inertial measurements units

Gyroscopes and accelerometers have also been used to measure kinematic variables. They consist of small electronic units measuring rotational positions and inertial accelerations. Kuo et al. (Kuo et al., 1983) and Louie et al. (Louie et al., 1984) used two *3D* gyroscopes to determine both the orientation of the ski boot and the pelvis. *IMU* consist of integrating gyroscopes and accelerometers in the same box. Such a device was also used to analyse aerodynamic factors in ski jumping, placing the *IMU* on the athlete's L5 vertebrae to approximate the *CoM* position (Ohgi et al., 2007). Waegli et al. (Waegli et al., 2009) proposed an algorithm merging data from low cost *GPS* and *IMU* sensors placed on the back of the ski boot allowing for determination of the skis' position, speed, orientation, edging and drift angle. The mean accuracy offered by the system was better then 0.4 m for the position, 0.2 m/s for the velocity and 2° for the orientations. Crossover and crossunder turn transitions have been investigated using four inertial modules placed on alpine skiers (two on the thighs and two on the ski boot) to determine knee joint angles (Chardonnens et al., 2010). Brodie et al. (Brodie et al., 2007, 2008; Brodie, 2009) presented a full body kinematic analysis using several *IMUs* and a *GPS*. *GRF* and dissipative forces were calculated allowing for estimation of energy changes from each force. Supej (Supej, 2009) investigated a fusion of differential high accuracy *GPS* and a Xsens inertial suit (Xsens,

Enschede, The Netherlands) reporting the accuracy of the *GPS* (1 cm horizontal and 2 cm vertical) and of the 3D orientation (0.5°). Unfortunately, the accuracy of the overall system was not reported. For this study, data was sent via Bluetooth to a computer carried by an experimenter following the skier. Finally, a full-body inertial measurement system was used to analyse snowboard freestyle (Krueger and Edelmann-Nusser, 2009). Mean knee angle errors of 4.8° were found when compared to an optical video-based system.

### 2.1.7. Summary

Kinematic analysis of winter sports is not a simple task and researchers constantly need to develop new ideas and find solutions to obtain consistent data. In alpine skiing, *3D* kinematics seems to be inevitable to capture the whole skier motion as important movements are performed in all directions. There is no system available yet which guarantees the necessary accuracy without the need of adding potentially disturbing equipment to the participants. Video based analyses are most common in full body motion kinematics, but the acquisition volume is limited to one or two turns. Several attempts using inertial sensors have been proposed, but the accuracy of such systems is still unclear, and the sensors that need to be worn are more disturbing than simple markers. As high accuracy but only limited acquisition volume was needed, the choice made for the current research was to use a video based approach.

## 2.2. Body segments parameters

To analyse human motion, it is also necessary to understand the physical and inertial behaviour of the segments composing the body. The mass, centre of mass location and moments of inertia of each segment have been measured using different methods. These methods are either based on cadaver studies, mathematical models, body scanning or indirect techniques using kinematic measurements.

## 2.2.1. Cadaver studies

In 1955, Dempster (Dempster, 1955) separated the segments of eight cadavers and measured their mass, *CoM* (using a balancing technique) and moment of inertia (using a pendulum technique). He published the procedure for measuring the segments properties (including the definition of the endpoints) and tables containing parameters needed for human motion analyses. The parameters were given as proportion of body mass and segments' length. Two years later, regression equations were proposed to increase the accuracy of the segments' masses computation (Barter, 1957). Joints centre were then defined using palpable landmarks instead of simple estimation (Clauser et al., 1969; Chandler et al., 1975). Based on Chandler's data, further improvements were proposed. Regression equations were applied to calculate segment's moments of inertia (Hinrichs, 1985). Then, non-linear equations were proposed (Yeadon and Morlock, 1989; Yeadon, 1990), and finally eleven anthropomorphic parameters (e.g. leg and thigh circumference, foot width…) were used in the equations to improve the estimation of the masses of the lower extremities (Vaughan et al., 1992).

## 2.2.2. Mathematical models

In 1964, Hanavan (Hanavan, 1964) proposed a mathematical model of the inertial properties of the human body. Based on the assumption that masses were uniformly distributed within each segment, he assimilates segments to geometric shapes (i.e. hands were represented as spheres, head as an ellipsoid, trunk segments as elliptical cylinders, and thighs, legs, feet, arms and forearms as truncated cones). Using the required anthropomorphic parameters needed to describe the geometric shapes of the different segments allowed him to determine the three principal moments of inertia of the 15 body segments composing his model. Measuring 242 anthropomorphic parameters allowed Hatze (Hatze, 1980) to determine a model composed of 17 segments with a total of 42 degrees of freedom. Mathematical methods were then enhanced using

photogrammetry, to provide more information about the body shape (Jensen, 1976, 1978).

### 2.2.3. Body scanning

New techniques involve scanning of living body to determine segments' properties. Zatsiorsky and Seluyanov (Zatsiorsky and Seluyanov, 1983; Zatsiorsky and Seluyanov, 1985) used gamma-ray scanning to compute mass distribution and inertial properties of a 15 segments human body. Regression equations allowed customizing body segments parameters. Others techniques have also been proposed (e.g. Magnetic Resonance Imaging (Mungiole and Martin, 1990; Cheng et al., 2000), and dual energy X-ray absorptiometry (Durkin et al., 2002; Durkin and Dowling, 2003; Ganley and Powers, 2004)). Nevertheless, none of these methods have been compared to one another.

These approaches pointed out the inaccuracy of using cadaver data to represent certain populations. Therefore, studies proposed investigated different kinds of population (e.g. children (Jensen, 1986, 1989), pregnant women (Jensen et al., 1996), infants (Schneider and Zernicke, 1992), and elderly (Jensen and Fletcher, 1994; Pavol et al., 2002).

### 2.2.4. Kinematic methods

Finally, kinematic methods have been used to deduce segments inertial properties and centre of mass. Drillis et al. (Drillis et al., 1964) and then Contini (Contini, 1972) used the quick release method, which consist of measuring the acceleration of a segment right after the release of a known force and applying the pendulum principle. Hatze (Hatze, 1975) proposed to use small damped oscillation of the segments. The investigated body part was set into oscillation using a spring. The properties of the joint and segment were estimated using equations based on small oscillation theory and the damped reduction of the oscillation. The kinematic approach allows in situ measurements but assumes a complete relaxation of all muscles. Another limitation is that these methods allow only for the

determination of terminal segments and measuring the trunk properties is impossible.

## 2.2.5. Summary

This subchapter presented four different type of methods developed to determine inertial properties of body segments. No studies comparing results obtained with the different approaches have been found. Kinematic methods provide incomplete data and are therefore unsuitable for full body analyses. Body scanning seems promising but results presented in the proposed studies are not directly usable. As mathematical models require a lot of anthropomorphic measurement, cadaver based method developed by .Clauser et al. (Clauser et al., 1969) and Chandler et al. (Chandler et al., 1975) has been chosen. This method simplifes calculation and field testing, as no anthropometric data are needed and segments' length can be deducted from *3D* reconstructed models.

## 2.3. Forces

Forces represent the action of one object on another. They are the causes of motion and the link to kinetics analyses. A force is represented as a vector, defined by its direction, magnitude and point of application. In alpine skiing, several forces have to be taken into account when investigating causes of motion. The force due to gravity, the centripetal force when turning, the ski-snow friction forces and the aerodynamic drag force are all interacting with skiers. This subchapter introduces the methods used to measure these forces.

### 2.3.1. Ground reaction forces

The first force plates have been developed to understand knee injuries mechanisms and to try to find solutions to improve bindings' safety. Hull and Mote (Hull and Mote, 1974, 1975, 1978) proposed a system consisting of two independent six degrees of freedom dynamometers integrated in the ski, one under the toe part of the binding and the other under the heel. The maximum error of the dynamometers was 4% for Fx and Fy, 100N for Fz, 2% for Mx, 4% for Mz and 27 Nm for My. The skier

had to wear a 5.8 Kg backpack containing a transmission system sending data wirelessly to a fixed station at 520 Hz. Lieu and Mote (Lieu and C. D. Mote, 1980) proposed to use *EMG* signals to control the release mechanism of an electronic binding.

Another design was proposed by MacGregor et al. (MacGregor et al., 1985), aiming to develop an electronic released binding system to be able to record data. The binding was integrated between the ski and the boot, with a height of 2.5 cm. It was composed of four octagonal strain rings, measuring the three moments. The average accuracy for the moments was approximately 10 to 15 %, with a worste case of 25 %. The non-linearity in the dynamometer didn't allow for a precise determination of forces. The acquisition system was able to record 1.5 min of data at 25 KHz across all recorded channel. The package containing the whole system weighted 8 Kg, and the release of the binding could be activated manually or electrically via a software included in the microcontroller. The release algorithm was discussed in another article (MacGregor and Hull, 1985). As this system was not able to measure forces accurately, the same research group proposed a second generation of measurement system. A six component dynamometer was built using seven instrumented flexure elements (Wunderly et al., 1988). An effort was made to maximize the mechanical decoupling of the load to reduce cross sensitivity between components. The plate was 4 cm thick, weighted 1.1 Kg and the weight of acquisition package was reduced to 2.5 kg. This new system was able to record 25 s of data at 200 Hz. The accuracy of the system was not clearly defined, but it was mentioned that it was better than that of the previous design. Maxwell and Hull (Maxwell and Hull, 1989) associated the force plate, *EMG* recording six surface muscles (i.g. rectus femoris, vastus medialis and lateralis, biceps femoris, semitendinosus and gastrocnemium) and the measure of the flexion of the hip and the knee with potentiometers.

A revised design of Hull's first force platform (Hull and Mote, 1974) was then proposed by optimising an uncoupled dynamometer using instrumented T-shaped Shear Panel Elements (*SPE*) (Quinn and Mote,

1990). Three pairs of SPE were used to measure forces components in the three directions. The dimensions of each pair of *SPE* were adapted to the estimated future load. The high linearity of the system allows an accuracy of less than 2% for all forces and moments components. Two devices were mounted on the ski (below the toe and the heel binding's component), elevating the binding by 3.2 cm and weighing a total of 3.4 Kg. The system was then used in addition to a potentiometer measuring the ankle flexion in order to calculate forces and moments both at the boot top and at the knee to predict constraints undergone by the knee during skiing (Quinn and Mote Jr, 1992). The calculated constraints were different from those measured at the base of the boot. Therefore, regression equations have been used to find the measured set of parameters that predict best the bending and torsional moments at the boot top and at the knee. Müller (Müller, 1994) used a four strain-gauge sensor on each ski to measure independently forces at the heel and the ball of the foot, as well as at the inner and outer sides of the foot.

Concerned by the possible effect of the bending of the skis on the measure of vertical load, Wimmer and Holzner (Wimmer and Holzner, 1997) developed two different devices measuring vertical reaction force. The first was inserted between the skis and the binding and the second between the binding and the boot. The first design was significantly perturbed by the bending but not the second.

More recently, new systems have been developed allowing measurements of forces and moments on both skis. Such measurements are needed for a complete understanding of the kinetics. The effect of binding position was analysed using skis equipped with an aluminium plate instrumented with two strain gauge cylinders (Nigg et al., 2001; Schwameder et al., 2001). A new device, based on strain gauges, placed instead of the plate on carving ski and elevating the skier by 6 mm compared to the usual position was proposed (Vodickova et al., 2005a). The given accuracy for the system was better than 7% for all components and the data acquisition system was placed in a backpack. At the same period, Kiefmann et al (Kiefmann et al., 2006) developed an interesting force platform where the

device could be fixed as an interface between the ski boot and the binding without modifying the overall system. The device used shear beam instrumented with strain gauges measuring the six components at 500 Hz, with the data being transferred wirelessly via Bluetooth to a Personal Digital Assistant (*PDA*). Unfortunately, the accuracy of the system was not specified and the platform suffered from mechanical weaknesses. A mock-up of the platform, with similar dimensions (4 cm height and 2 Kg each) was used to determine the influence of the material during moguls skiing, without finding any significant differences when using the devices (Kurpiers et al., 2009).

Several studies used a force platform based on piezoelectric sensors, developed by Kistler (Kistler AG, Winterthour, Switzerland). Knüz (Knüz et al., 2001) analysed loads when performing carved turns using either soft or hard snowboarding equipment. Lüthi et al. (Lüthi et al., 2005) compared three methods to determine forces and moments acting between the skier and the ski. The first method used Kistler force plate, the second used pressure insoles and the third used video based inverse dynamics. The results showed a precision of about 160 N when estimating forces based on video, and approximately 150 N for the vertical force using insole pressure measurements. The first details concerning the accuracy of the kistler force plate were found in the thesis dissertation of Klous (Klous, 2007). She gave a relative accuracy of ± 3 % for the forces and ± 8 % for the moments. The force platform was used for both skiing and snowboarding to calculate 3D joints loading of the lower extremities using inverse dynamics. The detailed protocol concerning the Kistler plate validation was published by Stricker et al. (Stricker et al., 2009). They studied the effect of temperature on the accuracy of the device and gave some information about the design of the plate: the achieved sampling rate can go up to 500 Hz and each dynamometer measured 3.2 cm and weighted 0.9 Kg. Data was recorded by a device carried in a backpack of unspecified weight. The cross talk between components ranged between 0.2 and 3.6 %, depending on the axis and the dynamometers had to be zeroed at the beginning and the end of the measure to control for the drift

induced by piezoelectric sensors. The results showed a very low influence of the temperature and an increase of the relative accuracy with the increase of the constraints.

Another way of measuring constraints has been proposed by Schattner et al. (Schattner et al., 1985). They introduced 3 mm thick pressure-measuring devices, called mats, composed of up to 192 sensors that could be placed along the tibia inside the ski boot. The processing unit operates at 25 Hz and sends data by telemetry via UHF transmitter. The main objective of this system was to help investigate ski boot characteristics to improve safety and reduce injuries due to material. The system was then used to analyse the influence of different boots and boot shaft on the learning process (Hauser et al., 1985). A second version of the system was then proposed, improving flexibility and reproducibility of the previous device (Schaff et al., 1987). The number of measured points in the mat was reduced from 72 to seven, allowing for a standardisation of the measurements. 14 participants tried a total of nine boots with different leg flexions, allowing to determine the quality of the upper boot shaft independently of the person wearing the boot. Nevertheless, individual pressure differences were found above the instep, inducing the need for personal fitting on this region.

Schaff et al. (Schaff et al., 1989) published the first article analysing pressure pattern underneath the feet. The 72 measuring points' mat was placed as an insole under the foot of ten subjects, to test five ski boots with different forward flexions. The pressure over the instep was also measured using a single point. With the unchanged objective to help reducing injuries pain in ski boots, Senner et al. (Senner et al., 1991) developed a new artificial leg to improve quality of ski boot testing. They used pressure distribution data from 14 participants and reproduced the shape of the leg of the person showing the nearest curve compared to the average distribution. The leg's characteristics were then adapted to reproduce the average pressure distribution pattern. A review described the possibilities offered by pressure sensor systems, highlighting enhanced acquisition frequencies up to 500 Hz, data-logger weight of only

0.5 Kg, possible repartition of the measured points all around the foot and leg and even simplified biofeedback system, beeping when the heel pressure exceeds a predetermined threshold (Schaff et al., 1997).

Novel Pedar insoles (Novel Gmbh, Munich, Gm) with 99 capacitive sensors and an acquisition frequency of 50 Hz were used by Lafontaine et al. (Lafontaine et al., 1998) to investigate different turns performed by alpine ski instructors. Parallel and carving turns were compared using the Pedar insole, *3D* model reconstruction and *EMG* measurements of seven right leg muscles (Raschner et al., 2001). As seen previously, methods using pressure insoles, force platforms or video based inverse dynamics to determine forces were compared (Lüthi et al., 2005). When comparing to the vertical component of the force platform, the authors were able to establish that pressure insoles introduced an average error of 150 N. The experiment showed that in average, 90 % of the total force was acting in the vertical direction during the turn. A more detailed comparison between pressure insole and force plate was achieved by Stricker et al. (Stricker et al., 2009). The pressure insole induced an average underestimation of the vertical force of 21 % for the outside ski and 54 % for the inside ski and maximum deviations of 55 % and 86 % respectively. These values were obtained during the turn transition, when vertical applied forces were lower than 200 N. Spitzenfeil et al. (Spitzenpfeil et al., 2009) estimated energy expenditure in slalom, giant slalom and super giant using Parotec pressure insole system (Paromed Medizintechnick, Neubevern, Germany) and goniometers. Maximal isometric strength was previously recorded for each participant at different knee angle and a dynamic model was created to compute the muscular expenditure. Finally, Footscan pressure insoles (RS-scan Lab Ltd, Ipswich, UK) were used to estimate ground reaction forces and snow friction in the development of a fusion motion capture system (Brodie et al., 2007; Brodie, 2009). The accuracy of the system was unspecified, as a high drift was measured between the start and the end of the trial.

## 2.3.2. Ski-snow interaction

Lots of efforts have been dedicated by researchers to better understand the mechanism of snow friction. The literature can be separated in two distinct parts. First the study of the parameters influencing the friction mainly focused on the microscopic level. A synthetic review of the subject has been proposed by Colbeck (Colbeck, 1994b) and some updates are given by Federolf et al. (Federolf et al., 2008). The second part concerns the way to estimate ski-snow friction during field experiments. This subchapter introduces investigations related to the second part described above.

Bowden and Hughes (*Bowden* and *Hughes*, *1939*) first investigated the snow and ice friction using a refrigerated turntable. Watanabe and Ohtsuki (Watanabe and Ohtsuki, 1978) estimated the snow friction using a straight 100 m running course with coil magnets positioned along the ski course to measure the skier's speed. Three different postures were tested in the field and reproduced in a wind tunnel to determine the aerodynamic drag and consequently deduct the ski-snow friction coefficient. Snow friction of both straight and traverse downhill have been determined using photocells (Nachbauer et al., 1992; Kaps et al., 1996). The equations of motion were resolved using the constraints given by the path and timing of the skier, taking into account the gravitational force, the drag force and the friction force. Collbeck (Colbeck, 1994a) investigated the way to improve the measurement of high speed friction on snow and proposed to use a slider instead of a skier to increase the accuracy and reproducibility. Friction coefficients during turns have also been analysed (Sahashi and Ichino, 1998; Tada and Hirano, 1998). Several studies have been focusing on carving turns. A modelling of the ski snow contact during carving turns was proposed (Mössner et al., 2006), the deformation of the snow was measured (Federolf et al., 2006), and the contact pressure between ski and snow was calculated (Heinrich et al., 2009). Fauve et al. (Fauve et al., 2005) quantify the influence of different snow and weather characteristics (e.g. Snow temperature, snow surface hardness, mean snow grain diameter, air temperature, net radiations...) on gliding performance.

Finally, a prototype allowing to measure the friction coefficient has been proposed based on load cells and accelerometers determining friction force and normal force acting on the skis (Miller et al., 2006).

### 2.3.3. Aerodynamics

Athletes performing disciplines like running, speed skating, cycling or cross-country skiing have always been interested in optimizing their aerodynamic drag to increase speed and achieve better performance (Shanebrook and Jaszczak, 1976; van Ingen Schenau, 1982; Spring et al., 1988; Lopez et al., 2008). In alpine skiing, the gravitational force is used to increase the skier's kinetic energy, whereas the aerodynamic drag is one of the two non-conservative forces doing negative work on the skier. Quantifying this parameter is therefore important to understand skier's performance.

A number of studies have examined skier aerodynamic drag. The effect of varying skiing postures on aerodynamic drag was investigated in a wind tunnel study (Watanabe and Ohtsuki, 1977), and the effect of skiing velocity in a field study (Watanabe and Ohtsuki, 1978). As seen in the previous sub-chapter, a method based on motion equations has been proposed to calculate snow friction and drag area during straight and traverse downhill skiing using photocells (Nachbauer et al., 1992; Kaps et al., 1996). Performance coefficients taking into account factors like mass, frontal area, and drag coefficient have been developed with wind tunnel tests (Luethi and Denoth, 1987). Theoretical drag analysis based on tridimensional models of speed skiers and on two-dimensional body part projections have been conducted to compare different postures, and determine factors limiting speed (Savolainen, 1989). Thompson and Friess (Thompson et al., 2001) performed wind tunnel tests to improve the aerodynamic efficiency of speed-skiers by optimizing their posture and equipment.

While these studies have made valuable contributions towards our understanding of the aerodynamic properties of static skiing postures, they are limited in that alpine skiing is primarily a dynamic sport where the skier

continually moves and changes position. To allow the drag analysis of skiers performing turns, Barelle et al. (Barelle et al., 2004) modelled the drag coefficient based on athlete segments' length, and inter-segmental angles, thereby allowing the determination of aerodynamic properties through a complete span of positions typically encountered in skiing. In his estimation of the air drag force, Reid (Reid, 2010) used the projection of a 3D model on a plan perpendicular to the velocity of the skier's CoM to determine the frontal area. Air drag coefficients were taken from the literature for different postures and regression equations used to calculate the appropriate drag coefficient depending on the height of the skier.

## 2.3.4. Summary

The only way to record accurately ground reaction force seems to be integrated force platform. The systems proposed in this review all imply modification of the skier's equipment except the device proposed by Kiefmann et al (Kiefmann et al., 2006), but no data concerning the accuracy are available. Insole systems, even if practical to perform measurements, are not accurate enough to quantify forces in alpine skiing due to the high quantity of constraints going around the boot shell and not only going through the sole. Ski-snow friction can either be measured using antero-posterior component of the ground reaction force, or deducted from estimation of the friction coefficient and of the force normal to the velocity direction. Finally, air drag should be determined using model estimating drag area from postures and anthropometric data.

## 2.4. Inverse dynamics

The only study dealing with inverse dynamic in both alpine skiing and snowboarding has been proposed by Klous (Klous, 2007). *3D* motion kinematics were collected using a multiple-cameras system ,the regression equations proposed by Yeadon (Yeadon, 1990) were used to determine segments' properties and the Kistler force plate was used to provide *GRF* data. Synchronization between cameras and forces data was achieved through to the execution of a jump at the beginning and the end of the trial, recorded both on the video and on the force platform. Stricker

(Stricker et al., 2009) used the same method to synchronize the same force platform with pressure insole.

## 2.5. Conclusion

This chapter introduced the current state of snow sports research. It is clear that further work needs to be developed to allow tests in outdoor environment leading to results similar to laboratory experiments. Adapted material and methods need to be developed, and the following chapters will explain the way followed in this research to analyse biomechanics of alpine skiers performing giant slalom turns. Each developed study will propose a dedicated literature review adapted to the investigated theme, which might contain some of the same elements as the ones just discussed.

# 3. Main results in the analysis of alpine skiing turning techniques

This chapter offers an overview of the main results obtained in the study of turning mechanisms in alpine skiing. First the way of describing a turn in different phases is discussed. Second, researches analysing skiers' movements and their effects on ski behaviour are exposed. Third, trajectories analysis are presented. Fourth, investigations on the friction forces affecting speed are described, and fifth, a review concerning the use of energy principles to describe skiers' performance is proposed.

## 3.1. Turn cycle

Analysing the mechanisms involved while performing turns in alpine skiing requires a comprehensive description of the turn cycle structure, to ensure the proposed results are correctly understood by the reader. Indeed, without knowing to which part a given result relates, it is impossible to interpret the data and compare them with other studies. Several approaches have been proposed and will be listed here.

Förg-Rob (Förg-Rob and Nachbauer, 1988) first proposed a structure based on ground reaction force measurements. The turn cycle was divided in two main phases, a preturning phase and a turning phase. Each one was than also separated in two, leading to:

- A weight transfer phase, where the weight on the future outer ski increases.

- An unweighting phase, where the weight on the future outer ski decreases.

- An edge setting phase, where the weight on the inside of the new outer ski increases.

- A steering phase, where the turn radius is controlled by the edging of the skis.

Müller (Müller et al., 1998) used a structure based on skier's movements. The turn cycle was separated in an initiation phase and two steering phases. The initiation phase was described by:

- The unweighting of the skis by bending or straightening the knees and hips.

- The edge change, from the uphill edge to the downhill edge.

- The turn initiation bringing the ski in the new direction using rotations.

- The speed control using skidding

The steering phase was separated in the part before the fall line and a part after, and described by:

- Turning, controlled by the pressure distribution along the skis, the variation of the edge angle and the variation of the body rotations.

- Controlling balance by varying inward leaning angle and distance between skis

- Controlling speed by varying ski position and skidding.

LeMaster (LeMaster, 1999) highlighted differences between turns. Basic turns were composed of four phases, with an initiation, a control, a completion and a traverse phase. When turns are directly following each other, the traverse phase disappears and the completion and the initiation phases merge into a transition phase.

Finally, Supej et al. (Supej et al., 2003) determined the beginning of a ski turn as the moment where the CoM of the skier crosses the average trajectory of the skis on the transverse plane.

## 3.2. Effects of skier's movements on ski behaviour

Several key movements are needed to perform ski turns and timing of execution of these movements is very important. Side leaning as well as knee and hips angulating induce edging of the skis. Rotations on the transverse plane are used to orientate the body and finally flexion/extensions of the legs, as well as fore/aft leaning help to control

respectively the load amplitude and location on the skis. The following paragraphs describe the effects of the key movements on ski behaviour.

### 3.2.1. Edging

As described above, edging of the skis can be achieved by leaning the centre of mass inward of the turn, or using angulations of the knees and the hips, which change the edging angle without significantly modifying the CoM position. Morawski (Morawski, 1973) first proposed to consider the skier as an inverted pendulum. The body was oscillating from one side to another, controlled by the lateral force acting at the ski-snow interface. A higher inclination of the body needed to be compensated by higher lateral forces, leading to higher oscillation frequency and therefore speed. In slalom, a maximal inward leaning angle of 40° was measured, occurring approximately at the gate crossing (Raschner et al., 1997). During parallel turns, experienced skiers had significantly larger edging angles than intermediate skiers (34.9° versus 30.6°, respectively) (Müller et al., 1998). A comparison between carving turns and parallel turns showed maximum edging values between 65° and 70° in carving, and approximately 10° less in parallel turns. Left and right legs edge angles were identical in carving and slightly smaller for the inner ski in parallel turns. The obtained values were a lot higher than the ones obtained by Müller (Müller et al., 1998). Observation of edging in both carving and parallel turns highlighted a higher use of side leaning in carving turns and a higher use of angulations in parallel turns (Yoneyama et al., 2001). In a study of slalom competitors' technique, knees angulation was used to initiate carved turns, directly followed by hips angulation to regulate inclination balance (Supej et al., 2005a). An analysis of short turns performed using carving skis indicated a large part of skidding by beginners, due to lower edging of the body (Vodickova et al., 2005b). Finally, it has been demonstrated that faster skiers had greater angulations, greater side leaning and larger distance between skis (Hraski and Hraski, 2009).

## 3.2.2. Rotations

Orientation of the body is usually used to help initiating turns and sustain ski driving during steering phases. Only few studies have reported results concerning rotations of body parts. In an extensive study investigating different turn techniques, pre-rotation was considered as the most important factor in the initiation phase, helping to transfer an angular momentum from the torso to the legs (Müller, 1994). In the comparison of carving and parallel turns, tight rotation was highlighted during steering phase in long parallel turns but not during long carving turns, whereas analysis of short turns indicated a gradual rotation of the thigh during short carving turns and fast initial rotation during short parallel turns (Yoneyama et al., 2001). Finally, when asked to perform short carving turns, beginners induced skidding due to over-rotation of the upper body during the steering phase (Vodickova et al., 2005b).

## 3.2.3. Loading

### 3.2.3.1. Binding safety

When performing turns, speed and radius influence the load acting on the skier, but as seen previously, legs flexion and extension help managing the amplitude of the force while forward and backward leaning controls the application point of the force and the torque applied on the skis. First investigations on ski loading were aimed at improving safety of bindings release mechanism. In early studies, it has been observed that load magnitudes at the boot sole were higher than static ultimate strength of the tibia measurements (Hull and Mote, 1974, 1975, 1978). As static measurements were used for binding release mechanism adjustment, it was concluded that this solution was not sufficient. They proposed to take into account body position and muscles contraction state for improving binding safety. The degree of muscle activity was then defined as the most reliable factor for calibration of binding release mechanism (Lieu and C. D. Mote, 1980). It was also observed that the level of axial load at the knee was a very good indicator of the level of muscle activity in the quadriceps group. As the axial loading at the knee joint is mainly derived from the

axial load at the binding, it was suggested that the level of muscle activity could be determined from binding loading measurements. Therefore, loads measured at the binding could be used to control the release mechanism. Also concern by safety issues, tight and loose closing of the buckles were compared, showing a lower total force on the insole when the buckles are tightly closed (Schaff et al., 1989). Moreover, the increase of the forward flexion induced an increase of the instep pressure and a reduction of the insole pressure on tight closed boots. On the contrary, higher forward flexion induced an increase of the total force on the insole for loosely closed boots. Considering the critical movements where the binding have to release, a study used the medial-lateral force at the toe as a predictor for the torsional moment applied to the leg. Additionally, the resultant medial-lateral force at the base of the boot was used to predict the vargus-valgus moment on the leg. Finally, vertical forces components at the heel and toe were used to determine anterior-posterior bending moments at the top of the boot and at the knee (Quinn and Mote Jr, 1992).

Injury risks during jump landings have also been analysed. Resulting knee joint forces acting on the tibia were around -1200 N in the vertical direction and slightly higher than 400 N. on the antero-posterior axis. Knee joint moments of approximately 400 Nm were acting on the tibia (Read and Herzog, 1992). It was measured that one leg landing almost doubled antero-posterior component of the knee joint force. In a similar study, maximal loads of the knee around 880 N were found for the anterior shear force, -2200 N for the compression force and -790 Nm for the extensor moment. All these measures were derived from kinematics data (Gerritsen et al., 1996; Nachbauer et al., 1996).

### 3.2.3.2. Turning technique

Transition between turns is initiated by unweighting the skis. This can be achieved either by a downwards acceleration of the CoM which directly unweights the skis (crossunder) or by an upwards acceleration of the CoM which once stopped, unweighs the skis (crossover). Observation of both initiation techniques showed that experienced skiers had higher amplitude

of movement with their CoM during turn transitions than beginners (Brierley and Bartlett, 1991).

In a study performed on 21 ski instructors, Müller et al. (Müller, 1994) observed that crossover turns were initiated either from the downhill ski only or from both skis. Crossunder turns were used mainly on mogul pistes and deep powder snow, and were considered not functional on even slopes, as knee extensors were almost always active. Sustained loads were also higher, due to the higher bend of knee and hips when resisting to external forces. On packed snow, vertical forces were approximately 1.4 times the bodyweight, with a ratio of 3:1 for the outside-inside distribution during steering phase. The body weight was shifted towards the rear of the skis, and knee angles were almost constant during the phase (125° and 115° respectively for the outside and inside ski). On icy surfaces, forces of 1.6 times the bodyweight were recorded, with the same distribution between skis. At the end of the steering phase, the total load increased to 1.75 times, with the additional load put on the outside ski.

Another study highlighted timing of vertical movements of the legs during turn transition. In crossover turns, extension of the outer leg began before the flexion of the inner leg, while crossunder showed an inverted pattern. No differences were found in the amplitude of the movements (Chardonnens et al., 2010).

Klous (Klous, 2007) measured forces and torques during carving turns. Graphs show averaged vertical loads around 1.5 times the bodyweight on the outer leg and less than one time the bodyweight on the inside leg. Medio-lateral and anterio-posterior forces were equally distributed between external and internal legs, but were a lot smaller than vertical forces (approximately 0.1 times the bodyweight for both components). Fore-aft torques were measured between -2 and 2 Nm/Kg for both legs. Averaged abduction-adduction moments around 0.2 Nm/Kg for the outside leg and 0.1 Nm/Kg for the inside were also recorded. Finally, internal-external rotations were around zero on the inside leg and approximately 0.2 Nm/Kg on the outside. The results obtained in this study demonstrated higher knee loading in skiing than snowboarding and higher ankle loading

in snowboarding. Carved turns also induced higher loads than skidding for both disciplines.

The comparison between basic parallel, dynamic parallel, giant slalom and short turns revealed higher vertical forces during short turns (mean of 1291 N) while basic parallel turns showed lower forces (mean of 1137 N). Except during dynamic parallel turns, where an equal pressure distribution was measured, more load was recorded on the outside ski for other techniques. Giant slalom turns also had a higher amplitude of anteroposterior displacement of the centre of pressure, with the centre of pressure migrating from the toes to the heel during the turn while moving only from the toes to the middle of the foot arch for other techniques (Lafontaine et al., 1998).

Differences in loading patterns have also been observed between parallel and carving turns. The inner ski was unloaded before the transition phase in parallel turns, while the load increased constantly during the carving turn. Vertical accelerations were more intense in parallel turns to unweigh and then turn the skis. The skier also was found to lean more backwards during the carving turn, increasing the heel pressure (Raschner et al., 2001). Confirming these results, an analysis of the CoM motion during turning phases revealed less vertical movement using carving skis instead of longer and less shaped skis, and a more harmonic locus of the CoM during turn transition (Schiefermüller et al., 2005). It has also been observed that it was possible to perform open carving turns using equal distribution on both skis, and that higher loads were recorded on the inner leg during closed carving turns (Vodickova et al., 2005a). A comparison between 10 m and 13 m slalom courses revealed a greater degree of carving and a prolonged initiation phase for the 13 m course. Using positions derivatives, snow reaction forces of 3.5 times the bodyweight were calculated. Peak forces occurred at about 50% and 65% of the turn on the 10 m and 13 m slalom races respectively (Reid et al., 2009; Reid, 2010).

Differences among skiers of different levels were also investigated. A study showed that during first steps of learning, participants having a

homogeneous pressure distribution on the shaft had low pain level on the tibia and had a quicker learning process (Hauser et al., 1985). Analysis of turning technique of skiers with different levels revealed a higher variability in intermediate skiers compared to the advanced group. Most of the significant differences between groups were found at the beginning of the transition phase (Müller et al., 1998; Schöllhorn et al., 2001)

Several studies have been focusing on racing technique. Analysis of one elite and six up and coming skiers in slalom reported constant hip angle during the first part of the steering phase and a quick reduction of the angle after the gate crossing. The outside knee was extended during the first steering phase and both knees were flexed after the gate passage. Stretch shortening cycle was highlighted for knee and hip extensor muscles of the inside leg but not those of the outside leg (Frick et al., 1997). Later, an average muscular load of 40% of the maximal strength was found for all racing disciplines (Spitzenpfeil et al., 2009).

A Slovenian group studied two different racing slalom techniques (Supej et al., 2004; Kugovnik et al., 2005; Supej et al., 2005a). The first technique consisted of a double cycle of flexion and extension of the CoM during a turn while the second used only a single movement cycle. Based on the technical possibilities offered by new ski geometry (carved skis) they highlighted the superiority of the single motion technique. A computer simulation of the movements was also proposed (Supej et al., 2004), revealing higher sustained forces during double motion. The skier's body was also in a more flexed position when the forces were maximum, increasing muscles power of legs. Timing of field tests of four highly skilled athletes on three different course setups showed improved times using the single motion technique for 82 % of the time (Kugovnik et al., 2005). Finally, vertical displacements of approximately 0.4 m were reported between the CoM and the slope for both techniques (Supej et al., 2005a). However, the CoM position was lower when using the single motion technique.

Several authors have been suggesting that effective extension movements of the CoM could contribute to increase the speed of the skier. Focusing

on undulating snow surface and supposing similar principle during turns, Mote and Louie (Mote and Louie, 1983) studied the theoretical aspect of the pumping mechanism. The vertical movements of skiers with specific timing was analysed, and they observed that the best timing to increase speed was to make the extension when the forces are maximal and flexion when forces are minimal. Takahahi and Yoneyama (Takahashi and Yoneyama, 2001, 2002) as well as Kagawa and Yoneyama (Kagawa and Yoneyama, 2001) theoretically demonstrated possible energy generation during turns when the CoM and the skis' trajectories are diverging and when forces are exerted at the same time. The phenomenon was highlighted at the beginning of the turn when the skier leaned inwards.

Finally, several researches have been focusing on the effect of the load on the mechanical ski behaviour. Using a mechanical model fixed on carving skis, Margane et al. (Margane et al., 1998) demonstrated a reduction of the radius of the turn when the model leaned forward. Fauve et al. (Fauve et al., 2009) obtained similar results in a field study using a ski equiped with eight strain gauges recording both torsion and bending stiffness of carving ski when performing giant slalom turns. Increased torsion and torsion vibrations were measured on hard snow compared to soft snow. De Cecco and Angrilli (De Cecco and Angrilli, 1999) built a calibration system allowing the measure of the elastic properties of skis since edging angles, applied load and forward and backward movements could be simulated. A forward position unloaded the ski tip and increased manoeuvrability, useful at the beginning of the steering phase. The stability of the ski was increased with higher edging angle, and this parameter was considered as the most important characteristic of a ski.

## 3.3. Trajectories

Skier trajectories have been one of the first focuses in alpine ski racing, looking for the optimal line leading to the best performance. Förg-Rob and Nachbauer (Förg-Rob and Nachbauer, 1988) studied the length of the outside toe binding trajectory on 34 ski racers performing slalom. They found correlation between performance time, velocity and trajectory:

shorter trajectories were correlated with higher speeds and better times. Skiers with a higher velocity also had a lower trajectory. For the best skier, the highest velocity was reached just after the gate crossing, shortly after the beginning of the steering phase, while the lowest speed was observed during the turn transition. His trajectory was also more direct, as his heading angle at the turn transition was below average.

Similar results were observed by Lesnik and Zvan (Lešnik and Žvan, 2003, 2007). They found correlation between higher speed and more direct line. In another study, Zvan and Lesnik (Žvan and Lešnik, 2007) found that skiers who had a direct line on the first analysed turn had a longer turn trajectory on the second one. On the contrary, Supej (Supej, 2008), observed that shorter turn radiuses, therefore leading to a more direct line, led to higher energy dissipation and thereby worse performance.

Goodwin (Goodwin, 1990) analysed the lateral distance between the front of the outside boot and the gate in slalom, finding significant correlation between high skier speed and thin lateral space, but several athletes too close to the gate achieved lower speed, suggesting an optimum gate crossing distance. Lesnik and Zvan (Lešnik and Žvan, 2007) found similar results in their study of giant slalom. Ankle joint positions of 18 elite skiers were compared. The authors found that skiers closer to the gate didn't achieve the faster velocity, which seemed contradictory with the correlation between high skier velocity and direct line exposed previously.

Ferrario et al. (Ferrario et al., 1997) used Fourier analysis to reconstruct trajectories of three different skiers performing three times a giant slalom. The less experimented skier achieved longer distances and lower speed, with a higher variability in his trajectory from one run to the next.

Investigating changing conditions during slalom ski course, Supej et al. (Supej et al., 2005c) observed that deterioration of the course increased trajectory lengths and reduced velocity of the five analysed top level slalom racers. With worse snow conditions, the apex of the turn also became lower.

Computer simulation has also been developed to determine the optimal turn trajectory. Seifriz and Mester (Seifriz and Mester, 2001) proposed genetic algorithms to optimise the trajectory based on skier, trajectory and slope parameters. Simulated runs highlighted situations where higher velocity at the cost of longer distance didn't lead to the best performance. The results obtained with the simulation were consistent with real trajectories measurements. A few more articles concerning numerical models have been published. Remondet et al. (Remondet et al., 1997) developed simplified equations for estimating the running time of a race. Reinisch (Reinisch, 1991) focused on the path of the quickest trajectory between two gates, and Von Hertzen et al. (von Hertzen et al., 1997) determined the optimal shape of a slope's portion to obtain maximum skier's final speed.

## 3.4. Friction forces

First investigations on snow and ice friction highlighted the increase of the friction coefficient with lower temperature or lower load on ice (Bowden and Hughes, 1939). The friction coefficient was divided by two when small ski models were waxed. Experiment on snow surfaces gave a kinetic friction coefficient of 0.04 for waxed hickory skis. Estimations of the skis-snow friction on the field reported coefficients of 0.13 and a negligible effect of posture (Watanabe and Ohtsuki, 1978). Spring (Spring, 1988) demonstrated the increase of the friction coefficient in correlation with speed. Coefficients between 0.008 and 0.25 for straight running and of 0.13 and 0.15 at respectively 11 m/s and 15 m/s for traverse skiing were also calculated (Nachbauer et al., 1992; Kaps et al., 1996). Moreover, low speed tests between 0 and 4 m/s on icy surface gave friction coefficient of approximately 0.04 (Miller et al., 2006).

Concerning aerodynamics, the advantage of the "egg-shaped" posture was established, as well as the negative effect of lateral extension of the arms. The increase of drag when opening the arms was comparable with the increase when raising the trunk (Watanabe and Ohtsuki, 1977, 1978). A drag area of 0.22 $m^2$ was calculated for a skier in upright position going

straight downhill, but the authors were unable to determine the drag area for traverse skiing (Nachbauer et al., 1992; Kaps et al., 1996). In speed-skiing, the torso had to be slightly lifted from the tangential direction of the slope to increase the lift effect and reduce the ski-snow friction (Savolainen, 1989). Moreover, wind tunnel tests showed a significant decreased of drag when the frontal area or the size of recirculation regions around the body was reduced. The most sensitive area were downstream the legs and buttock (Thompson et al., 2001). Finally, the model of drag area build by Barelle (Barelle et al., 2004) offered accuracy of 13 %. The model was based on a wind tunnel experiment which gave results for the drag area between 0.15 $m^2$ and 0.35 $m^2$ (respectively for the egg and the upright posture).

## 3.5. Energies

Recently, Supej et al. (Supej et al., 2005b) calculated the mechanical energy of skiers performing turns using the height and the velocity of the CoM to determine respectively the potential and the kinetic energy. Following the law of energy conservation, any decrease in mechanical energy is due to a loss of energy to the surrounding environment, and any increase is due to a gain of energy taken from this environment. Energy loss can either be induced by non conservative forces such as snow and air friction, but it can also take place through storage (e.g. in the skis when it is bended) or absorption (e.g. by the body). Gain of energy can come from muscles production or from energy restituted by the skis.

Supej et al. (Supej et al., 2005b) proposed to determine the rate of energy dissipated by vertical course distance. This allows to estimate the quality of a ski turn. The authors found cyclic behaviour of the dissipated energy curve in slalom. More energy was lost around the gate crossing and less at the turn transition. A positive correlation was drawn between this observation and the amplitude of ground reaction forces. Some negative energy dissipation was also found, suggesting external intake at the end of the turn cycle. Reid et al. (Reid et al., 2009) observed similar patterns in their study, and also found a relationship between the dissipated energy

and the reduction of the *CoM*'s turn radius, as well as with the fore/aft position. Nevertheless, no cause and effect was concluded. Giant slalom analysis performed by Supej (Supej, 2008) offered the same patterns. Maximum energy dissipation of 31.55 J/Kg*m was measured during the gate crossing, and minimum of -6.63 J/Kg*m during turn transitions, representing generation of energy. He suggested that this negative energy dissipation could be due to a vertical movement of the skier, artificially increasing his centre of mass position. Using their fusion motion capture suit composed of a *GPS* and *IMU*s, Brodie et al. (Brodie et al., 2008; Brodie, 2009) also found positive energy generation at several gates, but no detailed analysis of turn cycles was proposed. The diverging mechanism between *CoM* and feet trajectories mentioned in the previous subchapter was used to explain their results. However, the authors recommended to use the obtained results with caution, as the same mechanism also increased ski-snow friction forces.

## 3.6. Conclusion

This chapter made the inventory of the main results obtained this far in the biomechanics of alpine skiing. It has been seen that a high quantity of studies have been focusing on analysing movements required to perform turns. Different skis, slopes, snow conditions, skier levels and turns techniques have been tested, following the evolution of the technique over time. Nevertheless, only few studies have been focusing on analysing and improving athletes' performance and a question still remains unanswered: Can a skier increase his speed using active movements?

# 4. Aim and Objectives

This chapter introduces the aims of the current research: the motivations and the outline driving the seven studies proposed in this document are presented.

It appears from the previous chapter that performing field tests is very challenging as standard laboratory material is not adapted to external conditions. This is probably also the reason why few scientific researches have been performed on snow sports biomechanics, and even less in alpine skiing kinetics. Therefore, three primary objectives were defined for this work. The first was to develop tools dedicated to *3D* movement analysis and optimized for both outdoor field tests and larges acquisition volumes. The second aim was to identify relevant analysis parameters and to investigate the technique of skiers performing giant slalom turns. The third objective was to propose functional tools for performance analysis. To achieve these goals, intermediate steps have been defined and integrated in the different proposed studies.

As seen in the literature review, the common way to synchronize different measuring devices is to record a specific and recognisable movement such as a jump to allow post processing synchronization. No dedicated and versatile solution existed and it was therefore necessary to develop a new system allowing synchronization of cameras and other measurement devices such as embedded force platforms. The solution is proposed in the first study of this document, describing the design of a wireless synchronization system based on *GPS* technology.

A second gap exposed in the previous chapter is the measurement of intrinsic factors influencing energy dissipation. This reveals the need for accurate methods estimating aerodynamic drag and ski-snow friction of alpine skiers performing turns. The second study proposes an accurate and functional way to model drag area of skiers. The model was used in the third study to estimate the energy dissipated in aerodynamic drag during turns and the total energy balance of skiers performing turns was calculated.

Supej (Supej, 2008) and Reid (Reid et al., 2009) both found negative energy dissipation in their studies of slalom turns, but no evidence of the source of this created energy was given. The energy balance provided by the third study aimed at assessing this phenomenon in giant slalom, and the fourth study's objective was to investigate the possible contribution of muscles to the skier's total energy increase.

Several studies proposed analysis based on *GPS* data. There is however no indication of the influence of the *GPS* antenna placement on the investigated parameters. Placing the antenna on the skier's helmet, in a back pack or on the skis could indeed lead to different results. An estimation of the accuracy obtained using only one point of the skier's body to perform analysis is proposed in the fifth study. This investigation provides information about the reliability of the use of *GPS* or other methods using only one point on the body as a reference. Differences between using the centre of gravity or any other morphological point to estimate potential and kinetic energy of the skier as well as turn radius were analysed.

With the evolution of material and the emergence of carving skis, athletes and coaches have been trying new techniques to find the best strategies during the run. Drifting at the beginning of the turn seems an effective strategy depending on the situation. Nevertheless, no scientific paper has been investigating this technique, perhaps because no functional method exists. Therefore, the aim of the sixth study was to propose a new tool for skidding and trajectory analysis based on *GPS* and inertial sensors measurements.

Finally, a last gap identified in the literature review is the absence of reliable force platforms able to be used by elite skiers without requiring modifications to their usual equipment. As this thesis is the first part of a long term project, aiming at developing a platform dedicated to elite snow sports athletes' analysis, the development of a force platform began with the collaboration of the LCSM at the EPFL. The seventh study presents a first prototype of an adjustable force platform, placed between the ski

shoes and the bindings. Synchronization with other systems such as cameras is possible, allowing for full body kinematics.

*Figure 4-1* shows an overall diagram of the outline of the thesis project.
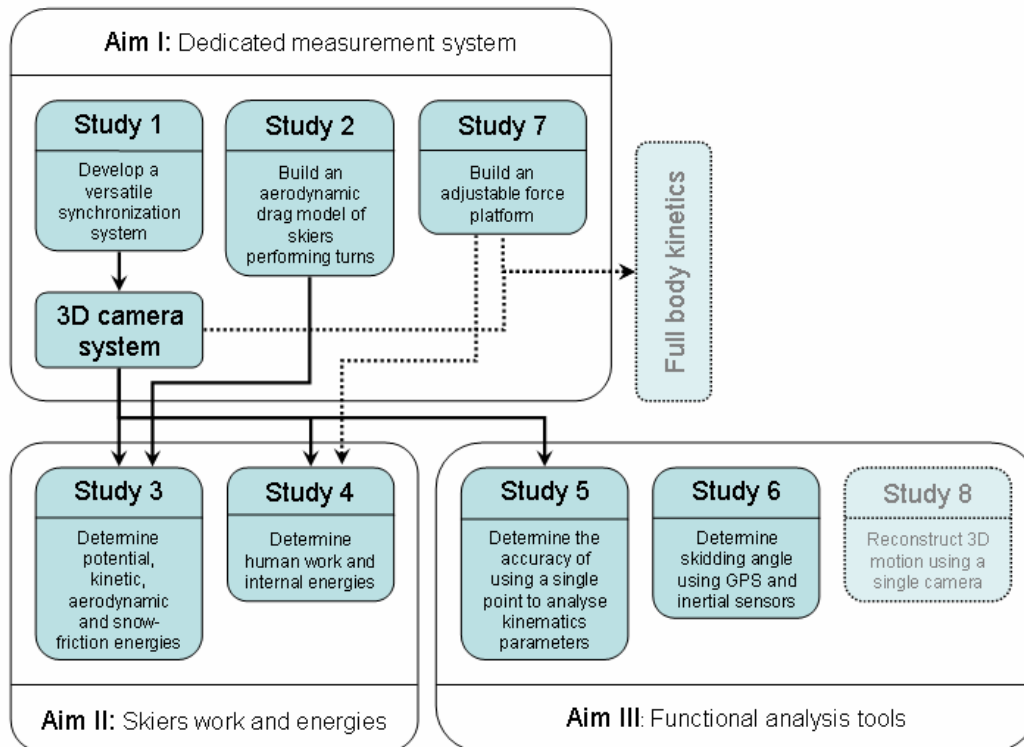


**Figure 4-1:** *Overall aims of the research project and contribution of each study.*

# 5. Study 1:

## Wireless GPS-based phase-locked synchronization system for outdoor environment

Frédéric Meyer[1], Alexander Bahr[2], Thomas Lochmatter[2], Fabio Borrani[3]

[1] Sport Science Institute, Lausanne University, Switzerland

[2] Distributed Intelligent Systems and Algorithms Laboratory, EPFL, Switzerland

[3] Sport and Exercise Science Institute, University of Auckland, New-Zealand

## 5.1. Abstract

Synchronization of data coming from different sources is of high importance in biomechanics to ensure reliable analyses. This synchronization can either be performed through hardware to obtain perfect matching of data, or post-processed digitally. Hardware synchronization can be achieved using trigger cables connecting different devices in many situations; however, this is often impractical, and sometimes impossible in outdoors situations. The aim of this paper is to describe a wireless system for outdoor use, allowing synchronization of different types of – potentially embedded and moving – devices. In this system, each synchronization device is composed of: **i)** a *GPS* receiver (used as time reference), **ii)** a radio transmitter, and **iii)** a microcontroller. These components are used to provide synchronized trigger signals at the desired frequency to the measurement device connected. The synchronization devices communicate wirelessly, are very lightweight, battery-operated and thus very easy to set up. They are adaptable to every measurement device equipped with either trigger input or recording channel. The accuracy of the system was validated using an oscilloscope. The mean synchronization error was found to be 0.39 microseconds and pulses are generated with an accuracy of < 2 µs. The system provides synchronization accuracy about two orders of magnitude better than commonly used post-processing methods, and does not suffer from any drift in trigger generation.

## 5.2. Introduction

Biomechanical studies often deal with multiple measurement devices that are recording data simultaneously. A recurrent difficulty is the synchronization among different devices. Mainly studies have investigated ways to synchronize images acquired by standard, free-running cameras in post-processing. Blievernicht (Blievernicht, 1967) placed rotating objects as visual references in the cameras' field of view, to allow synchronizing images afterwards. Walton (Walton, 1970) placed light-emitting diode (*LED*) clocks. As it is not always possible to place objects in the field of view, Cappozzo et al. (Cappozzo et al., 1983) placed devices pulsating at a known frequency on athletes, and Dapena and Chung (Dapena and Chung, 1988) used events such as foot contact with the ground to match images in post-processing.

A few years later, Yeadon and King (Yeadon and King, 1999) and Pourcelot et Al. (Pourcelot et al., 2000) made use of the direct linear transformation (*DLT*) method (Abdel-Aziz and Karara, 1971), leading to time variations of less than 1 ms between cameras. This method, called software genlock, uses digitized data to determine the phase difference between cameras by minimizing the reconstruction error of moving points. This solution was then improved by Kwon et al. (Kwon et al., 2004) using multiple target points to determine the frequency offset, resulting in a mean error of 0.13 ms.

More recently, Leite de Barros et al. (Leite de Barros et al., 2006) developed a synchronization method using the audio track of a camera. An audio signal is sent via radio frequency to the associated receivers, which are directly connected to the audio input of the cameras. A mean synchronization accuracy of 0.1 ms between cameras, with an additional drift of 0.15 ms/min was achieved with this technology.

Professional broadcasting equipment uses phase-locked (genlocked) systems where the clock of one camera (master) or a trigger generator is used to synchronize other cameras. Products such as the ES-292 GPS/IRIG B video synchronizer (Ese, El Segundo, USA) use GPS

technology to generate inter-range instrumentation group time codes (IRIG B) time stamping of the video frames, allowing only professional cameras synchronization (Pal and NTNC formats). Industrial cameras like the PiA1000-GM (Basler AG, Ahrensburg, Germany) can also be phase-locked using a trigger generator, and offer a wide range of acquisition frequencies (Lochmatter, 2010).

Additionally, the synchronization of embedded measurement devices (e.g. force plates, insole pressure measurement system or accelerometers) is a major issue in field experiments. A method commonly used consists of recording the jump of an athlete at the beginning of an experiment (Stricker et al., 2009); the peak value observed in association to the jump is recorded by the devices, and can be used to synchronize the different recordings, with accuracy depending on the lowest acquisition frequency. The relatively low accuracy of these approaches implicitly limits their reliability.

This paper presents a highly accurate wireless trigger synchronization (*WiTriSync*) system, which can be used outdoors to synchronize industrial cameras as well as other embedded devices.

## 5.3. Methods

### 5.3.1. Design

The *WiTriSync* system consists of multiple identical devices, which are needed to synchronise any connected equipment. Each *WiTriSync* device is composed of three main components (*Figure 5-1*). First, a *GPS* receiver (GPS 18 LVC, Garmin, Olathe, USA) that provides a one-pulse-per-second signal (*PPS*) on a dedicated line. According to the *GPS* specification, the error (*d*) between the *PPS* signal and the international atomic time (*TAI*) is within 1 µs (*Figure 5-2*). Second, a radio transmitter (MRF24J40MB, Microchip, Chandler, USA) that allows the devices to communicate with each other wirelessly. The transmitter operates in the 2.4 GHz band with an output power of 100 mW, allowing for a maximum distance between the devices of about 1 km. Third, a microcontroller

(dsPIC33F, Microchip, Chandler, USA) that generates the desired trigger signals. The *WiTriSync* devices are 120 mm x 90 mm x 60 mm in size, and weight 330 g. Their waterproof enclosure has three connectors: a power connector (8 – 18 V DC), a trigger signal connector, and a multi-purpose connector (for a status *LED*, a start button or a USB port). The latter enables configuring the devices using HyperTerminal in Windows, or Minicom in Mac OS X and/or Linux. All devices in the system can be configured with different frequencies (between 1 Hz and 3500 Hz, in steps of 1 Hz). All the devices are similar, but one must be equipped with a start button (*Figure 5-1*) and is considered as the master.
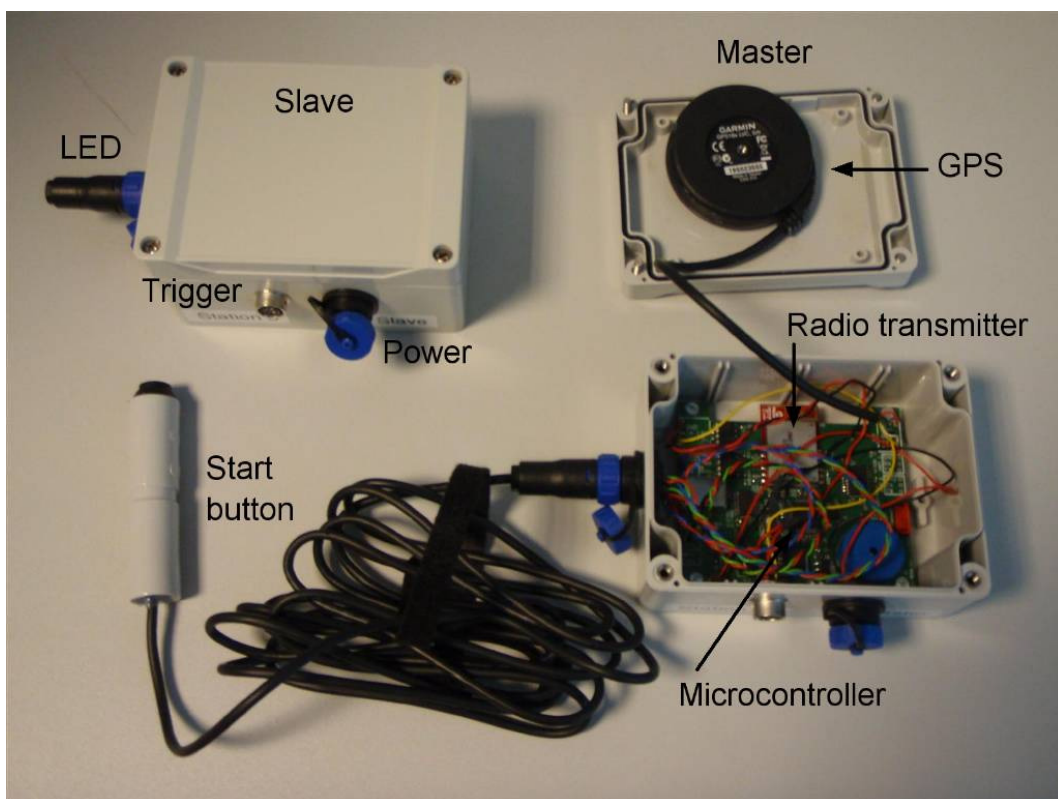


**Figure 5-1:** *A slave and a master device respectively setup with a LED indicator and a start button. The master is opened to show the different components*

When a *WiTriSync* device is powered on, it takes less than one minute for the GPS receivers to acquire (lock) satellites. Once acquisition is completed, the *LED* indicator starts blinking green, and the device is ready to operate. When the start button is pressed, a radio packet containing the

master's internal time status is sent to the other devices (slave). Along with the *PPS* signal from the *GPS* receiver, this time status signal allows all devices to set up and keep a common time base. Once the button is released, the master sends a second radio packet containing a start time phased by about 50 ms ahead to the slaves. This is a safety margin to account for the packet travel time through the radio channel. The devices then start generating the configured trigger sequence at the scheduled time. To keep the devices synchronized over a longer time span and avoid any drift, the frequency generator is realigned at each *PPS* (*Figure 5-2*).
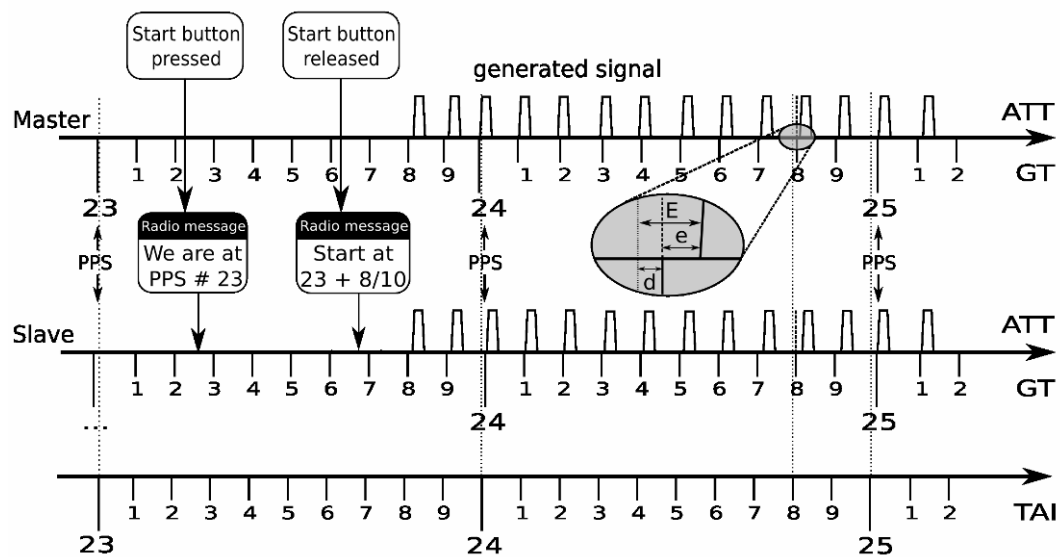


**Figure 5-2:** *System synchronization and trigger signal generation. According to the specifications of the GPS device, the error (d) of each PPS compared to the international atomic time (TAI) is < 1 µs. The error (e) is the difference between the time given by the GPS PPS (GT) and the actual time the trigger occurred (ATT). The absolute theoretical error (E) is the difference between the TAI planned for the trigger and the ATT.*

## 5.3.2. Validation

An oscilloscope (WS24Xs-A, Lecroy, New York, USA) was used to verify the accuracy of the WiTriSync system. Devices triggering at 10, 100, and 1000 Hz were recorded during one second with an acquisition frequency of 5 MHz. Each record therefore contained one of the *GPS PPS*, at which the device was resynchronized. Six trials were recorded for each

frequency. For each trigger signal, the absolute theoretical error ($E$) was defined as the time difference between the *TAI* and the actual time the trigger occurred (*ATT*) and was calculated as follows: $E = d + e$, where e is the difference between the time given by the *GPS PPS* (*GT*) and the *ATT* (*Figure 5-2*). This approach allowed analyzing the error of synchronization compared to the absolute time reference given by the *TAI*, and not only the error between the different *WiTriSync* devices, which would not take in consideration the drift due to frequency error. A two-way ANOVA was performed to estimate differences between devices, differences between frequencies, and any possible interaction between these two factors. The statistical analysis was carried out with SPSS 19 software (SPSS INC, New York, USA). An alpha value of 0.05 was set as the significance level for rejecting the null hypothesis of no difference between error means. All data are expressed as mean and standard deviation (mean ± *SD*).

## 5.4. Results

The mean error e between planned and actual trigger time during the recording second was 0.39 ± 0.19 µs, with a maximal value of 0.95 µs. Adding *d* led to a maximal theoretical error *E* of 1.95 µs. *Table 5-1* presents the errors *e* for the different frequencies and devices.

**Table 5-1:** *Mean synchronization error e ± SD of four boxes triggering at 10, 100 and 1000 Hz.*

| Error e (µs) | | | |
|---|---|---|---|
| | 10 Hz | 100 Hz | 1000 Hz |
| Device 1 | 0.36 ± 0.23 | 0.37 ± 0.19 | 0.42 ± 0.19 |
| Device 2 | 0.31 ± 0.22 | 0.34 ± 0.19 | 0.40 ± 0.20 |
| Device 3 | 0.36 ± 0.24 | 0.35 ± 0.20 | 0.37 ± 0.18 |
| Device 4 | 0.39 ± 0.21 | 0.32 ± 0.20 | 0.39 ± 0.18 |

No significant differences were found for mean error between devices ($p = 0.67$), and mean error between frequencies ($p = 0.18$). Furthermore, no significant interaction was found between the two factors ($p = 0.87$).

## 5.5. Discussion

The *WiTriSync* system presented here is both more accurate and more adaptable to a variety of experimental conditions than most other available solutions, as it can be used with a wide range of devices, not only cameras. As the system operates wirelessly, the devices needing synchronization can be embedded and moving during the recording. The accuracy recorded was two orders of magnitude better than the accuracy that can be achieved through the software method used by Kwon (Kwon et al., 2004), or through the audio band method proposed by Leite de Barros (Leite de Barros et al., 2006). Furthermore, unlike systems that depend on an internal crystal clock (e.g. Software genlock, Audio band and Cable genlock), the *WiTriSync* system doesn't have any long term frequency drift as the internal time of each device is realigned by the *GPS PPS* each second. Finally, the system did not require any sophisticated and time-consuming post-processing operations to recover synchronization of data. A synthesis of the main features of different commonly used synchronization systems is presented in *Table 5-2*.

*Table 5-2: Performance comparison for systems currently available.*

|  | Accuracy | Drift | Moving Device | Other than cameras | Post processing | Indoor use |
|---|---|---|---|---|---|---|
| WiTriSync system | 0.39 µs | No | Yes | Yes | No | No |
| Software genlock | 130.00 µs | Yes | Yes | No | Yes | Yes |
| Audio band | 100.00 µs | Yes | Yes | No | Yes | Yes |
| GPS/IRIG B | 70.00 µs | No | Yes | No | No | No |
| Cable genlock | <0.10 µs | Yes | No | Yes | No | Yes |

The design and construction of the *WiTriSync* devices is very robust, and this feature can have contributed to the lack of differences in the errors between devices, and between frequencies considered. Nevertheless, a limitation of the *WiTriSync* system is the suitability for outdoor use only. Indoors, unless close to windows, the *GPS* fails to acquire satellites, and would therefore be unable to provide the *PPS* signal.

The *WiTriSync* devices can be used with measurement devices managing the acquisition by themselves, but allowing for an external trigger to begin the recording. In this case, the *WiTriSync* device must be configured to send only one trigger signal. The *WiTriSync* devices can also be used with any kind of measurement device that offer a free recording channel. The trigger sequence generated by the *WiTriSync* device can be recorded on the free channel, and the synchronization post processed with accuracy depending on the measurement device's acquisition frequency.

# 6. Study 2:

## Aerodynamic drag modelling of alpine skiers performing giant slalom turns

Frédéric Meyer[1], David Le Pelley[2], Fabio Borrani[3]

[1] Sport Science Institute, University of Lausanne, Switzerland

[2] Mechanical Engineering Dept, University of Auckland, New Zealand

[3] Sport and Exercise Science Department, University of Auckland, New Zealand

## 6.1. Abstract

Purpose: Aerodynamic drag plays an important role in performance for athletes practicing sports that involve high velocity motions. In giant slalom, the skier is continuously changing his body posture and this affects the energy dissipated in aerodynamic drag. It is therefore important to quantify this energy to understand the dynamic behaviour of the skier. The aims of this study were to model the aerodynamic drag of alpine skiers in giant slalom simulated conditions, and to apply these models in a field experiment to estimate energy dissipated through aerodynamic drag. Methods: The aerodynamic characteristics of 15 recreational male and female skiers were measured in a wind tunnel while holding nine different skiing-specific postures. The drag and the frontal area were recorded simultaneously for each posture. Four generalised and two individualized models of the drag coefficient were built, using different sets of parameters. These models were subsequently applied in a field study designed to compare the aerodynamic energy losses between a dynamic and a compact skiing technique. Results: The generalized models estimated aerodynamic drag with an accuracy of between 11.00% and 14.28%, and the individualized models with an accuracy of between 4.52% and 5.30%. The individualized model used for the field study showed that using a dynamic technique lead to 10 % more aerodynamic drag energy loss than using a compact technique. Discussion: The individualized models were capable of discriminating different techniques performed by advanced skiers, and appeared more accurate than the generalized models. The models presented here offer a simple yet accurate method to estimate the aerodynamic drag acting upon alpine skiers while rapidly moving through the range of positions typical to turning technique.

## 6.2. Purpose

Athletes performing disciplines like running, speed skating, cycling or cross-country skiing have always been interested in optimizing their aerodynamic drag to increase speed and achieve better performance (Shanebrook and Jaszczak, 1976; van Ingen Schenau, 1982; Spring et al., 1988; Lopez et al., 2008). In alpine skiing, the gravitational force is used to increase the skier's kinetic energy, whereas the aerodynamic drag is one of the two non-conservative forces doing negative work on the skier. Quantifying this parameter is therefore important to understand skier performance.

A number of studies have examined skier aerodynamic drag. Watanabe and Ohtsuki analyzed the aerodynamic drag of a variety of skiing postures in a wind tunnel study (Watanabe and Ohtsuki, 1977), and skiing velocity in a field study (Watanabe and Ohtsuki, 1978). Later, Kaps et al. (Kaps et al., 1996) proposed a method to calculate snow friction and drag area during straight downhill skiing using photocells. Theoretical drag analysis has been conducted by Savolainen (Savolainen, 1989) to compare different skiers' posture, and determine factors limiting speed. Performance coefficients taking into account factors like mass, frontal area, and drag coefficient have been developed with wind tunnel tests by Luethi and Denoth (Luethi and Denoth, 1987). Thompson and Friess (Thompson et al., 2001) performed wind tunnel tests to improve the aerodynamic efficiency of speed-skiers by optimizing their posture and equipment.

While these studies have made valuable contributions toward our understanding of the aerodynamic properties of static skiing postures, they are limited in that alpine skiing is primarily a dynamic sport where the skier continually moves and changes positioning. To allow the drag analysis of skiers performing turns, Barelle et al. (Barelle et al., 2004) modelled the drag coefficient based on athlete segments lengths, and inter-segmental angles, thereby allowing the determination of aerodynamic properties through a complete span of positions typically encountered in skiing.

However, the segment lengths and inter-segmental angles required to use this model are often difficult to obtain in field research settings.

Despite these previous studies looking at the aerodynamic properties of alpine skiers, the importance of air drag toward performance in this dynamic sport is poorly understood. Mechanical energy (i.e. the sum of kinetic and potential energy) was used by Supej (Supej, 2008) to deduce dissipated energy during turns. Reid et al. (Reid et al., 2009) used the same method in slalom, but the intrinsic factors influencing this energy dissipation have not yet been analysed.

Therefore, the first aim of this study was to develop models of the aerodynamic drag coefficient of alpine skiers performing turns. The models should be able to take into account the skier's postural changes, using parameters that can be measured in the field. Furthermore, the second purpose of this study was to use the developed models to analyse the energy dissipated by the aerodynamic drag of a skier using either a dynamic technique, where the skier exposes a relatively large frontal area to the wind, or a compact technique, where the skier maintains an aerodynamic position, while performing giant slalom turns on a ski slope.

## 6.3. Methods

### 6.3.1. Wind tunnel experiment

#### 6.3.1.1. Participants

Fifteen recreational male and female skiers (mean $\pm$ *SD*; body mass 75.9 $\pm$ 9.7 Kg, height 1.79 $\pm$ 0.07 m, age 32.3 $\pm$ 6.7 year) volunteered for the study. All participants were healthy, without any joint motion problems. Written informed consent was obtained from each participant prior to participation in the study, which was approved by the University of Auckland Human Participants Ethics Committee.

#### 6.3.1.2. Wind tunnel setup

Testing was carried out at the University of Auckland in a wind tunnel with an open jet configuration, the jet having dimensions of 2.5 m (width) by 3.5

m (height), and a maximum flow speed of 18 m/s. Turbulence levels were approximately 0.5 % in the flow direction, and the velocity profile was uniform.

Participants were positioned on a force platform capable of measuring drag in the longitudinal wind direction. The drag force ($D$) was calculated through measurement of the displacement of a distorting force block, by using a Linear Variable Displacement Transducer (*LVDT*, RDP Ltd, Heath Town, UK). A 16-bit A/D converter (NI-6034, National Instruments, Austin, USA) was used to acquire the signal on a PC at a frequency of 200 Hz. The *LVDT* was previously calibrated over a suitable range of loads. This transducer exhibits a high degree of linearity and repeatability, with an accuracy of approximately 1 % of the measured reading, and a repeatability of 0.5 % (Flay and Vuletich, 1995). In accordance with Sayers (Sayers and Ball, 1983), no flow corrections were required in the open circuit tunnels, as the blockage model (in our case the person) was less than 1 m$^2$ and the open area 12.25 m$^2$.

The dynamic wind pressure was recorded with a Setra pressure transducer via a pitot-static probe (Airflow Developments Ltd, High Wycombe, UK) positioned in the wind tunnel, upstream of the contracted section. Prior to the experiment, a second probe was positioned in the middle of the testing volume to determine the ratio of dynamic pressure between the two locations. The measured pressure at run time was then adjusted accordingly. The accuracy of the dynamic pressure is approximately 2 % of the measured value with a repeatability of approximately 0.2 %. Dynamic pressure, air temperature and atmospheric pressure were recorded to enable the drag to be correctly non-dimensionalised.

A limitation with many wind tunnel systems is the inability to measure the frontal area ($A_F$) of an irregular, moving object. This only allows the drag area $C_DA$ to be calculated, which is of limited use in many subsequent calculations. To enable a true drag coefficient $C_D$ to be calculated, a real-time $A_F$ measurement system was developed. This consisted of a miniature camera (USB UI-1485LE, IDS Imaging, Obersulm, Germany)

positioned in the wind tunnel upstream of the participant. The background was coloured white and the area covered by each pixel was calculated by measuring the size of a reference object positioned at the average plane of the participant. During the test, the participant was dressed in a black suit, which served both to provide a contrast for the photography and to provide clothing uniformity for the drag measurements. A 50 % threshold was carried out on the greyscale image of the participant, generating a black and white picture. The total number of black pixels against the white background were then counted and converted into a true area in square meters which was displayed to the subject every 0.5 s. The accuracy of this system was approximately 0.001 m$^2$. The black and white images were also used to determine the skiers' height ($H$) and width ($W$) by counting the number of black pixels across the maximal horizontal and vertical distance between two anatomical reference points on the frontal plane.

### 6.3.1.3. Experimental procedure

Prior to the test, each participant's upright height ($UpH$) and mass ($M$) were measured respectively in meters and kilograms, and the corresponding body surface area ($BodyS$) which represents the total area of the skin, was calculated using Boyd's method (Boyd, 1935):

$$BodyS = 0.007184 \cdot (100 \cdot UpH)^{0.725} \cdot M^{0.425}$$

**Eq. 6.1**

To account for any weight-induced readings, the force transducer was zeroed with the participant on the balance under windless conditions at the start of each trial. The maximal frontal area ($MaxA$) of each participant (standing upright with the arms outstretched) was measured at the same time through the miniature camera. The wind tunnel was then run up to a speed of about 16 m/s, corresponding to typical gate entry speeds in giant slalom conditions, and therefore the Reynolds number was approximately the same as it would be experienced by the participants in the field.
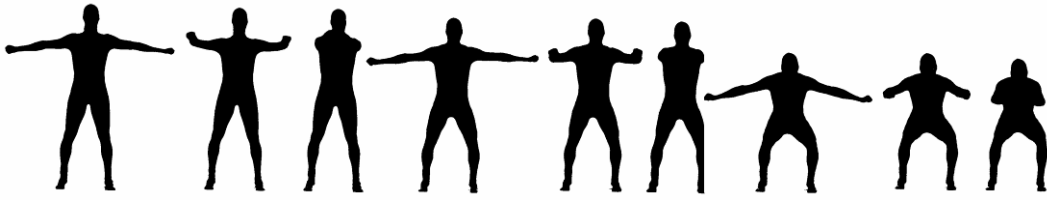
**Figure 6-1:** *The 9 tested skier positions as viewed by the frontal camera.*

After a settling period, the participants assumed nine postures, varying leg flexion and arm spacing (*Figure 6-1*). A red/green light switch was set up in front of the participants to let them know when they had to change posture. Each posture was repeated three times and held for 15 s over which $D$ and $A_F$ were measured and averaged.

The $C_D$ was calculated in the standard manner by:

$$C_D = \frac{2 \cdot D}{\rho \cdot V^2 \cdot A_F}$$

<div align="right">**Eq. 6.2**</div>

where ρ is the air density, and V is the wind speed. The dynamic pressure (½ $\rho$ $V^2$), was measured with the Setra pressure transducer, $A_F$ was measured with the miniature camera, and $D$ was measured with the force balance.

### 6.3.1.4. Models Construction

When conducting field tests, a participant's anthropometric data may not always be available (as in competition settings) while other information may be difficult to obtain (such as AF which can only be obtained from full frontal pictures). Therefore, models based on different combinations of parameters (2 to 7) were built to accommodate the information typically available in alpine field test conditions

Based on the possible sets of available data, six models were built: four generalized models using all participants' data, as well as two individualized models for each participant. *Table 6-1* summarizes the parameters that were used in each of the six models.

**Table 6-1:** *An overview of the parameters included in the six tested models.*

| CDA model | UpH | M | MaxA | BodyS | AF | H | W |
|---|---|---|---|---|---|---|---|
| GM1 | √ | √ | √ | √ | √ | √ | √ |
| GM2 |  |  |  |  | √ | √ | √ |
| GM3 | √ | √ | √ | √ |  | √ | √ |
| GM4 |  |  |  |  |  | √ | √ |
| IM1 |  |  |  |  | √ | √ | √ |
| IM2 |  |  |  |  |  | √ | √ |

Anthropomorphic parameters are inherent to an individual and do not vary with the position of the skier. They are therefore not relevant to build individualized models. However, the use of these parameters can improve the accuracy of the generalized models.

## 6.3.2. Field experiment

The field experiment was carried out on an indoor ski slope. One of the 15 participants volunteered to perform two giant slalom runs in a white suit dotted with black hemispherical markers. He was asked to execute ample active movements on the first run and to remain more compact on the second run. A total of six gates were set up with a linear gate distance of 24 m, and a lateral offset of 9 m. The first three gates were used to initiate the rhythm, and the last three were recorded. The slope angle was approximately 8 to 10 degrees. To record the skier's position during the turn, six piA1000-48gm cameras with 1004 * 1004 pixels resolution and running at 48 Hz (Basler AG, Ahrensburg, Germany) were placed around the slope, three on each side. The orientations of the two top and two bottom cameras were fixed. The two cameras in the middle were mounted onto specially built tripod heads that allowed operators to pan and tilt the cameras while maintaining camera sensor positions. Prior to the test, four

calibration poles with three markers each were set up around the centre of the capture volume and recorded with the cameras. Each calibration marker, reference point and camera position was measured with a reflectorless total station (Sokkia Set530R, Sokkia Topcon, Kanagawa, Japan). Each camera was connected by Gigabit Ethernet to its own laptop, a battery pack and a custom synchronization unit. The synchronization unit sent signals with the desired frequency to each camera, triggering the cameras to save images to the RAM memory of their associated laptops using a dedicated software (Swistrack, Lausanne, Switzerland). When the synchronization unit was switched off or when the RAM memory was full, all the images were transferred to the hard drive.

Sequences provided by the multiple cameras system, and *3D* positions of the points given by the total station were processed using SIMI motion software (SIMI Reality Motion Systems GmbH, Unterschleissheim, Germany). The calibration markers were first used to determine the 11 standard parameters of the Direct Linear Transformation calibration method (Abdel-Aziz and Karara, 1971). Reference points were affixed to the side of the ski hall to allow for the cameras' panning and tilting angles to be determined during the tests. The *3D* reconstruction accuracy was controlled by comparing the gate position given by the total station with the position calculated with the software for the three visible gates on the two runs. The centre of mass (*CoM*) of the skier was calculated using Hanavan method (Hanavan, 1964). Position trajectories of the head, feet and arms were exported to calculate the skier's *H* and *W*. As the anthropomorphic data were available but the $A_F$ was not, the *GM3* and *IM2* models were both used to determine the evolution of the aerodynamic drag coefficient over the turn cycle for the purpose of comparison. The energy losses due to aerodynamic friction (*ΔEaero*) were calculated at each step of the turn as follows:

$$\Delta Eaero \ = \ D \cdot \Delta dist$$

**Eq. 6.3**

where *Δdist* was the distance travelled by the skier's *CoM* and *D* was determined by rearanging *Equation 6.2* to give:

$$D = \frac{1}{2} \cdot C_D A \cdot \rho_{air} \cdot \left( V_{Skier} + V_{wind} \right)^2$$

**Eq. 6.4**

where *Vskier* is the speed of the skier's *CoM* and *Vwind* is the component of the wind speed, in the direction of the skier's speed. *GM3* and *IM2* were used to give an estimate of the $C_D A$, and combining *Equations 6.3* and *6.4* gives the dissipated aerodynamic energy during a *Δt* interval (*Δdist* is replaced by *Vskier * Δt*):

$$\Delta Eaero = \frac{1}{2} \cdot C_D A \cdot \rho_{air} \cdot \left( V_{Skier} + V_{wind} \right)^2 \cdot V_{Skier} \cdot \Delta t$$

**Eq. 6.5**

Since tests were performed in a ski hall, wind speed can be neglected in this study. However, it is an important parameter and must be considered during outdoor experiments. For a whole turn, the total aerodynamic drag energy dissipated is obtained by summing the previous equation between $t_0$, the beginning of the turn and $t_{end}$, the end of the turn:

$$Eaero = \sum_{t_0}^{t_{end}} \frac{1}{2} \cdot C_D A \cdot \rho_{air} \cdot V_{Skier}^3 \cdot \Delta t$$

**Eq. 6.6**

### 6.3.3. Statistical analysis

A Backward Stepwise Linear Regression was used to find the best predictive parameters of the models. Cut-off value for parameter acceptance was stated at $p <= 0.1$. Coefficient of determination ($R^2$), and the standard deviation of the estimate (*SD*) of the models was calculated.

The validation of the generalized models was performed by removing one participant from the dataset, recalculating the model coefficients with the remaining 14 participants, and then using the removed participant to compare the model prediction with an independent measure. A rotation through all 15 participants was performed and the mean error was used to describe the model accuracy. The individualized models were validated in the same way, by removing the result of one posture from the dataset, recalculating the model with the remaining eight postures and applying the models to the removed posture.

Bland-Altman plots (Bland and Altman, 1986) were used to compare the agreement between the generalized models and the experimental data. For the generalized and the individualized models, the 95 % limit of agreement ($\pm$ 1.96 * $SD$), was calculated. All the statistical analyses were performed with SPSS 16 software (SPSS INC, New York, USA), and significance was accepted at $P < 0.05$.

## 6.4. Results

### 6.4.1. Wind tunnel experiment

#### 6.4.1.1. Developed models

*Table 6.2* shows the multiplication coefficient of each parameter, as well as the coefficient of determination $R^2$, the standard deviation of the estimate ($SD$), and the significance of each model ($P$) developed to estimate the $C_DA$. The 0.1 cut off of parameter acceptance discarded *M*, *MaxA*, and *BodyS* from *GM1*, as well as *M*, and *MaxA* from *GM3*.

*GM1* offered the best accuracy with $R^2 = 0.972$, $p < 0.001$, and a standard deviation of the estimate $SD = 0.016$ m$^2$. For *GM2* and *GM3*, the coefficient of determination was $R^2 = 0.962$ ($SD = 0.019$ m2; $P < 0.001$) and $R^2 = 0.953$ ($SD = 0.021$ m2; $p < 0.001$), respectively. Finally, *GM4* represented the worst model with a coefficient of determination equal to $R^2 = 0.933$ ($SD = 0.025$ m2; $P < 0.001$).

**Table 6-2:** *Coefficients for the generalized models' parameters and accuracies of the models*

| CDA model | Cste | UpH [m] | M [kg] | MaxA [m2] | BodyS [m2] | $A_F$ [m2] | H [m] | W [m] | $R^2$ | SD [m2] | P |
|---|---|---|---|---|---|---|---|---|---|---|---|
| GM1 | 0.046 | -0.155 | \ | \ | \ | 0.649 | 0.181 | 0.039 | 0.972 | 0.016 | <0.001 |
| GM2 | -0.215 | | | | | 0.573 | 0.187 | 0.045 | 0.962 | 0.019 | <0.001 |
| GM3 | 0.121 | -0.373 | \ | \ | 0.156 | | 0.337 | 0.090 | 0.953 | 0.021 | <0.001 |
| GM4 | -0.248 | | | | | | 0.337 | 0.091 | 0.933 | 0.025 | <0.001 |

Bland-Altman plots between the generalized models and the experimental data are shown in *Figure 6-2* for all the generalised models. The 95 % limit of agreement is also reported for *GM1* (± 11.00), *GM2* (± 11.99), *GM3* (± 13.25), and *GM4* (± 14.18) respectively in *Figure 6-2A, B, C,* and *D*, respectively.
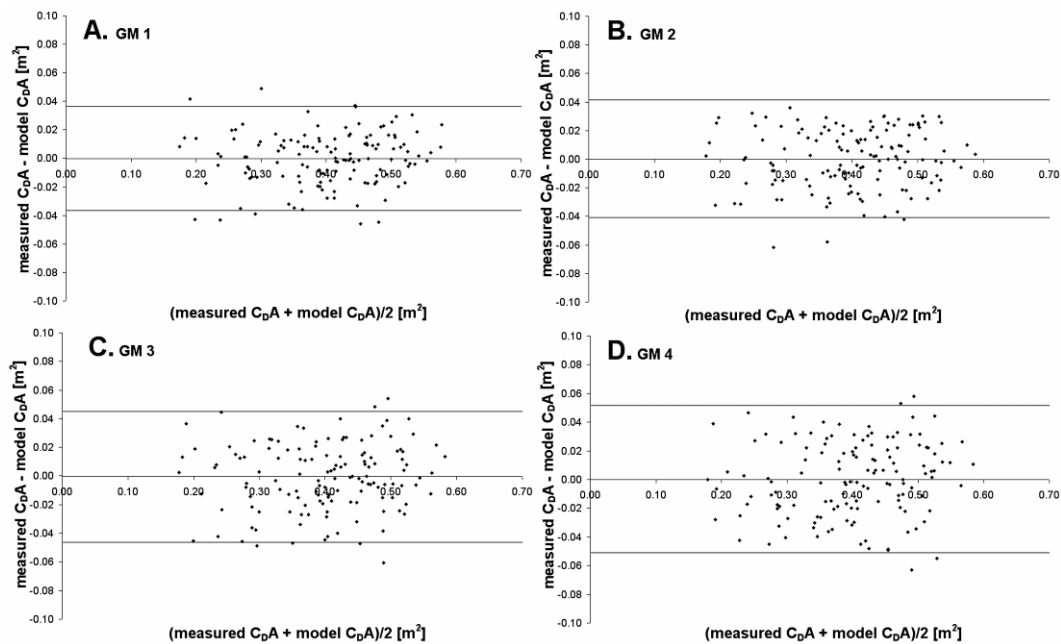
**Figure 6-2:** *Comparison of measured and calculated $C_DA$ with Bland-Altman plots for the four generalized models. Solid horizontal lines represent the 95% limits of agreement.*

For the individualized models, the backward linear regression did not remove any parameters. *IM1* reached an average coefficient of determination $R^2 = 0.995$ and a standard deviation of the estimate $SD = 0.009$ m$^2$. Validation between the models and the measures gave a 95 % limit of agreement of $\pm$ 4.52 %. *IM2* showed slightly worse results with $R^2 = 0.989$ $SD = 0.01$ m$^2$ and a 95 % limit of agreement of $\pm$ 5.30 %.

### 6.4.2. Field experiment:

To estimate his $C_DA$, the following *IM2* was individually developed for the skier who performed the field test:

$$C_D A = 0.349 \cdot H + 0.068 \cdot W - 0,272$$

**Eq. 6.7**

*Figure 6-3A* compares the evolution of $C_DA$ over a turn cycle, using the *IM2* defined in *Equation 6.7*, for the active and compact techniques. The limit of agreement of 5.30 % given for the *IM2* is also plotted for each technique, showing a possible differentiation between the dynamic and the compact skiing technique for 56 % of the turn. The darker grey area indicates an overlapping of the two techniques' limit of agreement.

*Figure 6-3B* shows the comparison of the same data set, but using *GM3*. The limit of agreement of 13.25 % is also plotted for each technique, showing an overlapping of the two techniques during the whole turn.
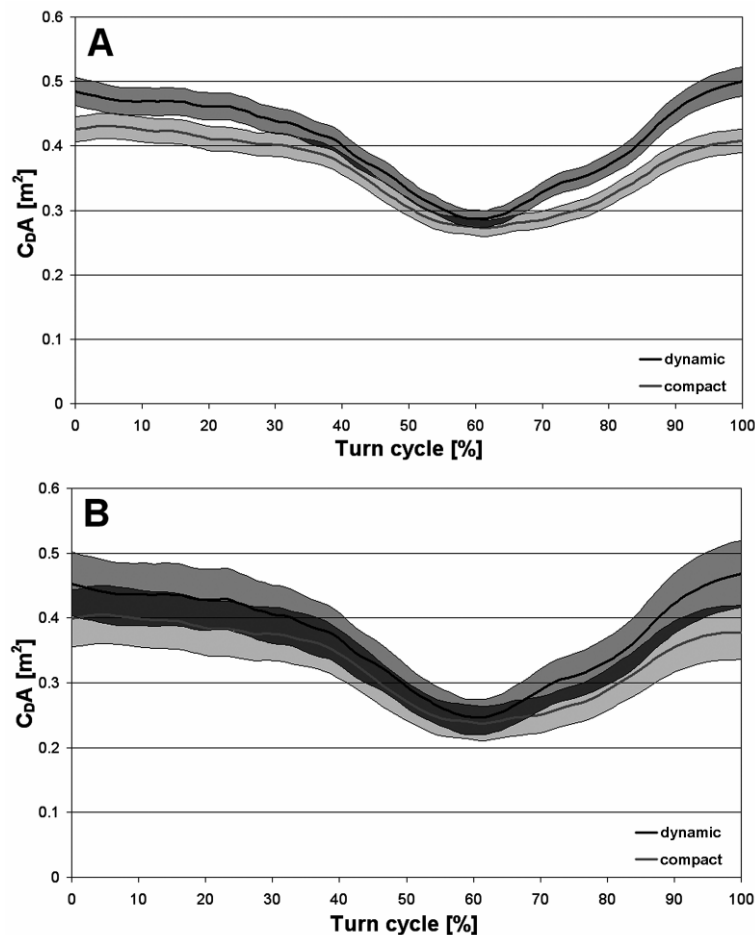


**Figure 6-3:** *Drag area ($C_D A$) for both the compact and dynamic techniques using the second individualized model (**A**) and the third generalized model (**B**).*

*Equation 6.5* gives the total energy dissipated due to the aerodynamic drag and is illustrated in *Figure 6-4* using either the *IM2* (*Figure 6-4A*), or *GM3* (*Figure 6-4B*) for one turn performed with the two different techniques. The 95 % limit of agreement is also reported, showing the disparity of energy dissipation. For the current giant slalom, an active technique gives around 3500 J of energy dissipated during one gate. This represents around 350 J more energy dissipation in one turn than a compact position, which means a loss of 10 % more energy during the whole run.

86
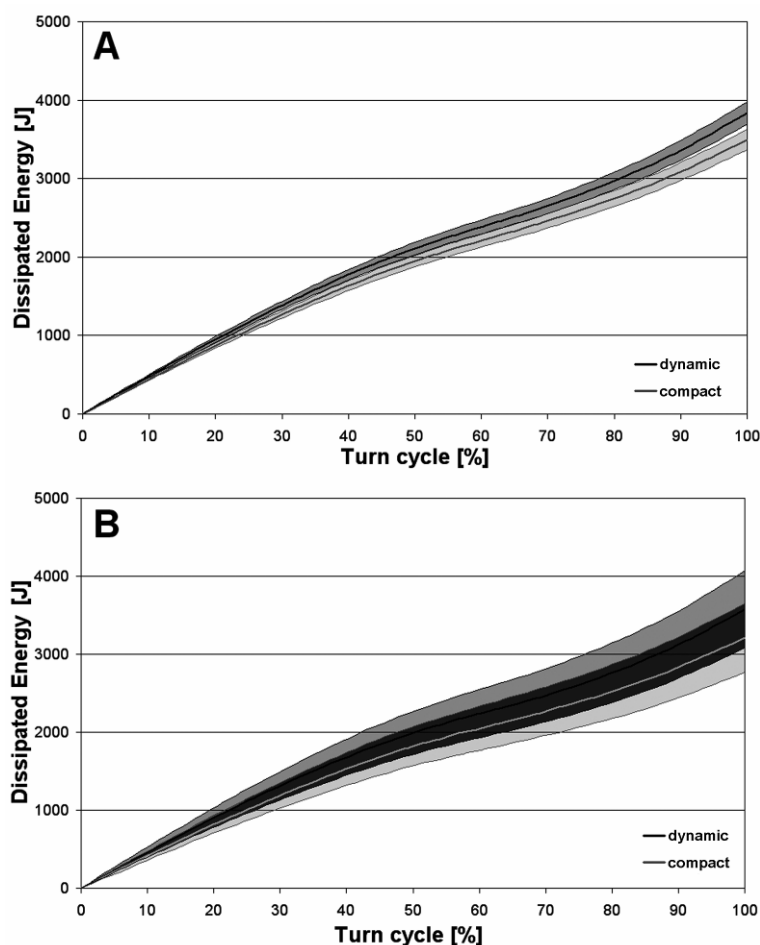
**Figure 6-4:** *Evolution of the energy dissipated due to aerodynamic drag for both the compact and dynamic techniques using the second individualized model (**A**) and the third generalized model (**B**).*

## 6.5. Discussion

The most important finding of this study is the accuracy of the individualized models, which allow for very good estimation of skier aerodynamic properties while performing giant slalom turns. Indeed, these models, which explain 98.9 % and 99.5 % of the experimental data, have accuracy better than 5.30 % to determine the skier's aerodynamic drag coefficient. The accuracy obtained is good enough for discrimination of different techniques performed by advanced skiers, as seen in *Figure 6-3A*.

The generalized models developed are a little less accurate, explaining between 93.3 % and 97.2 % of the experimental data, corresponding to

11.00 % and 14.18 % error for the 95 % limit of agreement. Using anthropomorphic data to build the generalized models led to an improvement of only 2 %. Therefore, the accuracy differences of about 8 % between generalized and individualized models should be due to other factors not measured in this study such as differences in individual body posture held in the wind tunnel.

Similar to the Barelle et al. (2) model, the generalized models developed in this investigation allow a global intra-individual comparison of a skier performing different techniques, but not accurate differentiation between skiers. However, the parameters used in this study are less specific than the segment lengths and angles used by Barelle et al. (2), and offer a wider and more generic use of the models. This allows the backward linear regression method to choose the relevant parameters and refuse parameters that are not necessary for the model. More flexibility is therefore possible for further parameter integration. Barelle et al. (Barelle et al., 2004) considered many more positions to allow the variation of the different parameters, but finally the drag coefficient found in both studies corresponds very well for the different positions a skier can reach during a run.

The developed models help to understand intrinsic factors of energy dissipation as calculated by Supej (Supej, 2008) and Reid (Reid et al., 2009). They both found high energy dissipation around the gate crossing and low energy dissipation during gate transition, which is inverted compared to the curves of *Eaero* in *Figure 6-4*. The energy dissipation due to snow friction, estimated by Meyer (Meyer and Borrani, 2010), indicates a higher importance of the ski-snow friction in giant slalom and curves corresponding to the results obtained by Supej (Supej, 2008) and Reid (Reid et al., 2009).

The study undertaken here is a first approximation of the skier's aerodynamic drag, which is correct in the field in the case of little or no ambient wind speed. In this case, the wind flow onto the skier will always be head-on, regardless of his/her direction of travel (no yaw angle). If there is a substantial wind speed, the aerodynamic drag experienced by

the skier will change depending on his/her direction of travel (yaw angle different from zero). To model this scenario, further tests would have to be conducted at a range of skier's yaw angles in the wind tunnel. Then a new dynamic model could calculate the skier's aerodynamic drag considering wind speed and relative direction, and the skier's yaw angle at each point of the turn. In contrast, for small yaw angles the current model serves as a good estimation of the aerodynamic drag.

One limitation of the current method is that the various postures in the wind tunnel used to develop the models (*Figure 6-1*) are symmetric, and differ from asymmetric skier positions achieved when turning, a fact which may jeopardize the model validity. Unfortunately, the repeatability of holding more turn-specific postures in the wind tunnel was poor due to the difficulty of holding unbalanced positions. A second limitation is that the models reported here use the wind tunnel measurements of a series of static positions to model skiers who change their position continuously while turning. It may be that the dynamic behaviour of the aerodynamic drag of a skier in continuous movement may somehow differ from that of a set of static positions. However, wind tunnel measurements are currently limited to static positions as the ground force platform would record each CoM acceleration, making it difficult to isolate the aerodynamic drag force.

In conclusion, this paper provides simple and functional models to calculate the aerodynamic drag of alpine skiers performing giant slalom turns. The developed models offer a mean accuracy between 4.52 % and 14.18 %, depending on the selected parameters. Using these models in skiing field studies may help to improve our understanding of the role of aerodynamic drag in skier performance. A functional model of ski-snow friction while performing turns still needs to be developed to have a full overview of where, how and when athletes lose energy during turns.

# 7. Study 3:

## 3D model reconstruction and analysis of athletes performing giant slalom

Frédéric Meyer, Fabio Borrani*

Institut des Science du sport, Lausanne University, Switzerland

* Sport and Exercice Science Institute, University of Auckland, New-Zealand

## 7.1. Introduction

Nowadays, giant slalom races are won by hundredths of a second. Difference between the athletes on the podium is generally less than 0.5 s, which represents less than 0.5% in time difference on a 2 min race. Very small details make the difference and it is important to understand where, when and how the top athletes make the difference. Approaches involving energy balance have been widely used to describe human locomotion such as walking (Cavagna et al., 1963; Willems et al., 1995), running (Belli et al., 1993; Kyröläinen et al., 2001) or cycling (Fregly and Zajac, 1996). In alpine skiing, if energy principles in Slalom have already been explored (Supej et al., 2005b; Supej, 2008; Reid et al., 2009), intrinsic factors affecting energy dissipation have never been analyzed. Due to larger acquisition volumes, giant slalom biomechanics have also never been explored. Nevertheless, there is a high demand from trainers and athletes to have access to news tools allowing for a better understanding of the giant slalom technique and its underlying mechanisms. Therefore, the aim of this paper is to propose a method allowing for the decomposition of the different factors affecting energy balance of highly skilled ski racers performing turns. Potential energy, kinetic energy, energy dissipation due to aerodynamic drag and ski-snow friction are separately calculated and summed to determine the athlete's ability to absorb, restitute or create energy.

## 7.2. Methods

### 7.2.1. Participants

Seven European Cup and FIS racers (mean ± *SD*: body mass 98.8 ± 9.1 Kg; height 1.82 m ± 0.07; Giant Slalom (*GS*) FIS points 26.45 ±14.58) participated in the study. All participants were healthy males without any joint motion problems. The study was conducted according to the 1964 declaration of Helsinki and all participants signed an informed consent form before beginning the test.

## 7.2.2. Experimental design

Participants had to wear a white racing suit equipped with 14 black markers, a black helmet and black gloves also used as markers, and ski poles with black markers at their centre of mass. In total, 19 markers were identified (*Figure 7-1B*). The athletes had to perform 3 trials of a giant slalom run, setup with gates distant of 24 m from each other, and a 9 m horizontal distance. For 6 consecutive gates, the slope was at a 20 to 22 degrees angle.

The runs were recorded and the time needed to go through 3 reference gates was estimated by counting the number of images captured on video. The fastest run of each skier was then analysed. The selected runs were processed with SIMI motion software (SIMI motion, SIMI, Germany), using the panning and tilting modules. The camera's internal (e.g., focal length, image format and principal point) and external (e.g., camera position and orientation) parameters needed for the analysis were determined using the DLT 11 calibration method (Hatze, 1988), using the position of the markers captured on video frames as reference points. The overall accuracy for the position of the markers' *3D* reconstruction was ±2 cm (Meyer et al., 2010b).
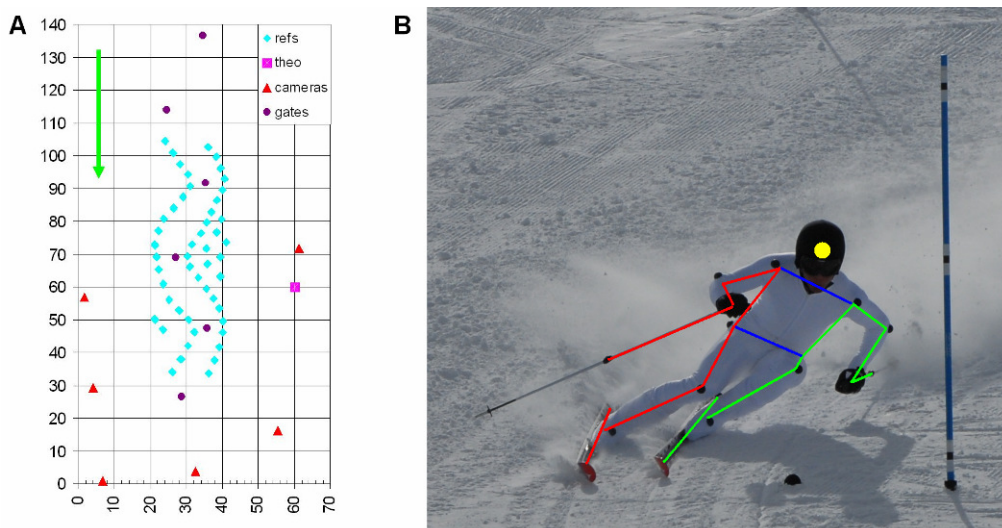


***Figure 7-1 A:*** *Slope setup,* ***B:*** *skier suit, markers and body segments*

*3D* models composed of 14 segments (*Figure 7-1B*) were built and the skiers' centre of mass were calculated using Hanavan model (Hanavan, 1964) modified to take the material's weight into account.

## 7.2.3. Measurements

Six panning and tilting cameras, 1004*1004 pixels resolution, 48 Hz (PiA1000, Basler, Switzerland) were positioned around a giant slalom run, about 35 meters from the center of the zone of acquisition (i.e., video captured). Each camera was mounted on a special tripod head, especially built to always keep the centre of the camera sensor in the same position even as the camera is panned or tilted to track the skier. Reference markers mounted on poles were positioned around the run to act as calibration and reference points for the panning and tilting reconstruction. The capture volume was around 60 * 20 * 2 meters (*Figure 7-1A*). The positions of each reference marker, each gate and each camera were measured with a reflectorless total station (theodolite + laser range finder, LQTS-522D, Longqiang, China). The cameras' positions were calculated as the median of two points on either side of the tilting axis of the camera. Each camera was connected with Gigabit Ethernet to a dedicated laptop which directly recorded the frames in the Random Access Memory (*RAM*) memory of the computer, using a software developed for this specific purpose (Swistrack, Thomas Lochmatter, Switzerland). Cameras were also connected to battery packs and dedicated synchronization boxes (Meyer et al., 2010b). Theses boxes achieve wireless synchronization of the cameras recording system and ensure images from the 6 cameras are taken simultaneously with error below 4 μs.

## 7.2.4. Parameters analysis

Following the law of conservation of energy, the total energy of a skier should remain constant during a run. The total energy (*Etot*) can be calculated using the potential energy (*Epot*), the kinetics energy (*Ekin*), the energy dissipation due to the aerodynamic drag (*Eaero*) and the ski snow friction (*Efrict*). Because energy can be absorbed, restored, created or

dissipated by the ski-skier entity a residual energy, (*Eres*) is introduced in the equation to help satisfy the conservation of energy law.

$$Etot(t) = Epot(t) + Ekin(t) + Eaero(t) + Efrict(t) + Eres(t) = \text{constant}$$ **Eq. 7.1**

*Epot* of the skier is calculated using the mass of the skier (*m*) and the vertical position (*z*) of the centre of mass (*CoM*) with the following formula:

$$Epot(t) = m \cdot g \cdot z(t)$$ **Eq. 7.2**

where *g* is the acceleration due to gravity. *Ekin* is calculated using the velocity of the skier's *CoM* (*Vskier*) and the mass of the athlete, using the following equation:

$$Ekin(t) = \frac{1}{2} m \cdot \vec{V}skier(t)^2$$ **Eq. 7.3**

Eaero is calculated using the skier shape coefficient (*C_D*), the frontal area of the skier (*A*), the air density (ρair), *Vskier* and the wind velocity (*Vwind*).

$$Eaero(t) = \int_0^t (\frac{1}{2} \cdot C_D(t) \cdot A(t) \cdot \rho_{air} \cdot \left( \vec{V}skier(t) + \vec{V}wind(t) \right)^2 \cdot \vec{V}skier(t)) \cdot dt$$ **Eq 7.4**

A model of the aerodynamic drag coefficient (*C_D A*) developed in (Meyer et al., 2010a) was used to estimate theses parameters during turns:

$$C_D A(t) = 0.337 \cdot H(t) + 0.091 \cdot W(t) - 0,248$$ **Eq. 7.5**

where *H* is the distance between the feet and the head of the skier and *W* the width of the arms. Theses two parameters are measured directly on the *3D* model reconstruction of the skier.

The energy dissipation due to friction between the skis and the snow *Efrict* is calculated using the standard formula:

$$Efrict(t) = \int_0^t \left( \mu \cdot Fcontact(t) \cdot Vskier(t) \right) \cdot dt$$ **Eq. 7.6**

Where *µ* is the ski-snow friction coefficient and *Fcontact* the contact force between the skis and the snow. The coefficient *µ* is considered constant for all the skiers, and determined using least square method. *Equation 7.6* was taken as the objective function and *µ* chosen to minimize the total of residual energy square. *Fcontact* is estimated in adding lateral forces due

to radial acceleration (*rad_acc*) and vertical forces, due to gravity (*g*) and vertical acceleration of the *CoM* ($A_{Z\_CoG}$).

$$Fcontact(t) = m \cdot \sqrt{(g + a_{z\_CoG}(t))^2 + rad\_acc(t)^2}$$  **Eq. 7.7**

As energy changes are more expressive and meaningful for analyses than energy state at a given time, deltas of energies occurring between two consecutive measurements were calculated using *Equation 7.1*. It corresponds to the energy that is won or lost during each time interval.

$$\Delta Eres(t) = \Delta Epot(t) + \Delta Ekin(t) + \Delta Eaero(t) + \Delta Efrict(t)$$  **Eq. 7.8**

For analysis purposes, a turn cycle is defined. The cycle starts (at 0%) and ends (100%) when the skis are flat on the slope, under the centre of gravity. A cubic spline interpolation method is used to achieve the normalisation (Greville, 1964). Each turn cycle is than separated in tree phases: the transition (*T*) corresponds to a turn radius of the skis higher than 25 m. The first steering phase (*S1*) corresponds to the end of the transition phase until the gate crossing. Finally, the second steering phase (*S2*) takes place between the gate crossing until the turn radius exceed 25 m. *ΔEkin*, *ΔEpot*, *ΔEaero*, *ΔEfrict* and *ΔEres* were also split according to the three phases, averaged and compared.

### 7.2.5. Statistical analysis

One-way repeated-measures analysis of variance (ANOVA) has been performed with SPSS 16 software (SPSS INC, USA) to compare the energies of the three phases for all participants and all parameters. Significance was accepted at $P < 0.05$ and located with post hoc analysis using the Tukey test. All data are expressed as means ± SD and the 95% interval of confidence (±1.96*SD) is represented on graphs.

### 7.3. Results

The least square method gave a ski-snow friction coefficient $\mu = 0.064$.

The radius describe by the *CoM* trajectory was over 25 meters between 0 % and 18 % of the turn, as well as between 85 % and 100 %,

corresponding to the *T* phase. The gate crossing occurred at around 53 % of the turn cycle. The *S1* phase is therefore between 18 % and 53 %, and the *S2* phase between 53 % and 85 %.

**Table 7-1:** *Mean and standard deviation of energy levels for the 3 phases.*

|     | $\Delta Ekin$ [J/Kg] | $\Delta Epot$ [J/Kg] | $\Delta Eaero$ [J/Kg] | $\Delta Efrict$ [J/Kg] | $\Delta Eres$ [J/Kg] |
| --- | --- | --- | --- | --- | --- |
| *T* | 0.43 ±0.24 | -1.04 ±0.05 | 0.29 ±0.03 | 0.50 ±0.08 | 0.20 ±0.20 |
| *S1* | -0.28 ±0.19* | -1.01 ±0.02 | 0.23 ±0.03* | 0.81 ±0.06* | -0.25 ±0.16* |
| *S2* | 0.21 ±0.22# | -1.01 ±0.04 | 0.22 ±0.03* | 0.60 ±0.06#* | 0.02 ±0.15# |

# Significantly different from *S1* ($P<0.05$)

* Significantly different from *T* ($P<0.05$)

As indicated in *Table 7-1*, $\Delta Ekin$ is significantly different between *T* (0.43 ±0.24) and *S1* (-0.28 ±0.19, $P<0.05$), as well as between *S1* (-0.28 ±0.19) and *S2* (0.21 ±0.22, $P<0.05$). ΔEpot doesn't have any significant differences between phases. *Figure7-2A* shows the two conservative energies for a turn cycle. $\Delta Ekin$ is negative during *S1* and positive during *T* and *S2*. $\Delta Epot$ is below zero and very stable during the turn cycle.

*Table 7-1* shows significant difference for the $\Delta Eaero$ between *T* (0.29 ±0.03) and *S1* (0.23 ±0.03, $P<0.05$) and between *T* (0.29 ±0.03) and *S2* (0.22 ±0.03, $P<0.05$). There is also a significant difference for all 3 phases for $\Delta Efrict$, between *T* (0.50 ±0.08) and *S1* (0.81 ±0.06, $P<0.05$), between *T* (0.50 ±0.08) and *S2* 0.60 ±0.06, $P<0.05$) and between *S1* (0.81 ±0.06) and *S2* (0.60 ±0.06, $P<0.05$). *Figure 7-2B* shows the dissipated energy occurring during a turn cycle. *S1* has the highest ski-snow friction energy, *S2* has a smaller dissipation compared to *S1* but higher than *T*. Concerning aerodynamic drag, *T* and *S2* have higher energy dissipation than *S1*. Ski-snow friction has more than two times higher average energy dissipation than aerodynamic drag.
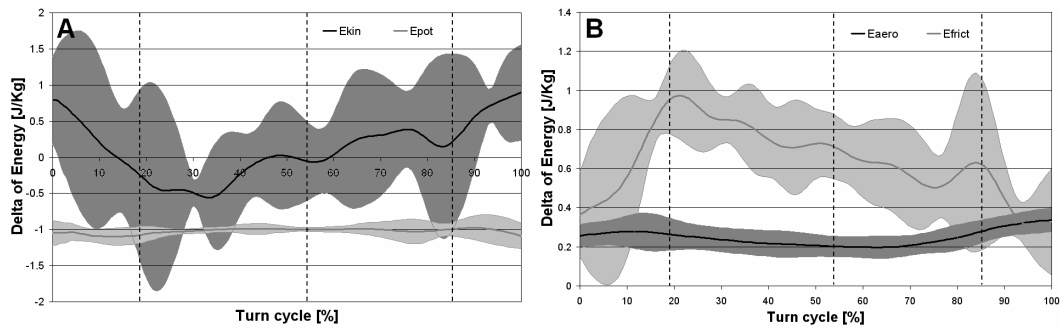
***Figure 7-2: A:*** *Evolution of conservative energy: ΔEkin and ΔEpot with a 95% interval of confidence.* ***B:*** *Evolution of dissipative energy: ΔEaero and ΔEfrict with a 95% interval of confidence. The dotted vertical lines indicate the separation between the 3 phases.*

The comparison of the three phases for *ΔEres* in *Table 7-1* indicates a significant difference between *T* (0.20 ±0.20) and *S1* (-0.25 ±0.16, *P*<0.05) as well as between *S1* (-0.25 ±0.16) and *S2* (0.02 ±0.15, *P*<0.05). *Figure 7-3* shows *ΔEres* of the seven athletes for a turn cycle with the 95% interval of confidence.
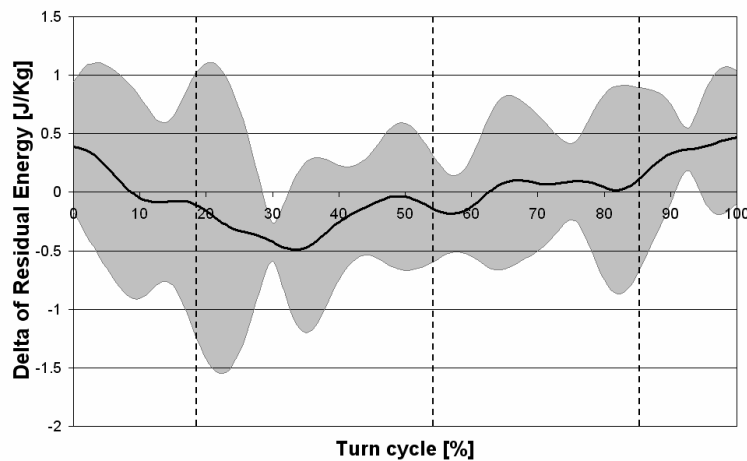


***Figure 7-3:*** *Evolution of ΔEres during a turn cycle with a 95% interval of confidence.*

## 7.4. Discussion

The main finding of this research is the significant difference of residual energy depending on the phase of the turn. It is the first time that evidence of energy absorption (when *ΔEres* is negative) and restitution (when *ΔEres* is positive) during turns performed by high level skiers is demonstrated. Various mechanisms can explain theses results. Firstly, the ski can absorb energy when it is bent, and restitute the energy when unbent during the transition between two turns. Secondly, vibrations of the skis-skier system can be a source of energy dissipation. Finally, the skier can absorb, restitute and also create energy with active movements. The results obtained show an increase of the system's total energy during the transition phases, implying restitution or creation of energy. The loss of energy between the transition and the gate involves energy absorption or dissipation. Eventually, the total energy is stabilized after the gate. Further investigations are needed to determine and understand the precise components of theses variations and therefore identify the exact causes.

Another important result is highlighted out of the energy dissipation analysis (*Figure 7-2B*). For the current test setup, aerodynamic drag is about half the ski-snow friction. The aerodynamic drag will take more importance when the speed increases, like in speed disciplines. The aerodynamic drag curve in *Figure 7-2B* also shows a variation of the drag during turns. Indeed, skiers are standing high during the transition phase, while they are in a more grouped position at the gate crossing, explaining the shape of the curve.

The *ΔEfrict* curve indicates low energy dissipation during *T*, which is quite intuitive because vertical forces and lateral acceleration are low. The interesting result comes from the *S1-S2* comparison. Indeed, *S1* has higher energy dissipation, probably due to the radius of the *CoM*, which is smaller during *S1*, inducing higher radial acceleration and therefore a higher *Fcontact*. There is also a moment just between S2 and T where the *ΔEfrict* increases slightly. This is probably when the skiers come back up with the *CoM*, increasing the force on the snow to trigger the next turn.

The least square method used to find the value for *μ* forced the sum of *ΔEres* to a minimum. The results given for the *ΔEres* are therefore the lower limit, and could be higher in reality. But as a variation of *ΔEres* is measured even with a minimum value, the results obtain are valid.

One limitation of the method is the use of models to estimate aerodynamic drag and ski-snow frictions. Even if they give a very good idea about the shape of the energy dissipated, they don't have very precise absolute accuracy. According to (Meyer et al., 2010a), the model used has a 13% accuracy to estimate the aerodynamic drag. The *Efrict* model doesn't take the possible skidding in consideration, so perhaps sometimes more energy is lost than described by the model.

This study proposed an experimental set-up for giant slalom analysis. Energy balance analysis of professional skiers was performed using conservative energy and dissipative energy models. This allowed computing residual energy which was found to vary significantly during the different phases of the turn, showing energy was absorbed and restituted during this movement. This absorption and restitution of energy still needs further investigation to understand the subjacent mechanisms operating during turns.

# 8. Study 4:

## External and internal work produced by alpine skiers performing giant slalom turns

Frédéric Meyer, Fabio Borrani*

Institut des Science du sport, Lausanne University, Switzerland

* Sport and Exercise Science Institute, University of Auckland, New-Zealand

## 8.1. Abstract

Identifying, understanding and quantifying mechanisms that lead to the best performance is a recurrent objective in the elite sport's community. Recent investigations in alpine skiing biomechanics allowed the determination of the mechanical energy of skiers performing turns. Kinetic energy increases measured around turn transitions exceeded that which can be explained by potential energy change suggesting that another source of energy is utilized. The aim of this project was to determine work produced by muscles of elite skiers during giant slalom turns. *3D* models of seven highly-skilled skiers performing a giant slalom were built using a multiple camera system and the SIMI motion software. An estimate of the skier's muscular work was calculated using leg extension and flexion movements and the ground reaction force, which in turn, was determined from the center of mass trajectory. The average total work calculated was close to zero. One skier managed to generate more than 150 J during a turn cycle, which represents approximately 1.5 % of the gravitational energy available. This increase of energy happened at the end of the second steering phase and during the turn transition, while the first steering phase indicated large negative work. This was the first time that work produced by muscles during giant slalom was quantified. The timing and the sum of work measured in this study confirms the negative mechanical energy dissipation found in other studies and previous theoretical researches. While this study demonstrated that the amount of work produced by skiers can contribute to a small increase of their overall performances, the authors believe that the role of parameters such as slopes inclination, snow conditions, and skier levels should be further investigated.

## 8.2. Introduction

Alpine ski racing is quite a unique sport because of the large number of parameters that influence towards the best performance. Indeed, slope profile, gates positions, snow quality, meteorological conditions are always changing and athletes have to adapt their technique. Nevertheless, at the end of the race, the victory is often won with less than a 0.1 s difference, which represents less than 0.1 % over a 100 s two runs race. Skiing technique and performance improve each year, taking advantage of the enhanced material developments and of the better understanding of the factors leading to the best performance.

Recent investigations have proposed / suggested new methods to analyze skiers' performance based on energy dissipation and allowed the determination of where and when athletes loose energy during the turns (Supej et al., 2005b; Supej, 2008; Reid et al., 2009). Negative energy dissipation, indicating increases in skier kinetic energy beyond which can be explained by potential energy change alone, have been observed through the transition between turns. One possible explanation for this excess energy may be mechanical work produced by the athlete's muscles as has been observed in other forms of human locomotion (e.g. in walking (Cavagna et al., 1963), in running (Cavagna et al., 1964), in cycling (Ericson, 1988), in swimming (Di Prampero et al., 1976), in ice skating (Saibene et al., 1989), or in cross country skiing (Formenti et al., 2005)). In theses studies of locomotion on a flat plane, the only engine to move the body is muscle work. In alpine skiing, gravitational force is the main contributor to increase and maintain speed. Nevertheless, the work developed by a skier's muscles may perhaps provide effective energy, although this has never been measured.

To explain how skiers could increase their speed on undulating snow surface and during turns, Mote and Louie (Mote and Louie, 1983) studied the theoretical aspect of the pumping mechanism. The reduction and augmentation of the turn radius with specific timing was analysed, similar to researches aiming to understand why the amplitude of a playground

swing increases when pumping (Tea and Falk, 1968; Siegman, 1969; Burns, 1970; Curry, 1976). Mote and Louie (Mote and Louie, 1983) observed that the best timing to increase speed was to make the extension when the ground reaction forces are maximal and flexion when they are minimal. This is coherent with the definition of work where maximial work is obtained for maximum distance and force. Based on the definition of work, Takahahi and Yoneyama (Takahashi and Yoneyama, 2001, 2002), theoretically illustrated possible work generation during turns, when the Centre of Mass (*CoM*) and the skis' trajectories are diverging and forces are applied at the same time. The phenomenon was highlighted at the beginning of the turn when the skier leans inwards. Finally, Coulmy et al. (Coulmy et al., 2010) proposed to see the skier as a parametric pendulum, where the length of the gyration radius is modified using flexion and extension of the legs. Greater vertical movement induced higher pressure during the turn transition as well as higher tangential velocity during the first steering phase.

The above concepts, theoretically describing energy increases, have never been verified through experimental data of skiers performing turns. Therefore, the aim of this study was to investigate the external work produced by highly skilled alpine skiers performing giant slalom.

## 8.3. Methods

### 8.3.1. Participants

Seven European Cup and FIS racers (mean ± SD: body mass 98.8 ± 9.1 Kg; height 1.82 m ± 0.07; Giant Slalom (*GS*) FIS points 26.45 ±14.58) participated in the study. All participants were healthy males without any joint motion problems. The study was conducted according to the 1964 declaration of Helsinki and written informed consent was obtained from each subject prior to participation in the study. In parallel, the study was approved by the local ethics committee.

## 8.3.2. Experimental design and setting

A six-gate giant slalom course was set using linear and lateral offsets of 24 m and 9 m, respectively. The first three gates were used to initiate the rhythm, while recordings were made during the last three. The slope angle was approximately 20 to 22 degrees. Six panning and tilting cameras, 1004*1004 pixels resolution, 48 Hz (PiA1000, Basler, Switzerland) were positioned around the giant slalom run, about 35 meters from the center of the capture volume. Each camera was mounted onto a tripod head designed to maintain the camera sensor in the same position as the camera is panned and tilted to track the skier. Fifty poles, each mounted by three reference markers were positioned on both sides of the trajectory to act as calibration and reference points for the panning and tilting reconstruction. The capture volume was around 60 * 20 * 2 meters (*Figure 8-1A*). The positions of each reference marker, each gate and each camera were measured with a reflectorless total station (theodolite + laser range finder, LQTS-522D, Longqiang, China). The cameras' positions were calculated as the average of two points on each side of the tilting axis of the camera. Each camera was autonomous, powered by a battery pack and synchronised using a dedicated GPS based wireless system (Meyer et al., 2011b). Moreover, each camera was connected with Gigabit Ethernet to a dedicated laptop which directly recorded the frames in the RAM memory of the computer, using a software developed specifically for this purpose (Swistrack, Thomas Lochmatter, Switzerland. The athletes had to perform three attempts at the giant slalom. Two consecutive turns were recorded and the time needed to go through the three reference gates was estimated by counting the number of images captured on video. The fastest run of each skier was then analysed. The selected runs were processed with SIMI motion software (SIMI motion, SIMI, Germany), using the panning and tilting modules. The camera's internal (e.g., focal length, image format and principal point) and external (e.g., camera position and orientation) parameters needed for the analysis were determined using the DLT 11 calibration method (Hatze, 1988), using the position of the markers captured on video frames as reference points.
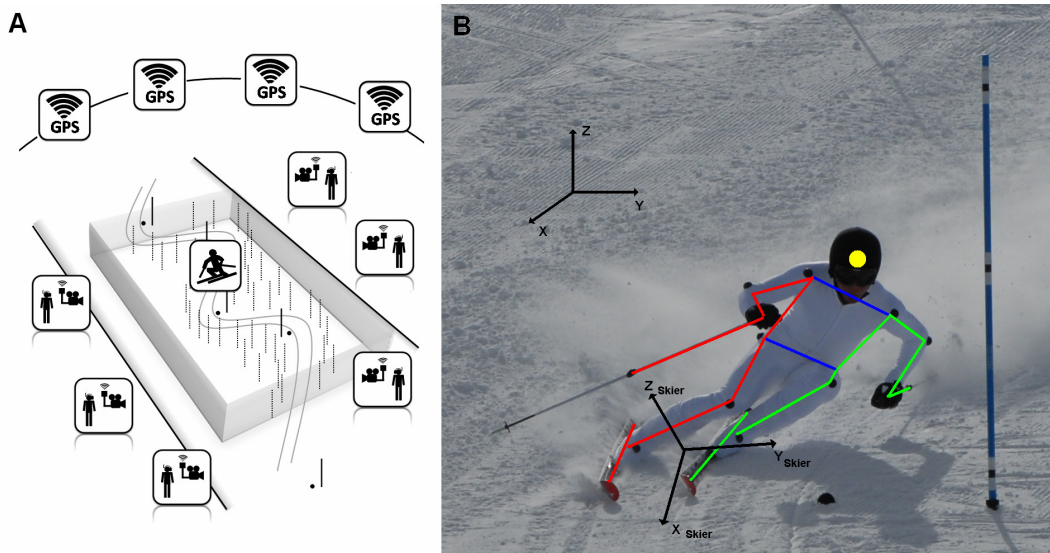
***Figure 8-1: A:*** *Slope setup showing the cameras, the gates and the reference points positions,* ***B:*** *Skier suit, markers,body segments and the two coordinate systems.*

Participants wore a white racing suit equipped with 14 black markers, a black helmet, black gloves also used as markers, and ski poles with black markers at their *CoM*. The 19 tracked markers were used to reconstruct a 14 segment model of the skier. The skier's center of mass was calculated using Clauser's model (Clauser et al., 1969) modified to take the material's weight into account. Two coordinate systems were defined: A global orthogonal referential with a vertical Z component, the Y component perpendicular to both the slope direction and the Z axis, and the X component perpendicular to the Z and Y axis. The skier orthogonal referential was than defined with the XY plane parallel to the slope surface, the X component following the skier speed direction, the Z component perpendicular to the XY plane.

### 8.3.3. Parameters analysis

### 8.3.3.1. 3D accuracy

The accuracy of the reconstruction method was measured in two different ways. First, the positions of three gates as given by the total station were compared with the positions calculated by the software. Second, the

length of the 14 segments defined by our markers was compared to the average calculated length.

### 8.3.3.2. Turn phases

For analysis purposes, each trial was normalized to fit a 100% turn cycle, where 0% and 100% were the beginning and the end of the curve when the skis were flat on the slope, under the *CoM*. A cubic B-splines interpolation method was used to achieve the normalisation (Greville, 1964; Lee et al., 1997 ). Each turn cycle was than separated in three phases: the transition phase (*T*) corresponds to a turn radius of the *COM* higher than 25 m, which is approximately the natural radius of giant slalom skis. The first steering phase (*S1*) corresponds to the end of *T* until the gate crossing. Finally, the second steering phase (*S2*) takes place from the gate crossing until the turn radius exceeds 25 m. The turn radii were calculated with the Frenet-Serret (Serret, 1851; Frenet, 1852) formula using the *CoM* 3D trajectory. All the analysed parameters were split according to these three phases and averaged.

### 8.3.3.3. External human work and power

As measurements gave discrete data, the work produced by the skier during a time interval *Δt* has been estimated by using the variation of distance between the *CoM* and the middle point between the feet (*ΔD*). The resultant external forces acting in the direction of the variation (*F*) can be calculated using:

$$\Delta W_{Hum} = F \cdot \Delta D \cdot \cos(\alpha) = F_{Lat} \cdot \Delta D_{Lat} + F_{Long} \cdot \Delta D_{Long} + F_{Ant} \cdot \Delta D_{Ant} \qquad \textbf{Eq. 8.1}$$

were *α* is the angle between the *F* and the *D* vector, and $F_{Lat}$, $D_{Lat}$, $F_{Long}$, $D_{Long}$, $F_{Ant}$ , $D_{Ant}$ are the projections of *F* and *D* in the mediolateral, longitudinal and anteroposterior directions of the skier referential, giving respectively $W_{Lat}$, $W_{Long}$ and $W_{Ant}$. Due to the gliding of the skis, $W_{Ant}$ is very limited on the anteroposterior direction and has been neglected. $D_{Lat}$ and $D_{Long}$ have respectively been defined as the mediolateral and longitudinal variations of the distance between the *CoM* and the feet. $F_{Lat}$ is composed by the centripetal force due to the turn radius, the lateral

component of the gravitational force in the skier's referential and the force due to the lateral acceleration of the feet relative to the *CoM* ($a_{Lat}$):

$$F_{Lat}(t) = \frac{m \cdot V_{CoM}^2(t)}{R_{CoM}(t)} + m \cdot g \cdot \sin(\beta \cdot \sin(\gamma(t))) + m \cdot a_{Lat}(t)$$

**Eq. 8.2**

where $R_{CoM}$ is the radius of the *CoM* trajectory, always positive; $\beta$ is the slope angle, also positive and $\gamma$ is the skier's heading (the angle between the falling line and the *CoM* direction, in the global referential), negative from the turn transition to the fall line and positive from the fall line to the next turn transition. $F_{Long}$ is composed by the longitudinal component of the gravitational force and the force due to the longitudinal acceleration of the feet relative to the *CoM* ($a_{Long}$):

$$F_{Long}(t) = m \cdot g \cdot \cos(\beta) + m \cdot a_{Long}(t)$$

**Eq. 8.3**

*Equations 1, 2* and *3* were used to determine the work generated during each time interval:

$$\Delta W_{Lat}(t) = \left( \frac{m \cdot V_{CoM}^2(t)}{R_{CoM}(t)} + m \cdot g \cdot \sin(\beta \cdot \sin(\gamma(t))) + m \cdot a_{Lat}(t) \right) \cdot \Delta D_{Lat}(t)$$

**Eq. 8.4**

$$\Delta W_{Long}(t) = \left( m \cdot g \cdot \cos(\beta) + m \cdot a_{Long}(t) \right) \cdot \Delta D_{Long}(t)$$

**Eq 8.5**

The speeds corresponding to the variation of distance ($V_{Lat}$ and $V_{Long}$ respectively), as well as the powers corresponding to the work production ($P_{Lat}$ and $P_{Long}$) were also calculated:

$$P_{Lat}(t) = \frac{\Delta W_{Lat}}{\Delta t} = F_{Lat} \cdot V_{Lat} = F_{Lat} \cdot \frac{\Delta D_{Lat}}{\Delta t}$$

**Eq. 8.6**

$$P_{Long}(t) = \frac{\Delta W_{Long}}{\Delta t} = F_{Long} \cdot V_{Long} = F_{Long} \cdot \frac{\Delta D_{Long}}{\Delta t}$$

**Eq. 8.7**

The evolution of the work $W_{Hum}$ developed during the turn cycle was calculated as follow:

$$W_{Hum}(t) = \sum_0^t \left( \Delta W_{Lat}(t) + \Delta W_{Long}(t) \right)$$

**Eq. 8.8**

### 8.3.3.4. Internal work

Using the the König theorem as described by Willems et al. (Willems et al., 1995), the internal work of a person subdivided into *n* rigid segments can be calculated as follows:

$$W\,int_{Tot}(t) = \sum_{i=1}^{n}(\frac{1}{2} \cdot m_i \cdot V_{r,i}^2(t) + \frac{1}{2} \cdot m_i \cdot K_i^2 \cdot \omega_i^2(t))$$

**Eq 8.9**

which consist in a linear part:

$$W\,int_{Lin}(t) = \sum_{i=1}^{n}(\frac{1}{2} \cdot m_i \cdot V_{r,i}^2(t))$$

**Eq 8.10**

and an angular part:

$$W\,int_{Rot}(t) = \sum_{i=1}^{n}(\frac{1}{2} \cdot m_i \cdot K_i^2 \cdot \omega_i^2(t))$$

**Eq 8.11**

where $m_i$ is the mass of the *i*th segment, $V_{r,i}$ is the velocity of the *i*th segment relative to the *CoM*, $K_i$ is the radius of gyration of the ith segment, given by Chandler (Chandler et al., 1975), and $\omega_i$ is the angular velocity of the *i*th segment around it's own *CoM*.

### 8.3.4. Statistical analysis

All data is expressed as mean plus standard deviation (mean ± *SD*). The 95 % limit of agreement (± 1.96 * *SD*) is given for the accuracy of the *3D* reconstruction. One-way analysis of variance (ANOVA) has been performed with SPSS 16 software (SPSS INC, USA) to compare the average powers developed on the three phases of the turn for both the $P_{Lat}$ and $P_{Long}$. Significance was accepted at $P < 0.05$ and located with post hoc analysis using the Tukey test.

## 8.4. Results

### 8.4.1. 3D accuracy

For the reconstruction of the gates' position using the *3D* reconstruction software, a horizontal mean absolute error of 14.0 ± 8.0 mm was calculated, giving a 95 % limit of agreement of 27.1 mm. For the vertical

axis, a mean absolute error of 5.9 ± 3.5 mm gave a 95 % limit of agreement of 11.6 mm. Adding the horizontal and the vertical errors led to a total *3D* reconstruction error of 15.7 ± 7.8 mm, and a 95 % limit of agreement of 28.3 mm. The segments' lengths mean absolute error of 13.0 ± 12.0 mm led to a 95 % limit of agreement of 32.7 mm.

## 8.4.2. Turn phases

The average radius described by the *CoM*'s trajectory was over 25 meters before 17.55 ± 3.82 % of the turn, as well as after 84.57 ± 4.04 %, corresponding to the *T* phase. The gate crossing occurred at 53.24 ± 4.38 % of the turn cycle, separating the *S1* and the *S2* phases.

## 8.4.3. External human work and power
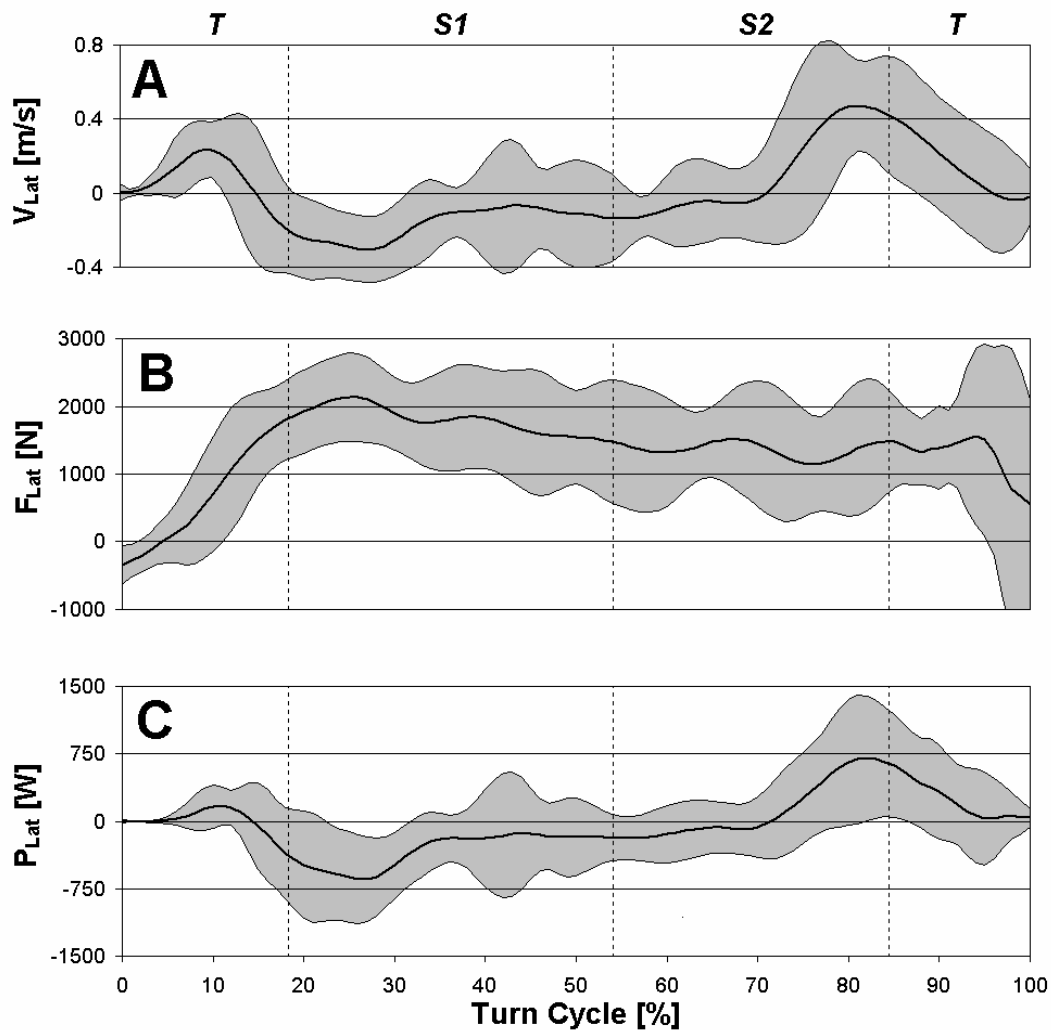


*Figure 8-2: **A:** Lateral velocity of the CoM's displacement relative to the feet. **B:** Lateral force sustained during the turn. **C:** External human power developed on the lateral axis. The grey areas indicate the 95 % limits of agreement and dotted vertical lines the limit between phases.*

The evolution of $V_{Lat}$ and $F_{Lat}$ sustained by the skier during the turn are respectively drawn on *Figure 8-2A* and 8-*2B*. Concerning $P_{Lat}$, *T* (93.83 ± 91.15 W) was significantly different from *S1* (-325.37 ± 106.80 W, *P* < 0.001), and *S1* (-325.37 ± 106.80 W) was significantly different from *S2* (127.01 ± 144.19 W, *P* < 0.001), but no significant difference was found between *T* and *S2*. *Figure 8-2C* shows the evolution of $P_{Lat}$ during the turn

111

cycle. Negative power is visible during *S1*, and positive power is developed at the end of the *S2* and during T.

*Figure 8-3A* and 8-*3B* show the evolution of $V_{Long}$ and $F_{Long}$, respectively. Averaged $P_{Long}$ on the three phases indicated significant difference between *T* (91.94 ± 78.14 W), and *S1* (-67.65 ± 18.51 W, *P* < 0.001), and between *S1* (-67.65 ± 18.51 W) and *S2* (67.87 ± 45.24 W, *P*<0.001), but not between *T* and *S2*. *Figure 8-3C* shows $P_{Long}$ during the turn cycle, with negative power during *S1* and positive power at the end of the *S2* and during *T*.
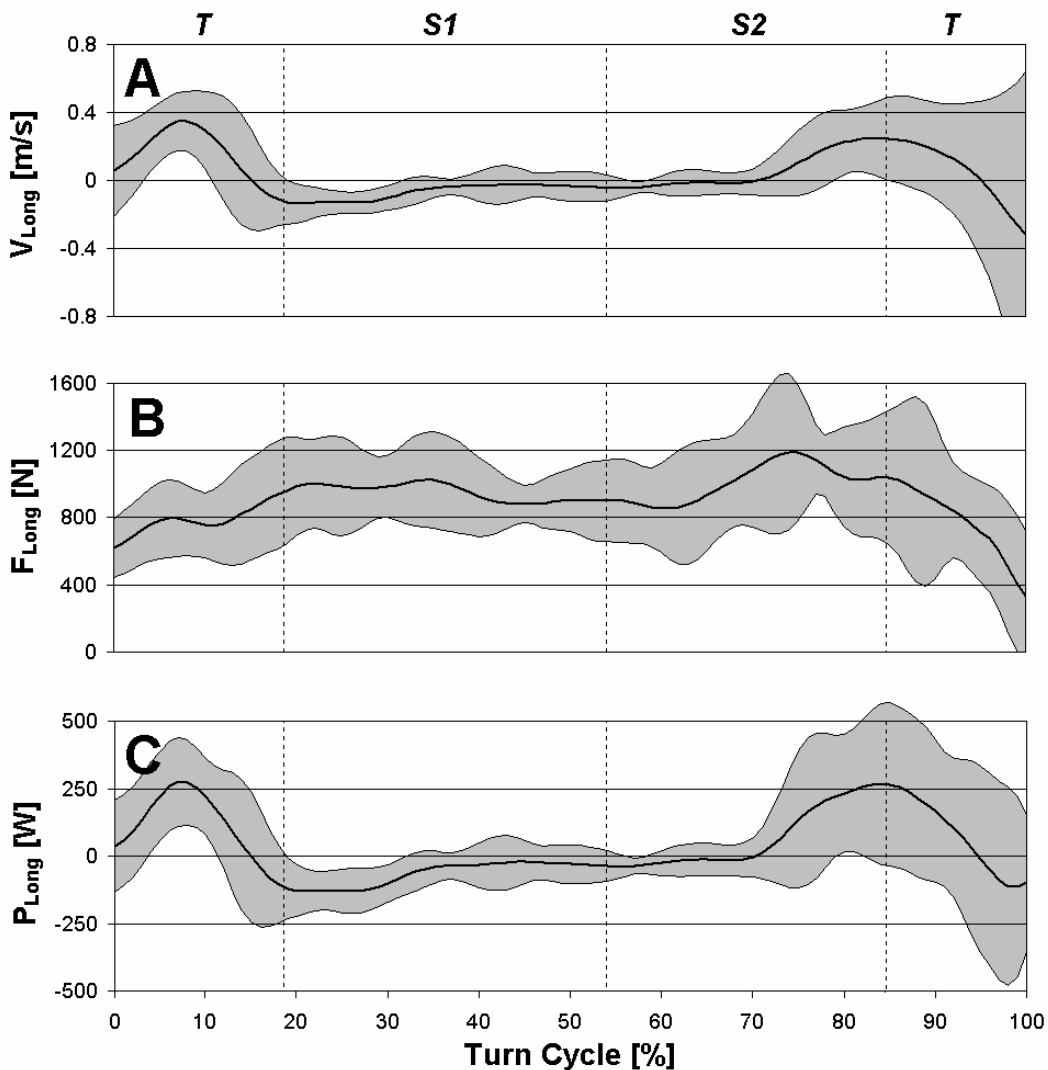


***Figure 8-3: A:*** *Longitudinal velocity of the CoM's displacement relative to the feet.* ***B:*** *Longitudinal force sustained during the turn.* ***C:*** *External human power*

*developed on the longitudinal axis. The grey areas indicate the 95 % limits of agreement and dotted vertical lines the limit between phases.*

The average $W_{Hum}$ produced by the skiers in a turn is 6.97 ± 112.79 J. *Figure 8-4* shows the evolution of the work during the turn cycle. The maximum $W_{Hum}$ produced during a turn cycle was 153.82 J.
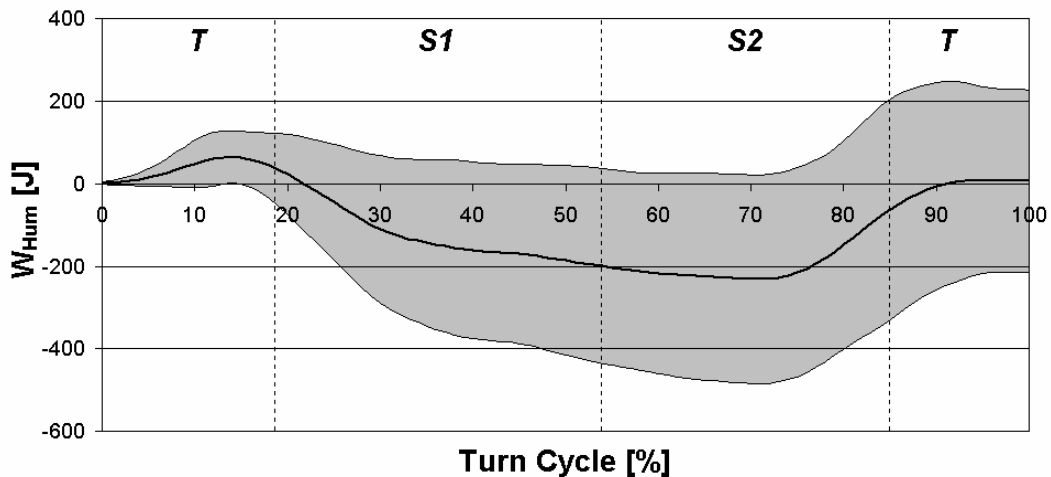


**Figure 8-4:** *Evolution of the total human work during a turn cycle. The grey area indicates the 95 % limits of agreement and dotted vertical lines the limit between phases.*

### 8.4.4. Internal work

*Figure 8-5A* shows the evolution of $Wint_{Lin}$ and $Wint_{Rot}$ during a turn cycle. $Wint_{Lin}$ is significantly different between *T* (51.89 ± 6.71 J) and *S1* (25.14 ± 8.54 J, p < 0.05), as well as between *T* (51.89 ± 6.71 J) and *S2* (24.00 ± 5.59 J, p < 0.05). $Wint_{Rot}$ shows the same pattern with a significant difference between *T* (13.18 ± 6.71 J) and *S1* (8.58 ± 2.46 J, p < 0.05), as well as between *T* (13.18 ± 6.71 J) and *S2* (7.35 ± 2.19 J, p<0.05). *Figure 8-5B* shows the evolution of $Wint_{Tot}$ during a turn cycle.
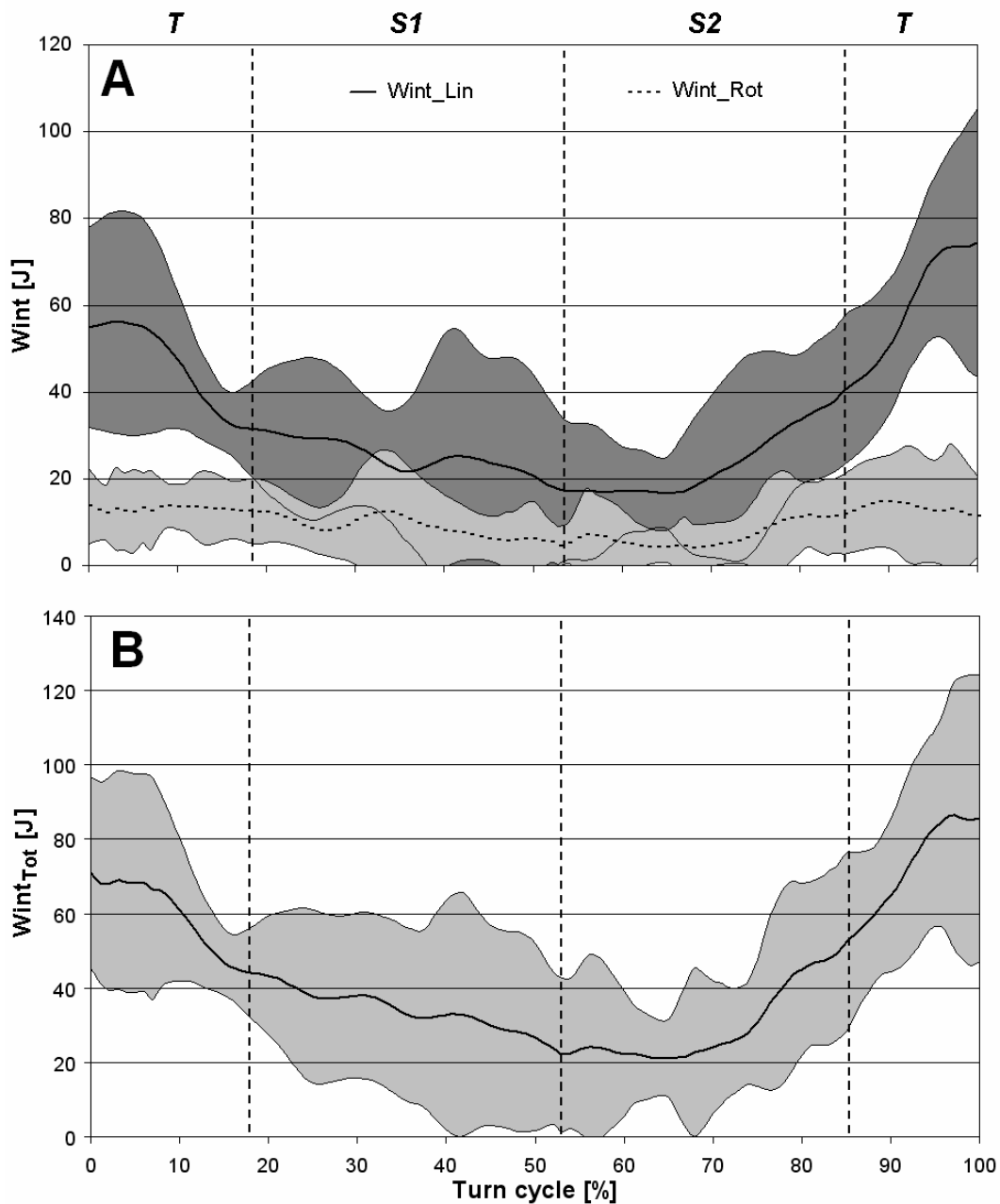
**Figure 8-5:** *Evolution of the internal work.* **A:** *Wint$_{Lin}$ and Wint$_{Rot}$,* **B:** *Wint$_{Tot}$. The grey areas indicate the 95 % limits of agreement and dotted vertical lines the limit between phases.*

## 8.5. Discussion

It was the first time that active work generation by alpine skiers performing turns was quantified using experimental data. Both lateral and longitudinal movements were shown to produce work. The resulting shape of the curve describing the evolution of the work developed by the skiers showed an

114

increase of energy during the last part of *S2* and during the *T*. A decrease of energy was found during *S1* and the first part of *S2*. Even though the average total work produced by the skiers was almost zero, one athlete managed to obtain a positive balance of more than 150 J during a turn cycle, amounting to approximately 1.5 % of the corresponding potential energy change during the turn (150 J versus 10'000 J for a 100 Kg athlete descending 10 m). This amount might not be very high, but should not be neglected as it can make a significant difference in terms of performance, as more energy is available to achieve the run. It is believed that the generation of energy is probably more efficient on flat slopes, as less potential energy is available, increasing the relative effect of the movement. On steep slopes, skiers might have more to loose trying to generate more speed than focusing on controlling their trajectory to avoid having to brake.

Supej et al. (Supej et al., 2005b; Supej, 2008) were the first to demonstrate negative energy dissipation in giant slalom turns. This dissipation was at the time explained by the vertical movement of the skier. This movement provides the skier with some additional potential energy during the turn transition. However, this energy is lost when the skier flexes during the steering phases. The evolution of the active work produced by the skier in the present study is very similar to the one obtained by Supej (Supej, 2008) (*Figure 8-2B*). Reid (Reid, 2010) also obtained negative energy dissipation in slalom for both a 10 m and a 13 m slalom course. The evolution of energy dissipation observed during the 10 m course is very similar to those proposed in this study. For the 13 m course the evolution shows a slightly shifted profile as the negative energy dissipation occurred only at the beginning of the initiation phase, after the edge change. This could be the results of a different pattern of motion due to the positioning and the rhythm of the gates. Meyer and Borrani (Meyer and Borrani, 2010) found a residual positive energy at the gate transition in giant when taking into account the kinetic energy, potential energy, aerodynamic drag energy dissipation and ski-snow friction energy dissipation. The results obtained in the present study concerning the work

produced and absorbed by the skiers using legs extensions and flexions can explain the energy balance results obtained by Supej (Supej, 2008), Reid (Reid, 2010) and Meyer (Meyer and Borrani, 2010).

As seen in the introduction, Mote and Louie (Mote and Louie, 1983) indicated that, when skiing on undulating sufaces, the best strategy to increase energy was to pump when the ground reaction force normal to the radius was the highest. This theoretical finding was confirmed in the present study. When turning, the direction of the turn radius is aligned to the slope's plane and therefore lateral extension should be exerted when lateral forces are the highest. A parallel can be drawn with the pumping of a swing when in a standing position, as described by Case and Swanson (Case and Swanson, 1990), and later by Wirkus (Case and Swanson, 1990; Wirkus et al., 1998). For swings, $T$ happens at the top of the swing trajectory as the body is unloaded, whereas the gate crossing corresponds to the lower position of the swing. Mote and Louie (Mote and Louie, 1983) also demonstrated an increase of the phenomenon when fore/aft rocking is performed. This technique could be assimilated to pumping a swing from the seated position (Case, 1996; Wirkus et al., 1998). It implies leaning progressively backwards during the two steering phases, and coming back to the front quickly at the end of the turn transition. This fore-aft leaning pattern has already been observed in several field studies (Brierley and Bartlett, 1991; Nigg et al., 2001; Schwameder et al., 2001; Federolf, 2005; Reid, 2010), but the efficiency of the movement still needs to be investigated.

Another parallel can be drawn between the flexions and extensions of the legs observed in the present study and the inverted pendulum principle described by Morawski (Morawski, 1973). The lateral force developed by the skier using longitudinal movements can be assimilated to the regulation force needed to keep the pendulum's equilibrium. The higher the lateral force at the end of the $S2$, the faster the skier will go from one turn to the other.

It is also the first time that internal work is calculated for alpine skiing athletes. Results showed the highest level of $Wint_{Tot}$ during $T$, a decrease

during *S1* and increase back to the initial level during S2. These results are quite intuitive as *S1* is qualitively a quiet part of the turn, while *S2* and *T* implies more gestures to control the balance and the efficiency of the movement. Average internal activity is in the same order of magnitude that results obtained in walking or running (Winter, 1979; Minetti and Saibene, 1992; Willems et al., 1995). Finally, even with significant differences between turn phases, $Wint_{Rot}$ is two to three time lower than $Wint_{Lin}$. This indicates that the major part of internal work is due to the linear speed of segments around the *CoM* of the body and not induced by the rotation of the segments around their own *CoM*.

One limitation of this research is the method used to calculate lateral forces. As described by Lüthi et al. (Lüthi et al., 2005) using video measurements lead to statistical noise due to the double derivative of the position needed to obtain accelerations. Additionnaly, this method does not allow to measure independently the forces sustained by each foot. Going forward, the accuracy of work determination could be improved by measuring the forces sustained by each foot using dedicated force platforms. Nevertheless, using a force platform or pressure insoles led to other issues (e.g. embedded captors, data processing and accuracy of the measures), and therefore the method used in the present study offered a good solution. Another limitation comes from the fact that the energy generation calculated here doesn't include the additional energy dissipated through the action forces on the snow.

In conclusion, this study demonstrated the possibility for athletes to increase their kinetic energy using extensions movements of the legs. Additionally, it offers new perspectives for the analysis of intrinsic parameters influencing performance in alpine skiing. Studying skiers of different skill level and different slope angles should lead to a better understanding of the most effective techniques. This in turn could help determining the efficiency of the active work of skiers performing turns.

# 9. Study 5:

## Differences between using the centre of mass or morphological points for the analysis of alpine skiing

Frédéric Meyer, Fabio Borrani*

Institut des Science du sport, Lausanne University, Switzerland

* Sport and Exercice Science Institute, University of Auckland, New-Zealand

## 9.1. Abstract

Purpose: Alpine ski analysis has always been very challenging, mainly due to the environmental conditions, large field and sharp skiers behaviours. High accuracy *GPS* offers a solution adapted to outdoor testing, but the relationship between the point where the *GPS* antenna is attached and the real centre of mass position is still unknown. This article proposes to analyze different points of the body used to quantify the performance of alpine skiers. Methods: models of seven elite skiers performing giant slalom were built using multiple camera system and SIMI motion software. Centre of mass as well as pelvis, head and feet trajectories were deduced from the data. The potential and kinetic energies corresponding to theses points were calculated, as well as the evolution of the turn radius during the turn cycle. Differences between values given by the centre of mass and the other morphological points were analysed. Results: The pelvis offered no significant differences in the turn entry and turn exit, and on the average kinetic energy calculation. Only 7 % of the turn indicated a different radius, 9 % a difference in the potential energy calculation and 30 % for the kinetic energy. The head was less accurate and the feet offered the worst results. Discussion: The best estimation of the centre of mass is proposed by the pelvis, for all the analyzed parameters. Energies and turn radius calculated by using pelvis in place of Centre of Mass offered similar patterns allowing the analysis of mechanical and dissipation energy in giant slalom. This may potentially enable easier testing methods to be proposed and tested.

## 9.2. Purpose

Human movement analyses are usually based on the body centre of mass (*CoM*) position determination. Mechanics of different sports have widely been studied, showing the necessity to calculate the *CoM* with a good accuracy to perform precise analysis e.g. walking (Cavagna et al., 1963; Willems et al., 1995; Saibene and Minetti, 2003), running (Kyröläinen et al., 2001), cycling (Cheze et al., 1995). However, *CoM* calculations usually require large infrastructures such as *3D* camera system (Richards, 1999) or force platform (Barbier et al., 2003). Kinematic arms (Belli et al., 1993) and global positioning systems (*GPS*s) (Terrier et al., 2005) have also been used, but theses methods use a point situated on the back of the subject to approximate the *CoM*. Slawinski et al. (Slawinski et al., 2004) analyzed the use of a lumbar point for the estimation of potential and kinetic mechanical power in running. With this method, they found an overestimation and underestimation of the kinetic and potential powers respectively. Nevertheless, results obtained by using either a fixed point on the back or the *CoM* were well correlated. In alpine skiing, the *CoM* has also been used as a reference to perform technical analysis (Kagawa and Yoneyama, 2001; Schiefermüller et al., 2005), trajectories and speed analysis (Lešnik and Žvan, 2003) and more recently to analyze energy balance of skiers performing turns both in giant slalom (Supej et al., 2005b; Supej, 2008) and in slalom (Reid et al., 2009).

Multiple camera systems are commonly used to reconstruct *3D* models of the athlete, and *CoM* is than calculated, with de Leva adjustments (de Leva, 1996), using mathematical models of the body like Hanavan (Hanavan, 1964), Clauser (Clauser et al., 1969) or Zatsiorsky (Zatsiorsky and Seluyanov, 1983). However, this method only enables the recording of a small acquisition volume (usually one or two gates). Alternatively, the use of low cost,high accuracy *GPS*s have expanded, allowing analyzing trajectories during a whole run (Waegli and Skaloud, 2007a; Gomez-Lopez et al., 2009; Waegli et al., 2009; Waegli and Skaloud, 2009). However, since the *CoM* is not a fixed body point, the link between the

*GPS* antenna trajectory and the real *CoM* of the skier is still missing. Therefore, the aim of this work was to compare the use of either the *CoM* or other morphological points to determine potential energy (*Epot*), kinetic energy (*Ekin*) and turn radius (*Trad*) of alpine skiers performing giant slalom.

## 9.3. Methods

### 9.3.1. Participants

Seven European Cup and FIS racers (mean ± standard deviation (*SD*): body mass 98.8 ± 9.1 Kg; height 1.82 m ± 0.07 m; Giant Slalom (*GS*) FIS points 26.45 ± 14.58) participated in the study. All participants were healthy males without any joint motion problems. The study was conducted according to the 1964 declaration of Helsinki and written informed consent was obtained from each subject prior to participation in the study, which was approved by the local ethics committee.

### 9.3.2. Experimental design and setting

A giant slalom run was set up with a total of six gates, with a linear gate distance of 24 m and a lateral offset of 9 m. The first three gates were used to initiate the rhythm, and the next three were recorded. The slope angle was approximately 22 degrees. Six panning and tilting cameras, 1004*1004 pixels resolution, 48 Hz (PiA1000, Basler, Switzerland) were positioned around the giant slalom run, about 35 meters from the centre of the zone of acquisition (i.e. video captured). Each camera was mounted on a special tripod head, specially built to always keep the centre of the camera sensor in the same position, even as the camera was panned or tilted to track the skier. Reference markers mounted on poles were positioned around the run to act as calibration and reference points for the panning and tilting reconstruction. The capture volume was around 60 * 20 * 2 meters (*Figure 9-1A*). The positions of each reference marker, gate and camera were measured with a reflectorless total station (theodolite + laser range finder, LQTS-522D, Longqiang, China). The cameras' positions were calculated as the median of two points on either side of the

tilting axis of the camera. Each camera was connected with Gigabit Ethernet to a dedicated laptop which directly recorded the frames in the RAM memory of the computer, using a software developed for this specific purpose (Swistrack, Thomas Lochmatter, Switzerland). Cameras were also connected to battery packs and dedicated synchronization boxes (Meyer et al., 2011a). Theses boxes achieve wireless synchronization of the cameras recording system and ensure images from the six cameras are taken simultaneously with an error of less than 2.00 µs.
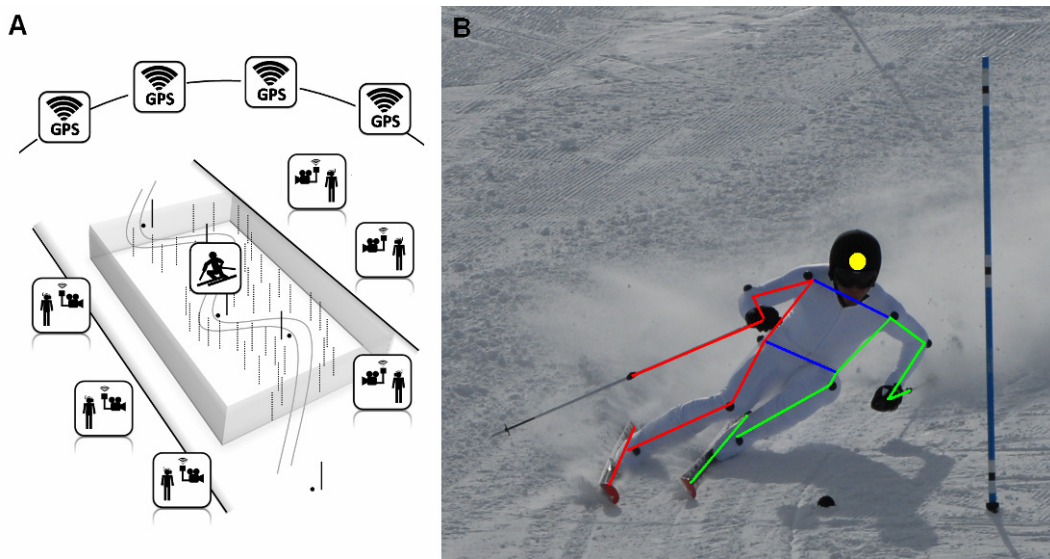


**Figure 9-1: A:** *Slope setup showing the cameras, the gates and the reference points positions,* **B:** *skier suit, markers and body segments.*

The athletes had to perform three trials of the giant slalom. The runs were recorded and the time needed to go through three considered gates was estimated by counting the number of images captured on video. The fastest run of each skier was then analysed. The selected runs were processed with SIMI motion software (SIMI motion, SIMI, Germany), using the panning and tilting modules. The camera's internal (e.g., focal length, image format and principal point) and external (e.g., camera position and orientation) parameters needed for the analysis were determined using the DLT 11 calibration method (Abdel-Aziz and Karara, 1971; Hatze, 1988).

Participants had to wear a white racing suit equipped with 14 black markers, a black helmet, black gloves, and ski poles with black markers at

their CoM. In total, 19 markers were identified, and *3D* models composed of 14 segments were built (*Figure 9-1B*). The *CoM* of the skiers were calculated using Clauser model (Clauser et al., 1969) modified to take the material's weight into account. For the further analysis, three morphological points were also defined: The *Pelvis* position was defined as the middle point between the two hips markers, the *Feet* position as the middle point between the two ankle-bone markers and the *Head* position as the centre of the helmet. The overall accuracy of the markers' *3D* coordinates reconstruction of the set up used in this study was 1.57 cm (Meyer et al., 2010b).

### 9.3.3. Analysis of parameters

The *Epot* and *Ekin*, (J/Kg), and the *Trad* (m), were calculated for the *CoM*, *Pelvis*, *Head* and *Feet*. The differences between the *CoM* and the other morphological points were than analysed.

For purposes of analysis, each trial was normalized to fit a 100% temporal turn cycle, where 0% and 100% were the time points at which the skis were flat on the slope, under the *CoM*. A cubic B-splines interpolation method was used to achieve the normalisation (Greville, 1964; Lee et al., 1997 ). The turn entry (*Tentry*) was arbitrary defined as the first time the turn radius of the considered point dropped below the natural turn radius of the skis (25 m) and the turn exit (*Texit*) as the last time the turn radius went over 25 m. *Tentry* time differences (*Tentry_diff*) between the *CoM* and the other morphological points were calculated, as well as *Texit* time differences (*Texit_diff*).

### 9.3.3.1. Potential energy

The *Epot* referred to the different morphological points, and was calculated for each participant for a time (*t*) given in percent of the turn cycle, using the mass of the skier and equipment (*M*), the acceleration due to gravity (*g*) and the height of the analysed point (*H*) in a global reference system. Since it is the variation of *H* of the analysed morphological point that is relevant and not the absolute height, the average *H* during the turn is subtracted to the *H(t)* during *Epot(t)* calculation:

124

$$Epot(t) = M \cdot g \cdot \left( H(t) - \frac{\int_0^{100} H(t) \cdot d(t)}{\int_0^{100} d(t)} \right)$$

**Eq. 9.9**

The time course of the differences between the CoM's Epot and the other morphological points (*Epot_diff*) (i.e. *Pelvis*, *Head*, and *Feet*) were calculated as follows:

$$Epot\_diff(t) = Epot_{CoM}(t) - Epot_{point}(t)$$

**Eq. 9.10**

### 9.3.3.2. Kinetic energy

The *Ekin* at different points of the curve were calculated using the speed (*V*) of the analysed morphological points and *M*, using the following equation:

$$Ekin(t) = \frac{1}{2} M \cdot V(t)^2$$

**Eq. 9.11**

The time course of the differences between the *CoM*'s *Ekin* and the other morphological points (*Ekin_diff*) were calculated as follows:

$$Ekin\_diff(t) = Ekin_{CoM}(t) - Ekin_{point}(t)$$

**Eq. 9.12**

The average differences in *Ekin* of the whole turn were also calculated, to show the global overestimation or underestimation when using a morphological point instead of the *CoM*.

### 9.3.3.3. Turn radius

The *Trad* of the *CoM*, the *Pelvis*, *Head*, and *Feet* were calculated directly with SIMI motion, using the *3D* point's positions (*x(t),y(t),z(t)*) and the Frenet-Serret (Serret, 1851; Frenet, 1852) formula:

$$Trad(t) = \sqrt{\frac{(x'^2 + y'^2 + z'^2)}{(z'' \cdot y' - y'' \cdot z')^2 + (x'' \cdot z' - z'' \cdot x')^2 + (y'' \cdot x' - x'' \cdot y')^2}}$$

**Eq. 9.13**

where primes and double primes refer to first and second derivatives with respect to parameter t.

125

The time course of the differences between the *CoM*'s *Trad* and the other morphological point (*Trad_diff*) were given as percentage differences and calculated as follow:

$$Trad\_diff(t) = \frac{Trad_{CoM}(t) - Trad_{point}(t)}{Trad_{CoM}(t)} \cdot 100$$

**Eq. 9.14**

### 9.3.4. Statistical analysis

For *Epot*, *Ekin*, and *Trad* parameters, one way ANOVA and Bonferonni post-hoc test were used to compare the values from the *CoM* to the *Head*, *Pelvis* and the *Feet* respectively at every one percent of the turn cycle. Significant differences (total %) of the turn cycle between the *CoM* and the other morphological points for these parameters were calculated. The 95 % limits of agreement (±1.96 * *SD*) are given to show the evolution of the disparity between athletes during the turn for *Epot_diff*, *Ekin_diff* and *Trad_diff*. A one way ANOVA with Bonferoni post-hoc test was also used to assess a statistical difference between the *CoM* and the morphological points of the average *Ekin* of the turn, *Tentry*, and *Texit*, given as mean ± *SD*. Finally, the 95 % limits of agreement of the average *Ekin* and *Epot* on the whole turn cycle are calcuated. For all statistical analyses, significance was accepted at *P* < 0.05.

## 9.4. Results

### 9.4.1. Potential energy

Using the Head instead of the *CoM* to estimate *Epot* led to 63 % of the turn in total that indicated significantly different values. During the turn, the 95% limit of agreement representing the variability between the athletes indicated a ± 0.62 J/Kg interval around the averaged curve, and the 95% limit of agreement of the average difference with the *CoM* over the whole turn represented a ± 1.20 J/Kg interval. The corresponding curves are plotted on *Figure 9-2A*.

When the *Pelvis* was used instead of the *CoM* to calculate the *Epot*, significantly different results were obtained for 9 % of the turn cycle. The

variability between athletes for the *Epot_diff* indicated a ± 0.37 J/Kg interval around the averaged curve for the 95 % limit of agreement. On average, the 95 % limit of agreement indicated a ± 0.39 J/Kg interval over the whole turn cycle. *Figure 9-2B* shows the evolution of the *Epot_diff* between the *CoM* and the *Pelvis*.

Concerning the use of the *Feet* to estimate *Epot* parameters, 82% of the turn had significantly different results compared to the values given by the *CoM*. As seen in *Figure 9-2C*, the *Epot_diff* showed ± 1.15 J/Kg variability between athletes for the 95 % limit of agreement, and an interval of ± 1.92 J/Kg for the average *Epot_diff* for the 95 % limit of agreement on the whole turn cycle.
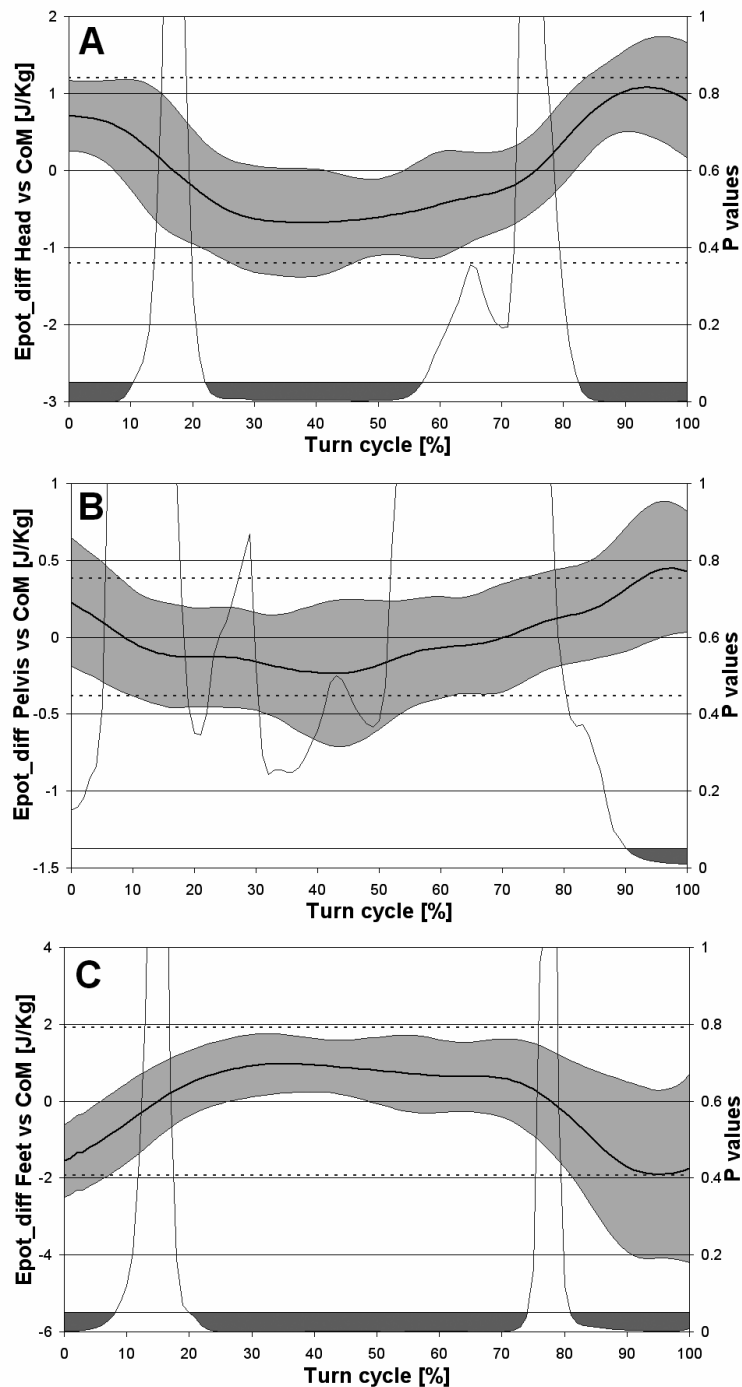
**Figure 9-2: A-B-C.** *The potential energy differences between the CoM and the Head, Pelvis and Feet respectively during a turn cycle. The bold black curve represents the potential energy difference over the whole turn for each morphological point compared to the CoM. The light grey area around the curve corresponds to the 95 % limits of agreement and represents the variability between athletes. The dotted horizontal line indicates the average 95 % limits of agreement over the whole turn. The evolution of P values for the Bonferroni Post-*

*hoc test are also plotted, indicating in dark grey the portions of the turns were it is statistically possible to differentiate the CoM with the other analysed point.*

### 9.4.2. Kinetic energy

*Figure 9-3A* shows the evolution of the *Ekin* values over the turn cycle for the different analysed points. From the *Ekin* calculations, it can be seen that the Head induced significantly different values for 30% of the turn compared to the results obtained using the *CoM*. The variability between athletes indicated a ± 3.48 J/Kg interval for the 95 % limit of agreement. The *Head* induced a significant underestimation of -2.57 ± 1.22 J/Kg ($P <$ 0.001) when calculating the average *Ekin* and an interval of ± 2.39 J/Kg for the corresponding 95 % limit of agreement. *Figure 9-3B* represents the evolution of the differences during a turn.

Over the whole turn cycle, estimating *Ekin* with the *Pelvis* induced no significant differences compared to using the *CoM*. The variability of the athletes around the averaged *Ekin_diff* curve represented a ± 2.70 J/Kg interval for the 95 % limit of agreement. No significant difference were found for the average *Ekin* (-0.22 ± 0.93 J/Kg, $P =$ 1.000) and the 95 % limit of agreement corresponded to a ± 1.83 J/Kg interval. *Figure 9-3C* illustrates *Ekin_diff* for the *Pelvis* compared to the *CoM*.

For the calculation of *Ekin*, using the *Feet* instead of the *CoM* led to significantly different values for 57 % of the turn cycle. The 95 % limit of agreement representing the variability of athletes around the average curve indicated a ± 5.22 J/Kg interval. The *Feet* also induced a significant overestimation of the average *Ekin* (5.77 ± 4.00 J/Kg ($P <$ 0.001)) compared to the result obtained with the *CoM*, and the 95 % limit of agreement indicated an interval of ± 7.84 J/Kg. *Figure 9-3D* displays the evolution of the *Ekin* curve during the turn cycle.
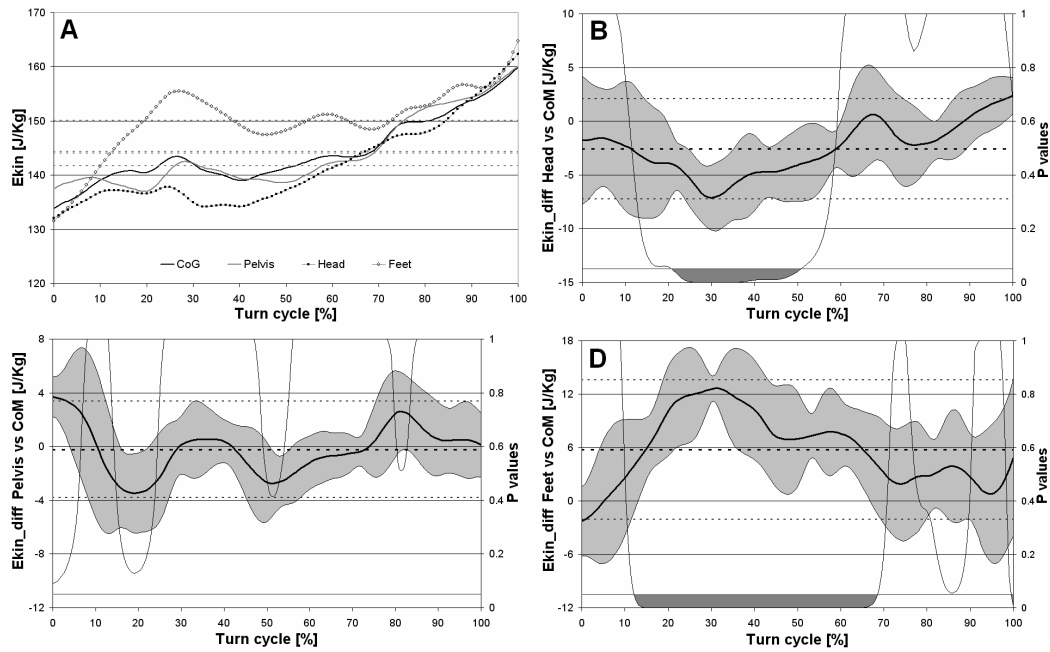
***Figure 9-3: A:*** *Kinetic energy of the athletes during a turn cycle calculated using the 4 analyzed points;* ***B-C-D:*** *The mean differences between the Ekin calculated based on the CoM and on the Pelvis, Head and Feet respectively are shown (black curves) with the corresponding 95 % limit of agreement (grey intervals around the curves), indicating the variability between athletes. The average differences over the turn cycle (dotted bold horizontal line) as well as the corresponding 95 % intervals of confidence (the dotted horizontal lines) are drawn. The evolution of P values for the Bonferroni Post-hoc test are also plotted, indicating in dark grey the portions of the turns were it is statistically possible to differentiate the CoM with the other analysed point.*

### 9.4.3. Turn radius

*Figure 9-4A* shows the evolution of the *Trad* values over the turn cycle for the different points. For the analysis of *Trad*, the results obtained using the *Head* indicated significant differences for 19 % of the turn. Evolution of the *Trad_diff* is described in *Figure 9-4B*, also showing the 95 % limit of agreement of the difference (± 22.02 %). *Texit* (74.67 ± 4.64 %) was significantly different from the *CoM* (84.67 ± 2.58 %, $P < 0.001$), whilst *Tentry* showed no significant difference (14.50 ± 3.02 % for the Head versus 12.33 ± 2.88 % for the *CoM*).

In the case of the *Pelvis*, only 7 % of the turn led to significantly different values to those obtained using the *CoM*. The curve representing *Trad_diff* is plotted on *Figure 9-4C* as well as the 95 % limit of agreement (± 44.82 %). There were no significant differences in the timing of *Tentry* (13.17 ± 3.19 % for the *Pelvis* versus 12.33 ± 2.88 % for the *CoM*), and *Texit* (84.17 ± 5.64 % versus 84.67 ± 2.58 %).

The use of the *Feet* to estimate *Trad* revealed that 33 % of the turn cycle had significantly different values. *Figure 9-4D* draws the *Trad_diff* between the *CoM* and the *Feet* with their corresponding 95 % limit of agreement (± 52.84 %). Both *Tentry* and *Texit* calculated with the *Feet* (6.50 ± 3.02 and 90.50 ± 1.98 respectively) were significantly different from values obtained for the *CoM* (12.33 ± 2.88, $P$ = 0.015 and 84.67 ± 2.58, $P$ = 0.048 respectively).
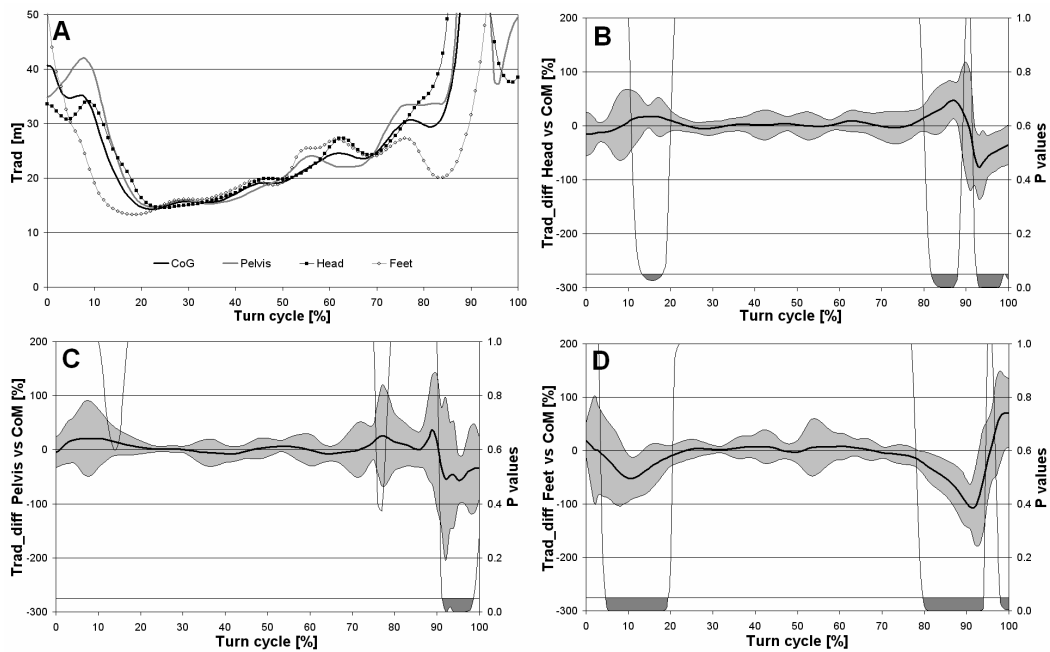


**Figure 9-4: A:** *Turn radius of the CoM, the Head, the Pelvis and the Feet during the turn.* **B-C-D:** *The differences between the trajectory's radius of the CoM and the Pelvis, the Head and the Feet respectively are shown with the corresponding 95% intervals of confidence in light grey. Evolutions of P values for the Bonferroni Post-hoc tests are also plotted in dark grey.*

## 9.5. Discussion

The most important finding of this study was the really good match between the *Pelvis* and the *CoM*. Indeed, when looking at the different parameters analyzed, the *Pelvis* offered the best estimation for the *Epot*, *Ekin* and *Trad* calculation. No significant differences were found for the *Ekin* during the whole turn whilst only 9% and 7% of the turn significantly differed in the case of the *Epot* and *Trad* respectively. These differences were encountered only at the end of the turn. Moreover, the small difference in the *Trad* should be put in perspective, as a 100 m or a 200 m radius during turn transitions would not affect the overall trajectory of the skier.

As a global observation, it is quite intuitive to see the *Feet* and the *Head* as extreme points of the skier, while the *Pelvis* is more centred and near the *CoM*. Nevertheless, the *Head* allowed slightly better estimations than the *Feet* for the analysed parameters showing more similar patterns of the *CoM*. The angulation of the hips during the second steering phase can probably explain this result, as the Head was more centred on the *CoM* trajectory and the *Feet* were more outside. With respect to inter-athlete variability, the magnitude of the interval used to estimate *Epot* and *Ekin* in increasing order was offered by the *Pelvis*, *Head* and *Feet*.

### 9.5.1. Energy

As the potential energy is linearly related to vertical displacement, the curves of *Epot* obtained in this study have been compared to those of Pozzo et al. (Pozzo et al., 2005), who calculated the vertical displacement of the *CoM* compared to the ground. This has been assimilated to the difference between the *CoM* and the *Feet* determined in the present study. As expected, the *CoM* was higher during transitions between turns and lower at gate crossings. This corresponds well to the *Epot_diff* between the *CoM* and the *Feet* found in the present study.

As the *Ekin* values depend on the square power of the speed, the shape of the curves obtained in this study have also been compared to those obtained by Pozzo et al. (Pozzo et al., 2005) for the speed of the skiers

during the turns. The measured speed attained its maximal value during gate transition, as it does in the present study.

Supej (Supej, 2008) and Reid (Reid et al., 2009) analyzed the mechanical energy of skiers (*Emech*), which involved addition of the *Ekin* and the *Epot*. They also calculated the corresponding dissipated energy (*Edissip*) as the change in mechanical energy per change of vertical distance (Supej et al., 2005b). To provide accurate comparison, *Figures 9-5A* and *9-5B* show the *Emech* and the *Edissip* respectively, calculated using the *CoM* and the morphological points of the present study.
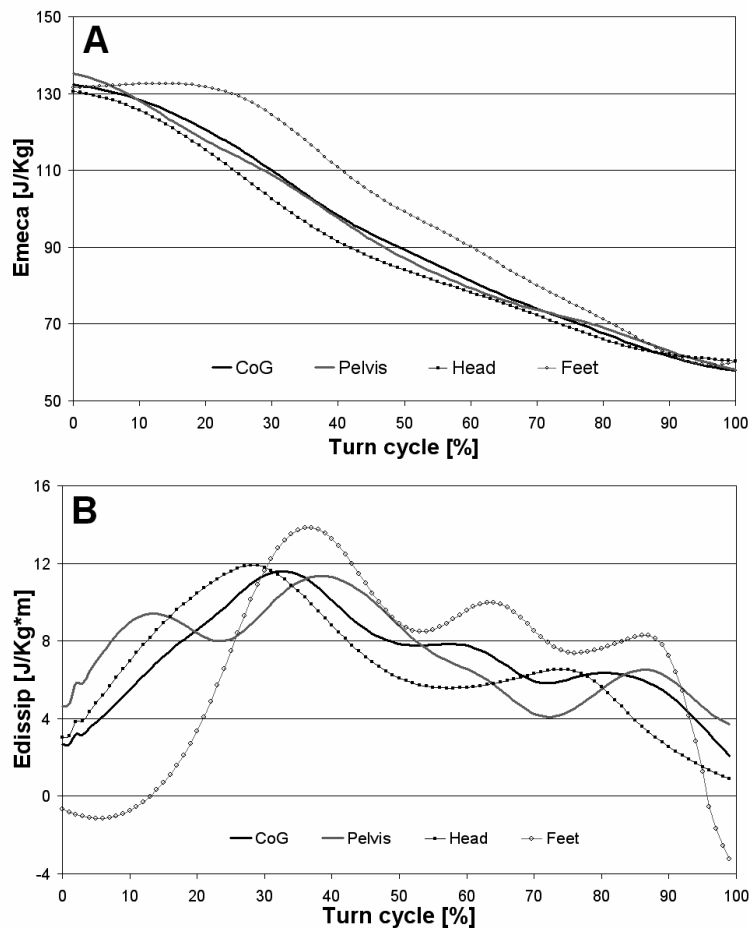


***Figure 9-5: A:*** *Mechanical energy calculated using the CoM and the morphological points,* ***B:*** *Energy dissipation during the turn.*

The curves obtained for the *CoM* are very similar to those obtained by Supej (Supej, 2008) in giant slalom and Reid (Reid et al., 2009) in slalom. The minimum energy dissipation occured at the turn transition and the

maximum during the first steering phase, between 20 % and 40 % of the turn cycle.

### 9.5.2. Turn radius

The *Trad* described by the *Feet* trajectory begun earlier and ends after the *Trad* of the *CoM*. The *Head* also finished the turn earlier than the *CoM*. Therefore, the *Head* had the longer time interval between two turns where its trajectory was almost straight, and the *Feet* had the shortest time interval with a straight trajectory. It was interesting to note that around the gate crossing, inter-athlete variability increased, suggesting that the gates induced perturbation. If the radius dropped during the transition phase to reach its minimum, the radius increased gradually during the steering phases. Supej (Supej, 2008) obtained a curve of a similar shape when calculating the *CoM*'s turn radius of four athletes performing giant slalom. For slalom turns, Reid (Reid et al., 2009) obtained a different curve in slalom, where the radius decreased slowly during the first part of the turn and increased rapidly at the end of the turn, without any greater variability at the gate crossing. This probably indicates a higher interference of the gate in giant compared to slalom.

The *Feet* trajectory radii showed a small reduction between the second steering phase and the transition phase, when the skier decided to engender the new turn. It was at this same moment that the skier made a longitudinal extension, when the *Epot_diff* between the *CoM* and the *Head* increased, at approximately 80 % of the turn cycle (*Figure 9-3A*).

Once again, the *Pelvis* gave the best approximation of the *CoM* concerning turn radius, followed by the *Head*. The *Feet*, with a time lag in the turn radius did not offer a good approximation of the *CoM*'s *Trad*, but it could be interesting to further explore the radius reduction around 85 % of the turn. Indeed, it may be possible that this radius reduction coincides with an increase in the force and an extension of the skier to trigger the next turn.

It is the first time that morphological points of the body have been used to estimate energetic parameters of alpine skiers. The results obtained with

the *Pelvis* offered very accurate approximations of the *CoM* and can be used to simplify further analyses. The *Head* also offered a good approximation for overall energy analysis and is a very accessible point for *3D* video tracking or *GPS* antenna placement, but side leaning profiles induced inaccurate estimations in the middle part of the turn. Finally, the Feet did not allow for a good estimation of the *CoM* as most of the parameters did not even have curves that look like those described by the *CoM*.

# 10. Study 6:

## Assessment of Timing and Performance based on Trajectories from low-cost GPS/INS Positioning

Adrian Waegli[1], Frédéric Meyer[2], Stéphane Ducret[3], Jan Skaloud[1] and Roland Pesty[3]

[1] École polytechnique fédérale de Lausanne, Switzerland

[2] Université de Lausanne, ISSEP, Switzerland

[3] TracEdge, Grenoble, France

## 10.1. Introduction

Traditionally, development and testing of materials or equipment has been based on repeated measurements with resources including timing cells or wind tunnels. Similarly, the analysis of athletes' performance often relies on techniques such as measuring race segments (chronometry) or video recordings. These methods however, either appear vulnerable to meteorological conditions (e.g. video), present the difficulty of replicating the posture and movements of test subjects from one trial to the next or have a discrete character (e.g. timing). On the other hand, researchers, coaches and athletes are interested in observing certain phenomena continuously and under all conditions. Satellite-based positioning offers continuous observation of the athletes' trajectory (timing, position, velocity). When coupled with inertial navigation systems (*INS*), it further allows observing accelerations and orientations. Not until recently, the cost, processing complexity and bulkiness of the *GPS/INS* technology often discouraged its regular employment (*Figure 10-1*). (Waegli and Skaloud, 2007a) have introduced an economic and ergonomic GPS/INS system based on differential *L1 GPS* receivers and Micro-Electro-Mechanical System (*MEMS*) inertial measurement units (*IMU*). In this paper, we first assess the accuracy of such low-cost system by comparison to a more precise reference. Then, we use its output to derive the ski's edging and skidding angles to illustrate the new possibilities in the application of this technology. Finally, we derive timing information and compare its performance to the chronometry provided by timing cells.

## 10.2. Methods

*MEMS-IMU*s are subject to large random and systematic errors (biases, scale factors, misalignment, and noise) which need to be suppressed in order to provide useful information on orientation and displacement. For instance, typical uncalibrated biases of a *MEMS* accelerometer reach 0.5 m/s2 which deviates the position by 50 m in 10 s. A solution for calibrating these errors consists in the integration of *MEMS-IMU* with satellite positioning where the *GPS* antenna is tightly attached to the inertial

sensors. However, the conventional *GPS/INS* integration strategies (Titterton and Weston, 1997) need to be adapted due to the error characteristics of the *MEMS-IMU* sensors (Waegli et al., 2007).
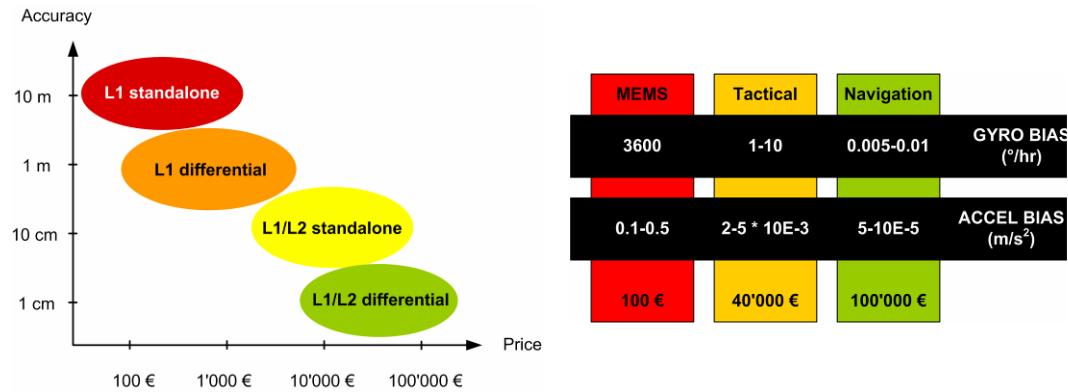


***Figure 10-1:*** *Accuracy versus prizing of current GPS (differential) methods and IMU hardware.*

To evaluate the position, velocity and orientation accuracy of the low-cost system, this one was mounted on an athlete together with a reference provided by dual-frequency *GPS* receivers and a tactical-grade *IMU*. The differential *L1 GPS* solution at 1 Hz was integrated with the triple-axis accelerometer and gyroscope measurements of the *MEMS-IMU* provided at 100 Hz. The reference system (Skaloud et al., 2006) yields cm accuracy for position, cm/s for velocity and 1/100° for orientation (*Figure 10-2*).
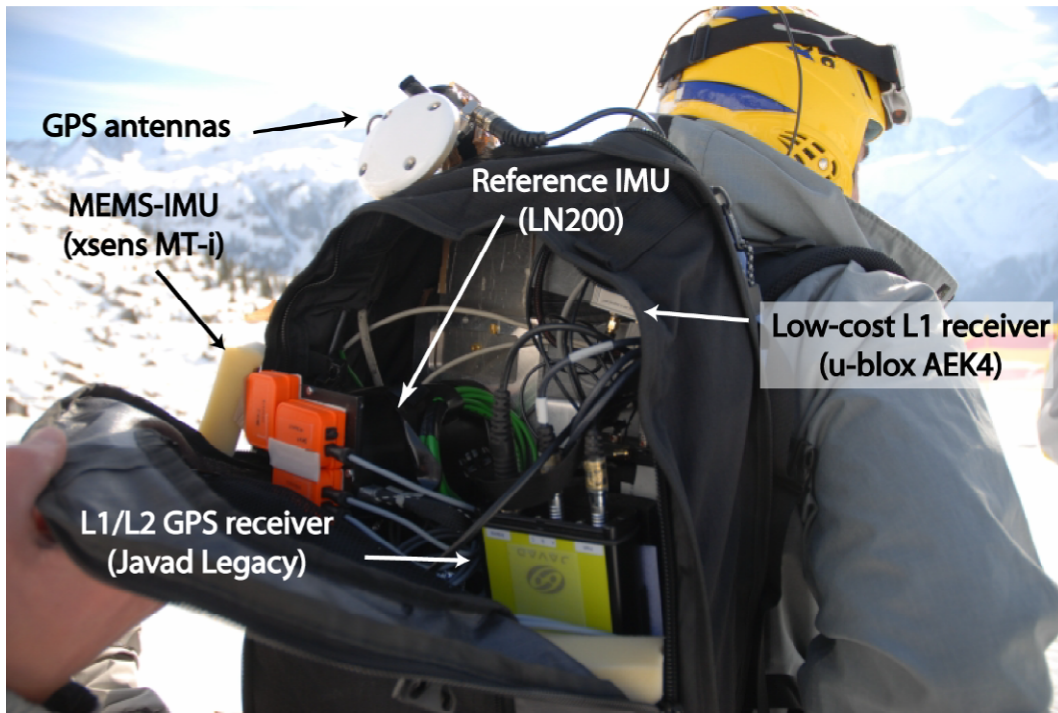
***Figure 10-2:*** *Low-cost and reference GPS and IMU mounted on a skier. In order to compare the systems accurately, all the sensors had to be installed on the same, rigid platform.*

The comparison of 6 runs of a giant slalom showed that the *GPS/MEMS-IMU* system offers mean accuracies (1 σ) better than 0.4 m for position, 0.2 m/s for velocity and 1-2° for the orientation. The accuracy indicators can be used to show clearly when the observed phenomenon is statistically significant as illustrated in *Figure 10-3* (dotted around the trajectory). Simulations outages in *GPS* data unveiled that these can be bridged by inertial navigation up to 10 s while maintaining accuracy (Waegli and Skaloud, 2007b).
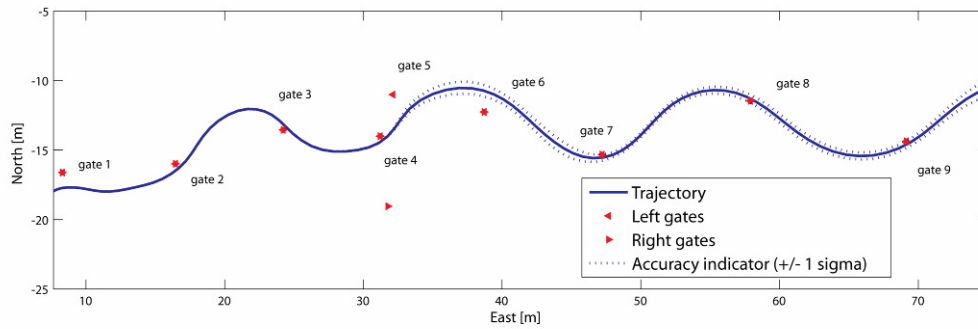
**Figure 10-3:** *GPS/MEMS-IMU trajectory with accuracy indicator (1 σ). Satellite masking decreased the positioning accuracy around gate 6 but the INS helped to bridge the GPS gaps efficiently.*

## 10.3. Resultats

### 10.3.1. Ski Orientation Determination

In alpine skiing, the determination of accurate orientations of a ski is the prerequisite for analyzing forces acting on the ski. Forces need to be decomposed with respect to the terrain in order to analyze potential and kinetic energies, as well as joint loading and energy transfers during a turn. Nowadays, the ski's orientation can be obtained from multi cameras system with a precision of 5 degrees for an object orientation (Richards, 1999). However, this method requires an important infrastructure and is not adapted for every-day use and training purposes. Skis equipped with *GPS/MEMS-IMU* provide a new method which is more accurate, faster, easier to setup and insensitive to the weather conditions. For a complete investigation, both skis need to be equipped with *GPS* and *MEMS-IMU* sensors to recover the position and orientation of both skis.

Based on the slope information derived from a digital terrain model and the trajectory derived from the *GPS/MEMS-IMU* integration, the orientation of the ski with respect to the slope can be computed. The local referential (*x,y,zslope*) is defined as follows (*Figure 10-4*): the *xy* plane represents the local surface with the x-axis aligned to the maximum slope of the terrain (fall line). The heading is the angle between the direction of the maximum

141

slope (*xslope*) and the direction of the ski (*xski*). The roll describes the edging angle of the ski.
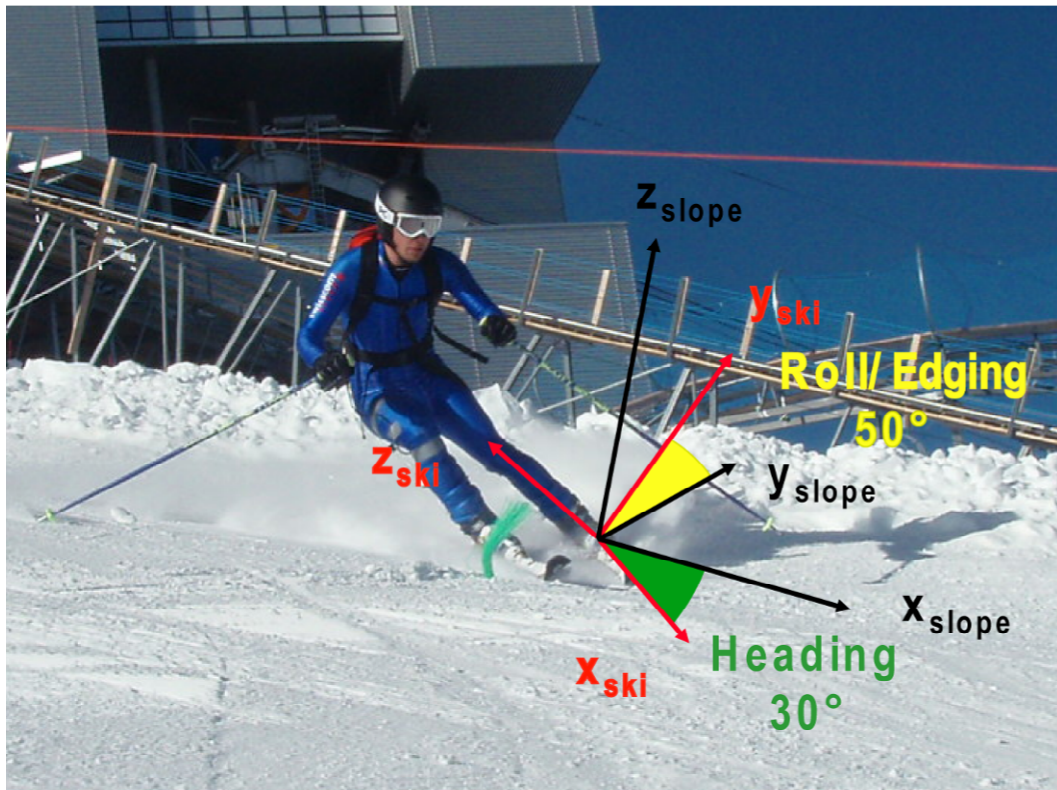


**Figure 10-4:** *Definition of the reference frames and illustration of the heading and roll (edging) angles.*

The zoom on the two turns illustrated in *Figure 10-5* allows studying the technique of the athlete:

During the turn initiation (①), the ski is flat (roll = 0°).

The steering phase of the turn (②) lasts until the ski's orientation reaches the fall line (heading = 0°). During this phase, the roll (edging) angle increases gradually and reaches its maximum (approximately 50°).

The skidding of the skis can be obtained by analyzing its orientation with respect to its velocity vector. In this example, this angle is zero at the initiation (①) and increases during the first phase of the curve (②, *Figure 10-5*). To study the carving and slipping phases of a turn, it is interesting to display the skidding angles with respect to the trajectory (*Figure 11-6*).
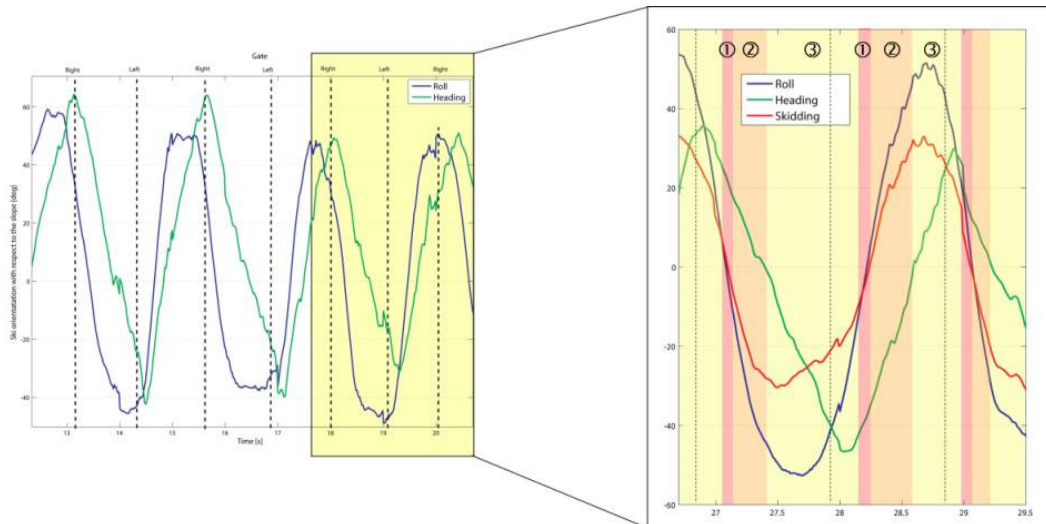
**Figure 10-5:** *Illustration of the roll (edging), heading and skidding angles during two turns.*
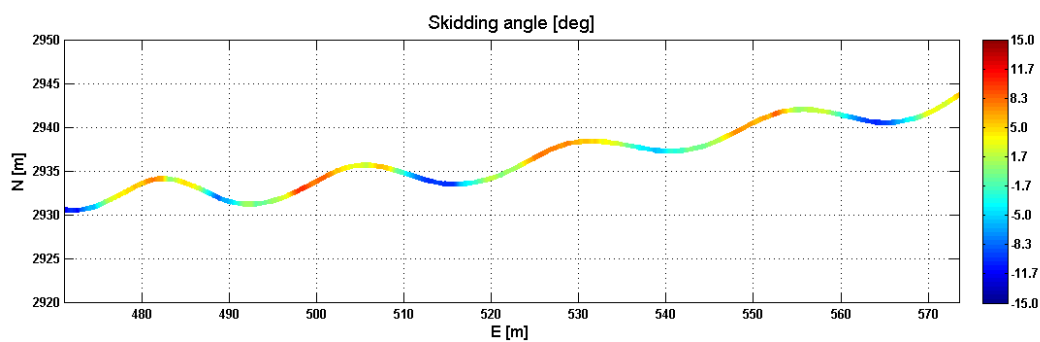


**Figure 10-6:** *Illustration of the skidding angle on the trajectory.*

### 10.3.2. GPS Timing Accuracy Assessment

On the contrary to traditional discrete character of chronometry with timing cells, the timing based on *GPS* (or *GPS/MEMS-IMU*) trajectories is continuous along the whole trajectory. This fact certainly has many advantages: The comparisons can be made over smaller sections (for example between two gates) and it can include topological aspects such as finding an ideal line by comparing different tracks. Furthermore, other parameters related to a defined section of the track (heart rate, velocity etc.) can be compared (Waegli and Skaloud, 2007b). In this section, we investigate the timing accuracy based on positioning.

143

The theoretical accuracy of timing derived from trajectories can be deduced from the following basic relation:

$$\Delta x = v \cdot \Delta t$$

<div align="right">**Eq. 10.1**</div>

Hence, considering a speed ($v$) of 80 km/h and a large (differential) positioning error ($\Delta x$) of 0.4 m leads to a timing error ($\Delta t$) of 1.8/100 s.

To verify this assumption, we set up an experiment where *GPS* synchronized timing cells (DATA Sports FRIWO) were placed along the trajectory. The positions of the gates were determined by static *GPS* sessions with an accuracy of 2-5 cm. As the *GPS* antenna was placed on the athlete's helmet while the timing cells were actuated by the feet, the virtual timing based on the *GPS* trajectory had to be corrected for this difference (*ΔT*). Knowing that *GPS* time is stable at the nano-second level, it was then possible to compare accurately the splits of the timing cells with that based on the trajectory (*Figure 10-7*).



**Figure 10-7:** *Timing cells versus virtual timing derived from GPS.*

After evaluation of 7 runs, an average timing difference ($\Delta t$) of 2.2/100 s was found. This value corresponds to the theoretical model and reflects the positioning accuracy. While timing cells provide only discrete measurements, trajectory-based timing provides a flexible approach which is independent of the skiers' posture. This result also confirms the findings of (Waegli and Skaloud, 2007b) where two pairs of skis were compared based on timing derived from *GPS* and traditional chronometry. There, the timing accuracies achieved with both methods were equivalent.

## 10.4. Discussion

Economical reasons and ergonomic constraints require the employment of small, low-cost *L1 GPS* receivers and inertial sensors of *MEMS*-type. The use of dual-frequency *GPS* receivers would increase the positioning accuracy to the decimeter level while the velocity and orientation accuracy would remain almost unaffected. However, the current pricing of dual-frequency *GPS* receivers restricts their use to a few athletes and applications with high accuracy requirements. To improve the orientation accuracy, higher-order IMU would have to be employed which reduces the portability and increases the cost of the system. An alternative consists in using redundant inertial system, a method which is currently investigated.

Trajectory and timing derived from *GPS/MEMS-IMU* present an interesting alternative to traditional methods applied for material testing and athletes' performance analysis. The presented low-cost system offers additional flexibility through continuous and accurate observation of an athlete's trajectory, including timing, position, velocity, acceleration and orientation. It has been shown that sufficient accuracy can be obtained even with low-cost sensors and that *MEMS-IMUs* are able to bridge lack of *GPS* data efficiently. We also illustrated in an example how these data can be further analyzed to retrieve additional knowledge. For instance by comparing the skis' trajectory with the skis' orientation, the skis' skidding angle can be derived. Integrating the information obtained from digital terrain models allows determining the heading and edging of the skis.

# 11. Study 7:

## Measurements of forces and torques at the skis-binding interface using a new embedded dynamometer

Frédéric Meyer[1], Alain Prenleloup[2], Alain Schorderet[2]

[1] Sport Science Institute, Lausanne University, Switzerland

[2] Mechanical Systems Design Laboratory, Swiss Federal School of Technology, Lausanne, Switzerland

This study presents the early results of an ongoing project in collaboration with the LCSM at the EPFL.

## 11.1. Introduction

In alpine skiing, force platforms were first developed to understand mechanisms leading to knee injuries and to find solutions to improve bindings' safety. Hull and Mote (Hull and Mote, 1974, 1975, 1978) proposed a system consisting of two independent six degrees of freedom dynamometers integrated in the ski, below the bindings. Another design was proposed by MacGregor et al. (MacGregor et al., 1985) aiming at the development of an electronic release binding system recording force data. The binding was integrated between the ski and the boot and the release algorithm was discussed in another article (MacGregor and Hull, 1985). A second generation of devices was presented by Wunderly et al. (Wunderly et al., 1988). They dedicated special attention to maximizing the mechanical decoupling of the load and reducing cross sensitivity between components. However, the accuracy of the system was not clearly defined. Quinn and Mote (Quinn and Mote, 1990) proposed a revised design of Hull's first force platform (Hull and Mote, 1974), equipped with T-shaped shear panel elements (*SPE*) and aiming at predicting constraints sustained by the knee during skiing to prevent injuries. Quinn and Mote (Quinn and Mote Jr, 1992) used their system in addition to a goniometer measuring angle of the ankle to determine forces and moments at the top of the boot and at the knee. Concerned by the possible effect of the bending of the skis on the measure of vertical load, Wimmer and Holzner (Wimmer and Holzner, 1997) developed two different devices measuring vertical reaction forces. The first device was inserted between the skis and the binding and the second one between the binding and the boot. The first design was significantly impacted by the bending of the skis but not the second.

More recently, new systems have been developed allowing measurements of forces and moments on both skis, necessary for a complete understanding of the kinetics. Vodickova et al. (Vodickova et al., 2005a) proposed a device, based on strain gauges, that substituted the plate on carving ski, raising the skier by 6 mm compared to the usual position.

Several studies involving the force platform, based on piezoelectric sensors and developed by Kistler (Kistler AG, Winterthour, Switzerland) have been published since 2001 (Knüz et al., 2001; Lüthi et al., 2005; Klous, 2007). In her study of carving turns, Klous (Klous, 2007) found maximal vertical loads around 2.5 N/Kg on the outer leg. Medio-lateral and anterio-posterior forces were equally distributed between external and internal legs, but a lot smaller than vertical forces (approximately 1 N/Kg for both components). Fore-aft torques were measured between -2 and 2 Nm/Kg for both legs. Maximum abduction-adduction moments measured were around 0.5 Nm/Kg and internal-external rotations moments were approximately 0.3 Nm/Kg on the outside leg. The detailed protocol concerning the Kistler plate validation was published by Stricker et al. (Stricker et al., 2009). Each dynamometer was 3.2 cm height and weighted 1.8 Kg. The achieved sampling rate can go up to 500 Hz. They also studied the effect of temperature and the accuracy of the device..The interactions among components ranged between 0.2 and 3.6 %, depending on the axis and the dynamometers had to be zeroed at the beginning and the end of the measure, to control for the drift induced by piezoelectric sensors. The results showed a very low influence of the temperature and an increase of the relative accuracy with the increase of the constraints. The persisting limitation of all the proposed solutions is the need for material adaptations and the impossibility for the skier to use his own material.

Finally, Kiefmann et al (Kiefmann et al., 2006) developed an interesting force platform. The device could be fixed as an interface between the ski boot and the binding without any modification of the system. Unfortunately, the accuracy of the system was not specified and the platform suffered from mechanical weaknesses. A mock-up of the platform, with similar dimensions (i.e. 4 cm height and 2 Kg each) was used to determine the influence of the material during moguls skiing (Kurpiers et al., 2009). No significant differences were found on kinematic parameters (i.e. knees angles, forward lean of the torso, hips forward and lateral inclinations) when using the devices.

There is a need for fully integrated force platforms, which will allow skiers to ride normally, without their performance and technique being affected by the device. Since there is approximately 2.5 cm unused height between the foot sole and the bottom of the ski boot, this space could be used to place the dynamometer. The aim of this project was therefore to design a compact dynamometer with dimensions that could be placed instead of the boot interface with the binding. In a first step, the prototype will be built as a removable interface inserted between a normal ski boot and the ski. Field test have also been conducted.

## 11.2. Methods

### 11.2.1. Dynamometer design

The force platform was designed to match the length of regular ski booths, i.e., 310 mm to 315 mm, and to be no higher than 25 mm. A standard ski-boot interface was needed on the front and the back part to fit in standard binding systems. Nominal loads were taken from the literature review as well as from theoretical models. The dynamometer was designed to measure maximal vertical forces $Fz$ of 3000 N, lateral forces $Fy$ of 1000 N, torques around the Y axis $My$ of 500 Nm, around the Z axis $Mz$ of 100 Nm, and around the X axis Mx of 150 Nm. Frontal forces Fx were not considered in this development, as they are very low in this direction. *Figure 11-1* shows the axis chosen to describe the platform referential.

**Figure 11-1:** *An athlete in the giant slalom equipped with the platforms and the backpack. The referential of the right force platform is also represented.*

A fully integrated solution was chosen to fulfill the specificied requirements. Strain gauges were positionned on flexible elements, decoupling lateral and vertical loads. *Figure 11-2* indicates the different constraints measured with the force platform. Vertical loads were measured at the front ($Fz_F$) and the back ($Fz_B$) of the platform. Adding the two components gives the forces while substracting them and multiplying them by the distance between the front and the back sensor gives the *My* torque. Lateral loads were also measured at the front ($Fy_F$) and the back ($Fy_B$) of the platform. The addition of the two components leads to $F_y$ while *Mz* torque is measured using the same method as *My* calculation. Finally, *Mx* was measured independently using both front and back sensors. *Figure 11-3* shows the two manufactured and fully equipped force platforms.
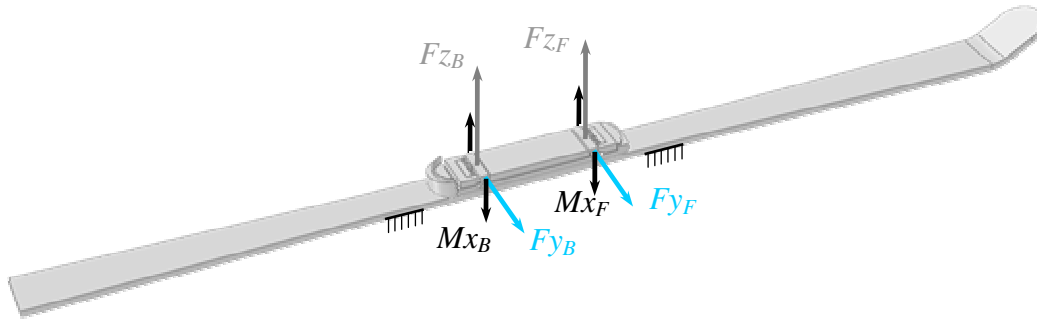
**Figure 11-2:** *Position of the sensors on the platform measuring the different components.*



**Figure 11-3**: *Manufactured force platforms.*

## 11.2.2. Calibration

Calibration tests were performed in laboratory to determine the relation between applied loads and recorded values given by the strain gauges on both the left and right force platforms. Specific situations were tested to determine the calibration coefficients. *Fz*, *Fy* and *Mx* were determined directly, while *Mz* and *My* were derived from *Fy* and *Fz* respectively. Each situation was tested three times and each test contained three trials. 5 loads within the nominal specifications were applied. For *Fz*, the plate was

first tested with the boot attached and mounted on the ski, using three different distances between fixation points (i.e. 0.5, 0.9 and 1.3 m) (*Figure 11-4A, B and C*). Second, off-centered loads were applied on the front and on the back of the platform. *Fy* was tested in a standard manner, applying loads laterally on the plate and finally *Mx* was tested by applying torques with a dedicated tool (*Figure 11-4D*).
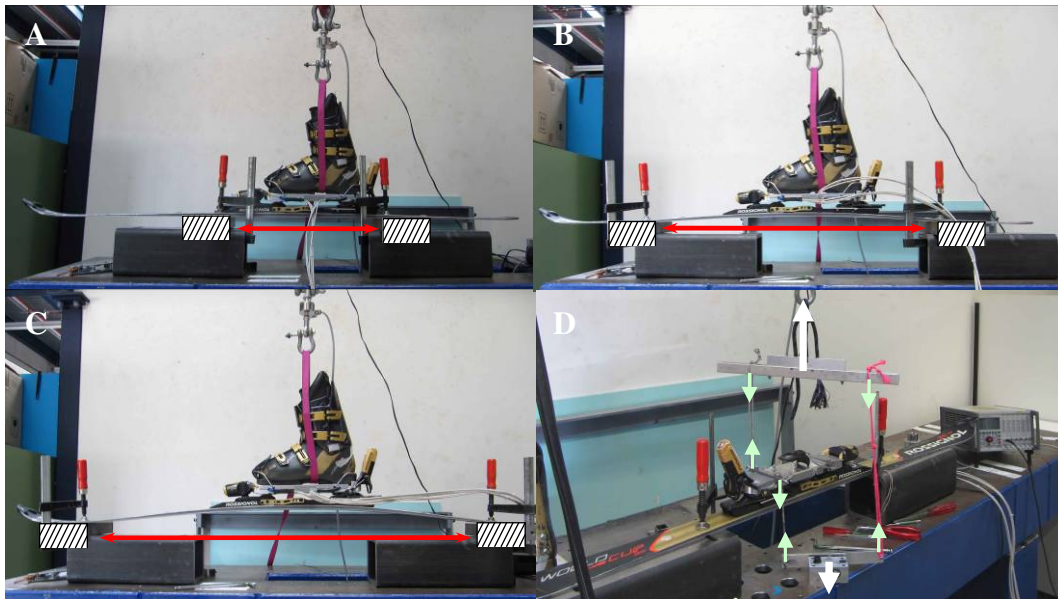


**Figure 11-4:** *Setup used for the calibration. A-B-C: the three different fixation situations. D: The tool for Mx measurements*

For each test, the coefficient of calibration was defined as the applied load divided by the tension measured on the sensor. Average coefficients were then calculated for each component and both force platforms. Coefficients of variation (the standard deviation of the calibration coefficient divided by the average calibration coefficient) were used to determine the accuracy of the measure along the different measured axis.

### 11.2.3. Field test

Three European Cup racers (mean $\pm$ *SD*: total weight with equipment 116.9 $\pm$ 6.5 Kg, height 1.82 m $\pm$ 0.07) participated in the field test. All participants were healthy males without any joint motion problems. The study was conducted according to the 1964 declaration of Helsinki and written informed consent was obtained from each subject prior to

participation in the study. In parallel, the study was approved by the local ethics committee.

Each participant was asked to perform three runs in a giant slalom composed of six gates set up with a linear gate distance of 24 m, and a lateral offset of 9 m. The slope's inclination angle was approximately 22 degrees. During the first three gates the athletes increased and stabilized their speed. Data for the analysis was recorded during gates four and five. The last gate was placed to keep the rhythm. Data was recorded with a frequency of 500 Hz in a datalogger placed in a backpack (*Figure 11-1*).

The raw data obtained was filtered using a moving average on a 5 points window. For each axis of mesure and each participant, mean and standard deviation were calculated. Participant's averages during a turn cycle are proposed in [N/Kg] to allow comparison of athletes of different weights. The 95 % limit of agreement (±1.96 * *SD*) is also plotted to show the disparity between athletes. The evolution of the load distribution between the outside and the inside skis is also represented for a turn cycle.

## 11.3. Results

### 11.3.1. Calibration:

The coefficient of variation on *Fy* and *Mz* calibration was 4.2 % of the applied load, 9.6 % for *Fz* and *My*, and 2.5 % for *Mx*.

### 11.3.2. Field test:

Data from the first run of each participant was removed due to the inconsistent results obtained compared to the other two runs. *Figure 11-4* illustrates the average results obtained with the two platforms for both inside and outside skis. For *Fy*, an average standard deviation within athletes' runs of 19.20 N was calculated, which represents 13 % of variation compared to the maximum load. The calculated *SD* was 109.11 N, or 9 % of variation for *Fz*, 46.13 Nm (12 %) for *Mx*, 202.21 Nm (13 %) for *My* and 57.50 Nm (19 %) for *Mz*.
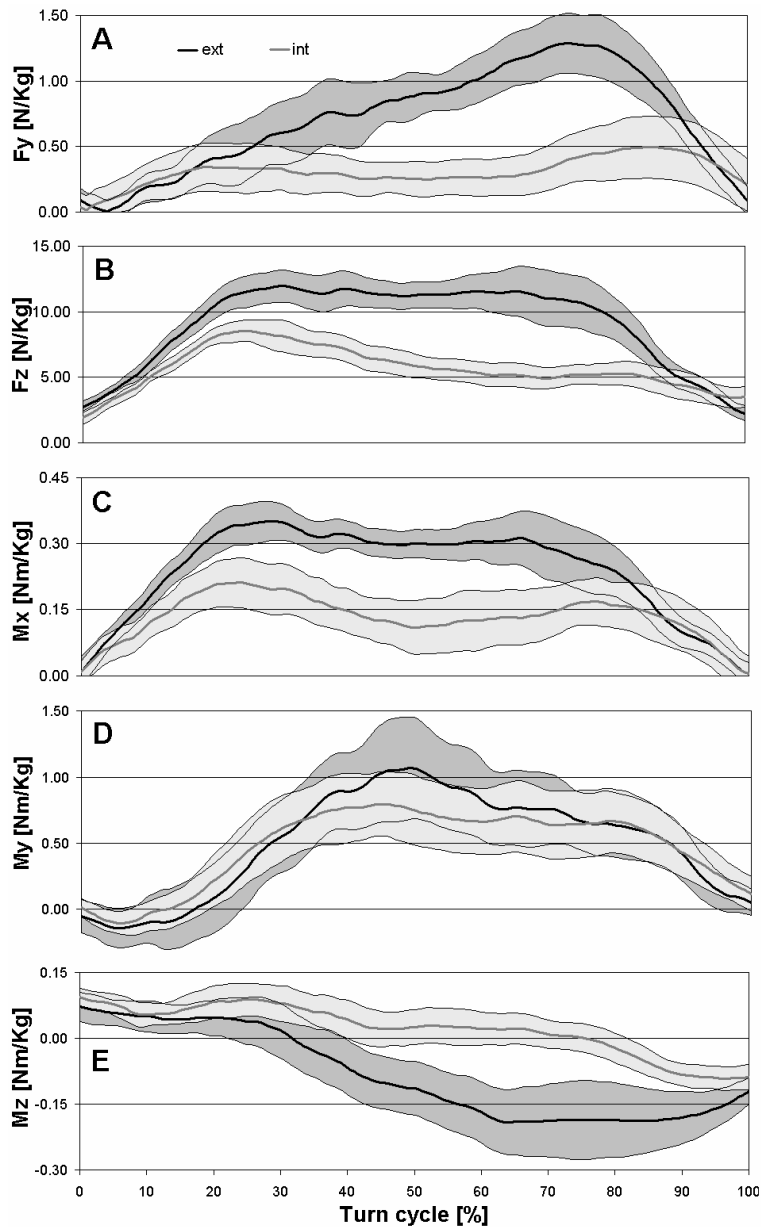
**Figure 11-5:** *Mean Fy (**A**), Fz (**B**), Mx (**C**), My (**D**), Mz (**E**) of 3 skiers and two runs for both skis during a turn cycle, with the 95 % limit of agreement (grey area).*

To highlight the load distribution between the skis, *Figure 11-5* plots the force distribution on the external versus the internal ski, as well as the torques along the turn cycle. The 50 % bold line represents an equal distribution. Parts of the graph on the right of that line indicate a higher proportion of load on the external ski, while parts on the left indicates higher load on the internal ski. *Fy* in *Figure 11-5A* indicates a distribution of about 80 % on the outside ski from 50 % to 70 % of the turn cycle. The

maximal sum of *Fy* int is attained around 80 % of the turn cycle. *Fz* in *Figure 11-6B* shows an upper limit of the external ski load at approximately 1.20 N/Kg. The limit is attained at 30 % and maintained until 70 % of the turn cycle. Regarding *Mx*, *Figure 11-6C* offers a pattern similar to *Fz*, while *My* on *Figure 11-6D* indicates a very balanced distribution of the fore-aft torque between skis.
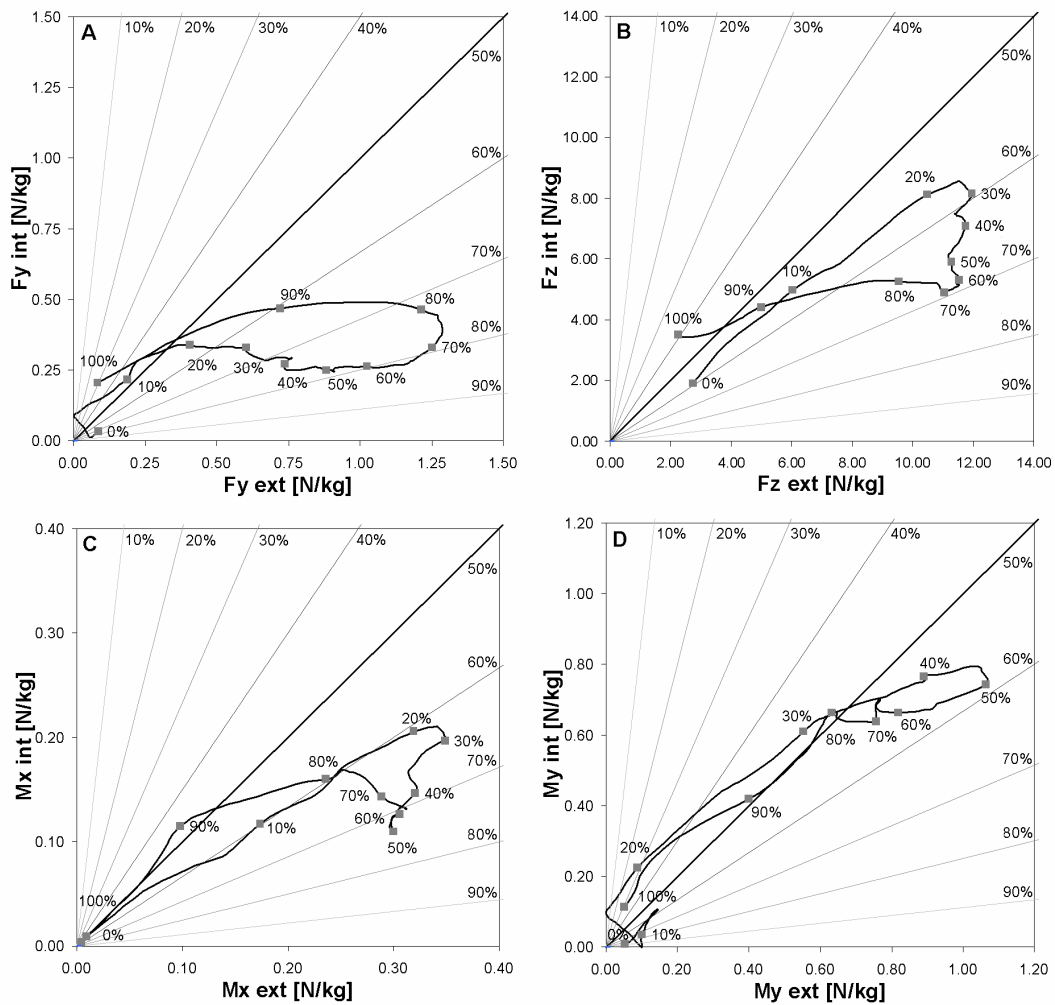


**Figure 11-6:** *Mean Fy (**A**), Fz (**B**) Mx (**C**) and My (**D**) loads distribution between external and internal ski along the turn cycle of 3 skiers and two runs for both skis during a turn cycle.*

## 11.4. Discussion

The main result of this study is the low percentage of error obtained for the calibration of the different components. Moreover, results obtained during the field tests indicated low variability between athletes as seen by

standard deviations ranging from 9 % to 19 %. This total variability measured includes both the variability inherent to the measurement system as well as the disparity between athletes. These low values are probably due to a good reproducibility of the system measurement as well as the very good and homogenous level of the skiers. Indeed, it has been demonstrated that skiers with higher skills are more capable of reproducing the exact same motion patterns than intermediate skiers (Müller et al., 1998). Every first trial of each participant had to be removed from the treatment as they were all inconsistent with the other two runs. This problem is probably due to the fitting of the platform inside the binding during the first turns leading to some small movements measured as noise during this first run. Further experiments should include one or two free runs before beginning recording. This issue could also question the start process and first few gates during races. Indeed, athletes put their skis on just before starting and their boots might not be perfectly fitted in the binding during the first part of the race.

The graphs obtained with the force platform are coherent with the results obtained by Klous (Klous, 2007) and Lüthi (Lüthi et al., 2005). Most of the total forces acting between the skier and the skis are measured on $Fz$ and a higher load is measured on the outside ski. Vodickova (Vodickova et al., 2005b) obtained similar results for $Mx$, with higher torque on the outside ski. The amplitude and distribution of $Fy$ found in this study are similar to the results obtained by Lüthi (Lüthi et al., 2005).

The graph representing the load distribution obtained for $Fy$ is different from $Fz$ (*Figure 11-6A* and 11-*6B* respectively). $Fy$ shows a progressive increase of the forces on the outside ski while the load on the inside remains constant. On the contrary, $Fz$ quickly reached a maximal load on both skis, followed by a decrease of the forces on the inside ski while the load on the outside ski remained constant until the next turn transition. Fore-aft movements, illustrated by $My$, indicated similar torques on both skis, with the skier leaning backwards during the turn transition and forward during the first steering phase.

The particularity of a force platform inserted as an interface between the binding and the ski boot led to several issues. The link between the ski boot and the dynamometer can be well controlled through design. Ski bindings have different designs and release systems meaning that the force platform is held differently depending on the bindings and the measurements could be affected. In this study, the skiers had the same binding manufacturer, but the effects of using different bindings should be investigated. Moreover, each first run performed by the skiers indicated adjustments of the plate interface in the binding, biasing results. Familiarization test should be provided before the real test to allow the binding to fall right into position and the skier to get used to the material.

Combined with kinematics measurements, the developed system allows a quantification of loads acting on the knee as proposed by Klous et al (Klous, 2007). Moreover, ground reaction forces determined with the force platform will allow accurate quantification of the work produced by skier muscles while performing turns. Finally, as described in the introduction, the system size makes it possible to insert it in the sole of a ski boot. The acquisition system could be significantly reduced in size and inserted on the back of each ski boot, offering a fully integrated force platform.

# 12. Conclusions

The main purpose of the present work was to determine the work produced by elite alpine skiers to increase their kinetic energy. Several steps were needed to reach this goal. First, dedicated tools were developed to allow accurate synchronization of different measuring devices (**study 1**) and to estimate aerodynamic drag coefficient of skiers performing turns (**study 2**). Additionally, a first prototype of an embedded force platform was developed to measure ground reaction forces (**study 7**). Second, skiers' technique was quantified using energy principles. Total energy balance was investigated (**study 3**), as well as work produced by the athletes during turns (**study 4**). Finally, two functional tools were examined to assess their suitability for simplified tests and analysis The accuracy of a method using a single point to estimate kinematic parameters of alpine skiers was compared to that of full body motion kinematics. Results showed that this is a suitable alternative for simplified analysis (**study 5**). A device composed of a low cost *GPS* and *IMU* sensors to determine the drift of the skis during turns was tested and proven to provide satisfactory measurements (**study 6**).

The overall idea of this project was not only to provide analysis of alpine skiing complex mechanisms, but also to develop tools dedicated to alpine skiing environment. The synchronization device developed in the **study 1** (Meyer et al.) answer to the difficulties encountered by Stricker (Stricker et al., 2009) and Klous (Klous, 2007), who needed to record a jump at the beginning of the experimental trial to synchronize (post field processing) the force platform to the video frames. The developed device therefore shortens post processing time as images are taken simultaneously with all cameras, without having to use methods such as software genlock to recover temporal delays between the different camera frames (Pourcelot et al., 2000; Kwon et al., 2004; Reid et al., 2009). Finally, the devices also simplify material set up as no cables are required and each camera can be placed independently of the terrain configuration, thereby having a

significant impact on the *3D* reconstruction accuracy (Nachbauer et al., 1996).

The second methodological contribution of this work was the development of an experimental model aiming at estimating aerodynamic drag coefficient of skiers depending on the evolution of their posture while performing turns (Meyer et al., In press). Aerodynamic drag is a very complex mechanism impossible to measure directly on the field. It was therefore important to provide a functional method to determine this factor based on accessible parameters. Barelle et al. (Barelle et al., 2004) proposed another model based on different parameters and reaching approximately the same accuracy, but no practical application of the model was proposed. Aiming to analyse factors affecting energy dissipation in slalom, Reid (Reid, 2010) used a virtual mannequin of the skier to estimate his frontal area and took drag coefficients from existing literature to determine aerodynamic coefficient. He pointed out the limitations of such method and the need for accurate aerodynamic drag measurements to achieve precise analysis of energy dissipation in slalom. The models developed in **study 2** resolve several of these limitations such as frontal area measurement and drag coefficient determination, but some other limitations remain. Air density should be controlled and wind speed during testing should be carefully measured even if lateral wind could not be integrated in the models. In the present study, a validation of the developed models was proposed, verifying the accuracy of the method through previously acquired wind tunnel data,. The proposed models allow the estimation of the evolution of aerodynamic drag during ski turns, the comparison of efficiency of different techniques and they even provide a tool to virtually test results of different sequences of movements through computer simulation.

A recent method based on energy dissipation has been proposed to analyse the efficiency of the skier during slalom turn (Supej, 2008; Reid et al., 2009). Nevertheless, if the method indicates where skiers loose the most energy, it doesn't investigate the causes of that energy dissipation. Based on **study 1** and **2**, it has been possible to investigate the intrinsic

factors influencing energy balance of skiers performing giant slalom turns (**study 3**) (Meyer and Borrani, 2010). Kinetic and potential energies were calculated, aerodynamic drag estimated using the experimental model and ski-snow friction coefficient deducted using least square method. The friction coefficient was assumed constant, leading to a residual energy in the energy balance. Positive residual energy was found at the end of the turn and during the turn transition. This corresponds well to the negative energy dissipation found by Supej (Supej, 2008) and Reid (Reid et al., 2009) in slalom. Nevertheless, the methodology used in this work suffers from an important limitation: ski-snow friction coefficient is simplified to its minimum and a more accurate model should be developed. The assumptions that turns are fully carved, and that the friction coefficient is constant and equal for all skiers are really restrictive and could lead to important estimation errors. Reid (Reid, 2010) used a similar methodology in slalom without calculating the friction coefficient and just attributing the part of energy dissipation that is not due to aerodynamic drag to the snow friction force. The negative energy dissipation was explained by the skier's muscle contribution, corresponding to 3 % of the gravitational force contribution. The energy balance analysis led to a first estimation of human muscle work contribution to the increased energy of the skier, but several questions and hypothesis arose from this finding. The skier usually moves up at the end of the second steering phase to transit to the new turn. This movement coincides with the increase of the skier total energy during turn transitions. However, this vertical movement should not modify permanently the total energy as the skier moves back down during the next steering phase, loosing the previously earned energy.

The pumping mechanism first described by Mote and Louie (Mote and Louie, 1983) can also be useful to understand energy generation during turns. These authors applied the swing pumping principle to estimate the best way to increase speed when passing on undulating snow surfaces by pumping and rocking, and generalized the idea to skiers' turns. They observed that the best strategy was to make an extension with backward movement when forces were the highest. Brodie (Brodie et al., 2008)

found similar results in giant slalom with positive energy generation when ground reaction forces are at the highest during the steering phases. Reid (Reid, 2010) also found generation of energy in slalom, but with a different timing. Negative energy dissipation was found during transition on a 10 m course and just after turn transition on a 13 m course. An explanation of these patterns can be found in the work of Takahahi (Takahashi and Yoneyama, 2001, 2002), who showed that viewed from above, *CoM* and skis' trajectories are diverging right after the turn transition, when the skier leans inwards. As forces are exerted at this moment in the lateral component, work can be created. During skiing, this phenomenon can happen both in the longitudinal axis or the lateral axis of the skier, when the *CoM* and skis's trajectories are diverging.

An investigation of these mechanisms was proposed in **Study 4**, designed to quantify human work contribution and to estimate internal energies of athletes during the turns. *GRF* was estimated using *3D* kinematic data, and both longitudinal and lateral displacements of the *CoM* relatively to the feet were computed. Longitudinal positive work generated during the turn was not sufficient to explain negative energy dissipation found by Supej (Supej, 2008) and Reid (Reid et al., 2009). Moreover, results gave a small amount of positive work right after the transition phase and a larger quantity at the end of the second steering phase. The effet of the mechanism explained by Takahahi (Takahashi and Yoneyama, 2001, 2002) seems really low at the beginning of the turn in giant slalom. On the contrary, the sum of positive lateral work generated at the end of the second steering phase corresponds to approximately 2 % of the gravitational energy available in a turn. It has been observed that the legs' extension is accomplished at a moment of high *GRF*, in accordance with the work of Mote and Louie (Mote and Louie, 1983), as well as the results obtained by Brodie (Brodie et al., 2008). *GRF* obtained by Reid (Reid, 2010) in slalom are more centred on the gate crossing, perhaps meaning a shift of the template earlier in the turn. Contrary to actions performed on the longitudinal axis of the skier which don't contribute to long term energy increase of the skier's mechanical energy, lateral actions can provide a

meaningful energy intake. The approach proposed in this work (**study 4**) allowed to determine directly the work generated by alpine skiers during turns without complex model requirements and estimations. The main limit of this method was to use *3D* kinematic data to calculate *GRF*. Using a force platform would have led to more accurate results. Nevertheless, the results obtained in this study were comparable with the residual energy found in **study 3**. Indeed, summing the delta of positive residual energy led to a total of about 450 J, representing approximately 4.5 % of the gravitational energy available in one turn. Summing both the vertical and the lateral work components of **study 4** led to a total of 540 J, representing 5.4 % of the gravitational energy. The small difference between the two results could be explained by different factors: the accuracy of the models used in **study 3** to determine the energy dissipation or the limited accuracy of forces calculated in **study 4**. Additionally, one should consider noise as a possible difference factor. The assumption that efficiency of the work provided by the muscles is inferior to 100 %, can explain that the positive residual energy found in **study 3** is smaller than the muscle work calculated in **study 4**. Another factor that could possibly influence the energy balance calculated in **study 3** is the storage of energy in the skis when they are bent during the turn and later released at the end of the turn.

With the objective of simplifying analysing methods in alpine skiing and abolishing the need for complex *3D* kinematic system, **study 5** investigated the use of a single body point to estimate kinematic parameters. Potential and kinetic energy, as well as turn radius were best calculated using the Pelvis instead of the *CoM* as reference. This method allows determining energy dissipation as proposed by Supej (Supej, 2008) and Reid (Reid et al., 2009) using *DGPS* or single point tracking using two or more cameras. The results obtained for the turn radius of the feet can be compared to the distance between the feet and the *CoM* calculated in **study 4**. Body extension happened at the end of the second steering phase simultaneusely as the reduction in feet trajectory radius. This

suggests that work generation is also correlated to a reduction of the turn radius.

Collaboration with the Topo Laboratory of the EPFL led to the **study 6**, analysing a new method to determine skis' trajectories and orientations (Waegli et al., 2009). This tool, based on low cost *GPS* and *IMU* sensors, could be further used to estimate the quality of turns as well as the optimal drifting strategies in giant slalom. The device can also be used as a referential for force platforms, removing the need for *3D* camera measurements. This will also provide the directions of the forces and moments measured by the force platform, useful for *GRF* calculation or inverse dynamics.

Finally, the force platform prototype developed during this project showed the feasibility to integrate such a device in the ski boot, keeping external dimensions intact and staying within the limits set by the FIS rules. Prior works proposed different dynamometers design allowing determination of *GRF*, but skiers had to use material they were not familiar with. However, the prototype proposed in **study 7** doesn't allow measurements of frontal forces. Given the magnitude of vertical loads compared to frontal forces, the authors believe that the noise induced by the vertical load on the frontal component would significantly affect the accuracy. The different designs of ski bindings proposed by manufacturers would also have probably influenced correct measurements. The forces and moments measured on top athletes performing giant slalom revealed a very satisfactory repeatability. *GRF* measured with the force platform offers similar shapes and amplitudes that the *GRF* calculated in **study 4** using kinematics of the skier. Direct measurements have the advantage of proposing differentiation between the two legs, allowing for more precise analysis.

# 13. Perspectives

Following this work, further investigations can be suggested to increase our understanding of alpine skiing biomechanics. The first point consists in proposing further research directions based on the force platform development. The second point discusses the need for accurate ski-snow friction model development and possible improvement for the actual aerodynamic drag model. The third point concerns new techniques for *3D* model reconstruction and finally the fourth point discusses possible ways to improve testing of material to reach the goal of performing scientific experiments without impacting the athlete's technique with measurement devices.

The force platform prototype built in collaboration with the LCSM at the EPFL (**study 7**) should be further developed. A dedicated calibration rack should allow testing of interactions among components, and the platform should be validated with different binding systems. The force platform could then be used to determine precisely *GRF* for both skis, allowing more accurate quantification of human work as proposed in **study 4** and using direct forces measurements instead of video based analysis. The force platform could also be used to determine full body kinetics of skiers with different skills, to investigate potential injury risks depending on the skier's strength and technical abilities.

As seen in the literature review, several attempts to understand and model snow friction have been produced, but no functional tool allowing friction coefficient estimation has been proposed. Future work should investigate ways to model ski-snow friction coefficient of alpine skier performing turns based on different set of parameters. Regression equations could use variables such as skier's speed, snow temperature and humidity, edging angle and skidding angle to estimate friction coefficient. The force platform should then provide reliable *GRF* to calculate accurately the ski-snow friction force.

Aerodynamic drag coefficient estimation could also be further investigated and improved. The main actual limitation is the static position held by the

subjects in the wind tunnel when running the tests, as seen in **study 2**. Indeed, skiers performing turns always have dynamic movements. Their shape changes continuously and the dynamic behaviour of the aerodynamic drag may change accordingly. An idea is to develop a dynamic aerodynamic drag model for skiers performing turns. The participants would have to simulate turns directly in the wind tunnel. Initial tests have been performed, and the results seem promising. *Figures 13-1* gives both the dynamic measurements made in real time in the wind tunnel for two consecutive turns and the corresponding coefficients calculated for each position (with the fourth model developed in the wind tunnel article).
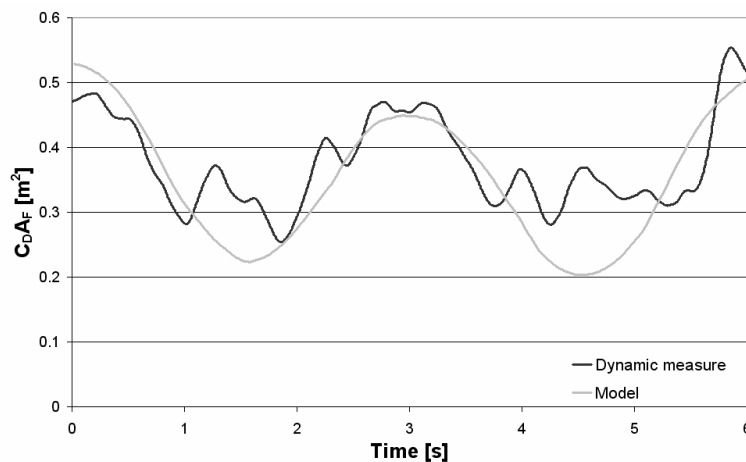


**Figure 13-1:** *Comparison of the $C_DA$ given by the dynamic measurements and by the model.*

Several issues need to be resolved when performing dynamic measurements, such as the influence of a person's movements on the drag measurement and the absence of inertial forces induced by the skier's speed. Moreover, the slope's angle is not simulated in usual wind tunnels.

Developing accurate models for aerodynamic drag and ski-snow friction is required to improve analysis of energy balance as proposed in **study 3.** Precise estimation of parameters that can't be directly measured would allow to determine more accurately the effectiveness of human work to

increase the energy of the skier during turns. The method developed in **study 5**, using a single reference point to determine energies could be used to simplify data acquisition. Several conditions should be tested, such as different slope angle, snow quality or skier's level. The results obtained could be compared to direct measurements of work as proposed in **study 4**, analysing the effect ot the different parameters, in order to better understand this mechanism. An investigation of the use of the drift depending on the situation could also be proposed, using the tool developed in **study 6** to measure the required parameters.

Biomechanical analysis of human movement usually involves wearing additional testing equipment. While this could be an insignificant concern when determining global technical concepts, it becomes important when analysing elite athletes and very precise movements and behaviours,. In those situations, equipment should not have any influence on motion and performance of the test subjects. Actual state of technology could allow for integration of a force platform in the ski boot or ski binding, maybe leading to a slight weight increase but offering dimensions remaining within FIS rules. Data logger and/or transmitter could also be included directly in the equipment without a need for the participant to wear a backpack and inconvenient connecting cables. Working with equipment manufacturers would be necessary to develop such fully integrated measuring systems. Using a high number of these devices and collecting a wide set of data should lead to a better understanding of the constraints sustained when skiing. This in turn should allow to detect injury risks and finally help develop improved binding release systems. Using such devices during training could permit to test different steering strategies and idenitfy the best option, but also help develop appropriate force and coordination training programs adapted to the conditions found on ski slopes.

The video based *3D* kinematics analysis used in this work used markers positioned on the skier's body, and determination of the markers coordinates via panning and tilting cameras system. In the future, testing could be performed during training or racing, without the need for markers or extra equipment. The athlete should be able to ski normally, without

even noticing the ongoing test. Since 2000 (Deutscher et al., 2000), more and more researches have been conducted on markerless full body motion tracking, using multiple fixed cameras. Several techniques have been used e.g. *3D* voxel reconstruction (Caillette and Howard, 2004), visual hull (Mündermann et al., 2006), silhouette based (Rosenhahn et al., 2006). Several issues arise when performing markerless tracking: the need for a *3D* model of the tracked person (Rosenhahn et al., 2007) and the criticality of initiating the model with the correct posture (Schmidt and Castrillon-Santana, 2008). Another persisting issue is the presence of occlusions that could not always be detected. Moreover, all the developed algorithms are dedicated to fixed cameras and there is no available solution for large field acquisition. Brightness and white background on ski slope should be advantages for further developments adapted to the encountered condition during field tests. Markerless solutions should also provide more accurate body inertial measurements as weight densities could be defined very precisely for each part of the body model. Even body shape modifications due to muscle contractions could be taken into account. Finally, a single camera tracking system could be further developed to obtain full *3D* capture of skiers' motion (Fossati et al., 2009).

# 14. References

Abdel-Aziz, Y.I., Karara, H.M., 1971, Direct linear transformation from comparator coordinates into object space coordinates in close-range photogrammetry, Proceedings of the American Society of Photogrammetry Symposium on Close-Range Photogrammetry, 1-18.

Barbier, F., Allard, P., Guelton, K., Colobert, B., Godillon-Maquinghen, A.-P., 2003, Estimation of the 3-D Center of Mass Excursion From Force-Plate Data During Standing, IEEE transactions on neural systems and rehabilitation engineering 11, 31-37.

Barelle, C., Ruby, A., Tavernier, M., 2004, Experimental model of the aerodynamic drag coefficient in alpine skiing, JOURNAL OF APPLIED BIOMECHANICS 20, 167-176.

Barter, J.T., 1957, Estimation of the Mass of Body Segments, WADC Technical Report (TR-57-260), Wright-Patterson Air Force Base, OH,

Bartlett, R., Bussey, M., Flyger, N., 2006, Movement variability cannot be determined reliably from no-marker conditions, Journal of Biomechanics 39, 3076-3079.

Belli, A., Avela, J., Komi, P.V., 1993, Mechanical energy assessment with different methods during running, Int J Sports Med 14, 252-256.

Bland, J.M., Altman, D.G., 1986, Statistical methods for assessing agreement between two methods of clinical measurement, Lancet 1, 307-310.

Blievernicht, D.L., 1967, A multidimensional timing device for cinematography, Res Q 38, 146-148.

Bohm, H., Hosl, M., Senner, V., 2008, Safety in big jumps: relationship between landing shape and impact energy determined by computer simulation, Journal of ASTM International 5,

Bowden, F.P., Hughes, T.P., 1939, The mechanics of sliding on ice and snow, Proc R Soc London, pp. 280-298

Boyd, E., 1935, The growth of the surface area of the human body, Minneapolis: University of Minnesota Press, 52-112.

Brierley, H., Bartlett, R., 1991, A three-dimensional video analysis of the kinematic differences between experienced and novice skiers performing two types of parallel ski turn, Journal of sport sciences 9, 395.

Briggs, S.M., Tyler, J., Mullineaux, D.R., 2003, Accuracy of kinematic data calculated using SIMI motion, Journal of sport science 21, 235-236.

Brodie, M., Walmsley, A., Page, W., 2007, Fusion motion capture: The biomechanics of alpine ski racing., Journal of Biomechanics 40 (Suppl. 2), S399.

Brodie, M., Walmsley, A., Page, W., 2008, Fusion motion capture: a prototype system using inertial measurement units and GPS for the biomechanical analysis of ski racing, sports technology 1, 17-28.

Brodie, M.A., 2009, Development of fusion motion capture for optimisation of performance in alpine ski racing, PhD Thesis, Massey, Wellington, New Zealand

Burns, J.A., 1970, More on Pumping a Swing American Journal of Physic 38, 920.

Caillette, F., Howard, T. (2004) Real-Time Markerless Human Body Tracking with Multi-View 3-D Voxel Reconstruction. British Machine Vision Conference

Canclini, A., Pozzo, R., Cotelli, C., Baroni, G. (2005) 3-D kinematics of double poling in classical technique of elite cross-country skiers engaged in world championships races (1999-2003). In: E. Müller, D.B., R. Klika, S. Lindinger, & H. Schwameder (ed) Science and Skiing III. Oxford: Meyer & Meyer Sport (Uk), Ltd, pp. 308-316

Cappozzo, A., Leo, T., Macellari, V., 1983, The CoSTEL kinematics monitoring system: Performance and use in human movement measurements, Proceedings of the Eighth International Congress of Biomechanics, 1067-1074.

Case, W.B., 1996, The pumping of a swing from the standing position American Journal of Physic 64, 215.

Case, W.B., Swanson, M.A., 1990, The pumping of a swing from the seated position American Journal of Physics 58, 463.

Cavagna, G.A., Saibene, F.P., Margaria, R., 1963, External work in walking, Journal of applied physiology 18, 1-9.

Cavagna, G.A., Saibene, F.P., Margaria, R., 1964, Mechanical Work in Running, J Appl Physiol 19, 249-256.

Chandler, R.F., Clauser, C.E., McConville, J.T., Reynolds, H.M., Young, J.W., 1975, Investigtion of the inertial properties of the human body, Wright-Patterson Air Force Base AMRL-TR-74-137,

Chardonnens, J., Favre, J., Gremion, G., Aminian, K., 2010, A new method for unconstrained measurement of joint angle and timing in alpine skiing: Comparison of crossover and crossunder turns., ISBS - Conference Proceedings Archive, 28 International Conference on Biomechanics in Sports,

Cheng, C.-K., Chen, H.-H., Chen, C.-S., Lee, C.-L., Chen, C.-Y., 2000, Segment inertial properties of Chinese adults determined from magnetic resonance imaging, Clinical Biomechanics 15, 559-566.

Cheze, L., Fregly, B.J., Dimnet, J., 1995, A solidification procedure to facilitate kinematic analysis based on video system data, J Biomech 28, 879-884.

Clauser, C.E., McConville, J.T., Young, J.W., 1969, Weight, volume and center of mass of segments of the human body, Wright-Patterson Air Force Base, Ohio AMRL-TR-69-70,

Colbeck, S.C., 1994a, An error analysis of the techniques used in the measurement of high-speed friction on snow, Annals of Glaciology 19, 19-24.

Colbeck, S.C., 1994b, A review of the friction of snow skis, J Sports Sci 12, 285-295.

Contini, R., 1972, Body segment parameters. II, Artif Limbs 16, 1-19.

Coulmy, N., Antichan, F., Reinisch, G., 2010, Effect of different movement strategies on tangantial and perpendicular velocity of skis and plantar pressure in slalom skiing, Poster presentation at the 15th European Congress on Sport Science, Antalya, Turkey,

Curry, S.M., 1976, How children swing American Journal of Physic 44, 924.

Dapena, J., 1978, Three dimensional cinematography with horizontally panning cameras, Sciences et Motricite 1, 3-15.

Dapena, J., Chung, C.S., 1988, Vertical and radial motions of the body during the take-off phase of high jumping, Medicine and Science in Sports and Exercices 20, 290-302.

De Cecco, M., Angrilli, F., 1999, Testing ski stability, Measurement Science and Technology 10, N38-N43.

de Leva, P., 1996, Adjustments to Zatsiorsky-Seluyanov's segment inertia parameters, J Biomech 29, 1223-1230.

Dempster, W.T., 1955, Space requirements of the seated operator, WADC Technical Report (TR-55-159), Wright- Patterson Air Force Base, OH,

Deutscher, J., Blake, A., Reid, I., 2000, Articulated Body Motion Capture by Annealed Particle Filtering, ieee 1063,

Di Prampero, P.E., Cortili, G., Mognoni, P., Saibene, F., 1976, Energy cost of speec skating and efficiency of work against air resistance, J Appl Physiol 40, 584-591.

Drillis, R., Contini, R., Bluestein, M., 1964, Body Segment Parameters; a Survey of Measurement Techniques, Artif Limbs 25, 44-66.

Durkin, J.L., Dowling, J.J., 2003, Analysis of body segment parameter differences between four human populations and the estimation errors of four popular mathematical models, J Biomech Eng 125, 515-522.

Durkin, J.L., Dowling, J.J., Andrews, D.M., 2002, The measurement of body segment inertial parameters using dual energy X-ray absorptiometry, J Biomech 35, 1575-1580.

Ehara, Y., Fujimoto, H., Miyazaki, S., Mochimaru, M., Tanaka, S., Yamamoto, S., 1997, Comparison of the performance of 3D camera system II, Gait and Posture 5, 251-255.

Ehara, Y., Fujimoto, H., Miyazaki, S., Tanaka, S., Yamamoto, S., 1995, Comparison of the performance of 3D camera systems, Gait and Posture 3, 166-169.

Ericson, M., 1988, Mechanical muscular power output and work during ergometer cycling at different work loads and speeds, European Journal of Applied Physiology and Occupational Physiology 57, 382-387.

Fauve, M., Auer, M., Lüthi, A., Rhyner, H., Meier, J. (2009) Measurement of dynamical ski behavior during alpine skiing In: E. Müller, S.L., & T. Stöggl (ed) Science and Skiing IV. Maidenhead: Meyer & Meyer Sport (Uk), Ltd, pp. 195-206

Fauve, M., Buhl, D., Rhyner, H., Schneebeli, M., Ammann, W. (2005) Influence of snow and weather characteristics on the gliding properties of skis. In: E. Müller, D.B., R. Klika, S. Lindinger, & H. Schwameder (ed) Science and Skiing III. Oxford: Meyer & Meyer Sport (Uk), Ltd, pp. 401-410

Federolf, P., JeanRichard, F., Fauve, M., Lüthi, A., Rhyner, H., Dual, J., 2006, Deformation of snow during a carved ski turn, Cold Regions Science and Technology 46, 69-77.

Federolf, P., Scheiber, P., Rauscher, E., Schwameder, H., Lüthi, A., Rhyner, H.U., Müller, E., 2008, Impact of skier actions on the gliding times in alpine skiing, Scandinavian Journal of Medicine & Science in Sports 18, 790-797.

Federolf, P.A., 2005, Finite element simulation of a carving ski, PhD Thesis, EPFZ,

Ferrario, V.F., Sforza, C., Michielon, G., Dugnani, S., Mauro, F. (1997) A mathematical method for the analysis of trajectories in giant slalom. In: E. Müller, H.S., E. Kornexl, & C. Raschner (ed) Science and Skiing. London: E & FN Spon, pp. 107-115

Flay, J., Vuletich, I.J., 1995, Development of a wind tunnel test facility for yacht aerodynamic studies, Journal of Wind Engineering and Industrial Aerodynamics 58, 231-258.

Förg-Rob, W., Nachbauer, W., 1988, The use of spline functions in the smoothing of film data for slalom ski racers, International journal of sport biomechanics 4, 166-177.

Formenti, F., Ardigo, L.P., Minetti, A.E., 2005, Human locomotion on snow: determinants of economy and speed of skiing across the ages, Proc R Soc B, 1561-1569.

Fossati, A., Salzmann, M., Fua, P. (2009) Observable subspace for 3D human motion recovery. IEEE Conference on Computer Vision and Pattern Recognition

Fregly, B.J., Zajac, F.E., 1996, A state-space analysis of mechanical energy generation, absorption, and transfer during pedaling, Journal of Biomechanics 29, 81-90.

Frenet, F., 1852, Sur les courbes à double courbure, J de Math 17,

Frick, U., Schmidtbleicher, D., Raschner, C., Müller, E. (1997) Types of muscle action of leg and hip extensor musles in slalom. In: E. Müller, H.S., E. Kornexl, & C. Raschner (ed) Science and Skiing. London: E & FN Spon, pp. 262-271

Fukuoka, T., 1971, Changes in the knee angle and in the load of the ski during swing motion in alpine skiing, Medicine and Sports 6: Biomechanics II, Basel, Karger eds., 246-248.

Ganley, K.J., Powers, C.M., 2004, Determination of lower extremity anthropometric parameters using dual energy X-ray absorptiometry: the influence on net joint moments during gait, Clinical Biomechanic 19, 50-56.

Gerritsen, K.G., Nachbauer, W., van den Bogert, A.J., 1996, Computer simulation of landing movement in downhill skiing: anterior cruciate ligament injuries, J Biomech 29, 845-854.

Gomez-Lopez, P.J., Hernan, O., Ramirez, J.V. (2009) Analysis of skiers' performance using GPS. In: E. Müller, S.L., & T. Stöggl (ed) Science and Skiing IV. Maidenhead: Meyer & Meyer Sport (Uk), Ltd, pp. 207-215

Goodwin, D.A. (1990) Kinematic considerations of elite alpine slalom ski racers. In: J. Hamill, T.R.D., & E.H. Elliott, B. (ed) *XI Symposium of the International Society of Biomechanics in Sports* Amherst, MA

Greimel, F., Virmavirta, M., Schwameder, H.I.E., (pp. ): . (2009) Kinematic analysis of the landing phase in ski jumping. In: E. Muller, S.L.T.S. (ed) Science and Skiing IV. Meyer and Meyer Sport (UK), pp. 721-727

Greville, T.N.E., 1964, Numerical Procedures for Interpolation by Spline Functions Journal of the Society for Industrial and Applied Mathematics: Series B, Numerical Analysis 1, pp. 53-68.

Hanavan, E.P., Jr., 1964, A mathematical model of the human body. Amrl-Tr-64-102, AMRL TR, 1-149.

Hatze, H., 1975, A new method for the simultaneous measurement of the movement of inertia, the damping coefficient and the location of the centre of mass of a body segment in situ, Eur J Appl Physiol Occup Physiol 34, 217-226.

Hatze, H., 1980, A mathematical model for the computational determination of parameter values of anthropomorphic segments, J Biomech 13, 833-843.

Hatze, H., 1988, High-precision three-dimensional photogrammetric calibration and object space reconstruction using a modified DLT-approach, J Biomech 21, 533-538.

Hauser, W., Asang, E., Schaff, P. (1985) Influence of ski boot design on skiing safety and skiing performance. In: R. J. Johnson, C.D.M. (ed) Skiing trauma and safety: Fifth International Symposium. ASTM, Philadelphia, PA

Heinrich, D., Mössner, M., Kaps, P., Nachbauer, W., 2009, Calculation of the contact pressure between ski and snow during a carved turn in Alpine skiing, Scand J Med Sci Sports 20, 485-492.

Hinrichs, R.N., 1985, Regression equations to predict segmental moments of inertia from anthropometric measurements: an extension of the data of Chandler et al. (1975), J Biomech 18, 621-624.

Howe, J.G. Skiing mechanics 1983. Poudre press, Colorado

Hraski, Z., Hraski, M. (2009) Influence of the skier's body geometry on the duration of the giant slalom turn. In: E. Müller, S.L., & T. Stöggl (ed) Science and Skiing IV. Maidenhead: Meyer & Meyer Sport (Uk), Ltd, pp. 252-259

Huber, A., Waibel, K.-H., Spitzenpfeil, P. (2009) Description of race courses and estimation of ground reaction forces by GPS-Data and video. In: E. Müller, S.L., & T. Stöggl (ed) Science and Skiing IV. Maidenhead: Meyer & Meyer Sport (Uk), Ltd, pp. 260-271

Hull, M.L., Mote, C.D., 1974, Pulse code modulation telemetry in ski injury research. I. Instrumentation, Biotelemetry 1, 182-192.

Hull, M.L., Mote, C.D., 1975, Pulse code modulation telemetry in ski injury research. II. Preliminary results, Biotelemetry 2, 276-276.

Hull, M.L., Mote, C.D., 1978, Analysis of Leg Loading in Snow Skiing, Journal of Dynamic Systems, Measurement, and Control 100, 177-186.

Ikai, M., 1970, Scientific report report for Sapporo olympic games. Tokyo commettee of sports science of Japan amateur sports association, 1-54.

Janura, M., Cabell, L., Elfmark, M., Vaverka, F., 2006, A 10-year longitudinal study of the in-run position kinematic changes in ski jumping, Journal of Biomechanics 39, S553.

Jensen, R.K. (1976) Model for body segment parameters. In: Komi, P.V. (ed) Biomechanics V-B. University Park Press, Baltimore, pp. 380-386

Jensen, R.K., 1978, Estimation of the biomechanical properties of three body types using a photogrammetric method, J Biomech 11, 349-358.

Jensen, R.K., 1986, Body segment mass, radius and radius of gyration proportions of children, J Biomech 19, 359-368.

Jensen, R.K., 1989, Changes in segment inertia proportions between 4 and 20 years, J Biomech 22, 529-536.

Jensen, R.K., Doucet, S., Treitz, T., 1996, Changes in segment mass and mass distribution during pregnancy, J Biomech 29, 251-256.

Jensen, R.K., Fletcher, P., 1994, Distribution of mass to the segments of elderly males and females, Journal of Biomechanics 27, 89-96.

Joubert, G. Skiing. An art. A technique 1980. LaPorte, CO: Poudre Publishing Company. (Original work published 1978)

Joubert, G., Vuarnet, J. How to ski the new french way 1966. Kaye and Ward, London

Kagawa, H., Yoneyama, T. (2001) Effective action of skier's center of mass in skiing. In: E. Müller, H.S., C. Raschner, S. Lindinger, & E. Kornexl (ed) Science and Skiing II. Hambourg: Verlag Dr. Kovač

Kaps, P., Nachbauer, W., Mössner, M., 1996, Determination of Kinetic Friction and Drag Area in Alpine Skiing, Ski Trauma and Skiing Safety 10, 165–177.

Kiefmann, A., Krinninger, M., Lindemann, U., Senner, V., Spitzenpfeil, P. (2006) A New Six Component Dynamometer for Measuring Ground

Reaction Forces in Alpine Skiing. In: Moritz, E.F., Haake, S. (ed) The Engineering of Sport 6. Springer New York, pp. 87-92

Klous, M., 2007, Three-dimensional joint loading on the lower extremities in alpine skiing and snowboarding. , PhD Thesis, University of Salzburg, Salzburg, Austria

Klous, M., Muller, E., Schwameder, H., 2010, Collecting kinematic data on a ski/snowboard track with panning, tilting, and zooming cameras: is there sufficient accuracy for a biomechanical analysis?, J Sports Sci 28, 1345-1353.

Knüz, B., Nachbauer, W., Schindelwig, K., Brunner, F. (2001) Forces and moments at the boot sole during snowboarding. In: E. Müller, H.S., C. Raschner, S. Lindinger, & E. Kornexl (ed) Science and Skiing II. Hambourg: Verlag Dr. Kovač, pp. 242-249

Krueger, A., Edelmann-Nusser, J., 2009, Biomechanical analysis if freestyle snowboarding: application of a full-body inertial measurement system and a bilateral insole measurement system, sports technology 2, 17-23.

Kugovnik, O., Supej, M., Nemec, B. (2005) Time advantage using an improved slalom technique. In: E. Müller, D.B., R. Klika, S. Lindinger, & H. Schwameder (ed) Science and Skiing III. Oxford: Meyer & Meyer Sport (Uk), Ltd, pp. 87-95

Kuo, C.Y., Louie, J.K., Mote Jr, C.D., 1983, Field measurements in snow skiing injury research, Journal of Biomechanics 16, 609-624.

Kurpiers, N., Kersting, U.-G., McAlpine, P.R. (2009) Effect of a mock-up force plate on riding technique and perception - a prerequisite for a comprehensive biomechanical analysis in modul skiing. In: E. Müller, S.L., & T. Stöggl (ed) Science and Skiing IV. Maidenhead: Meyer & Meyer Sport (Uk), Ltd, pp. 327-336

Kwon, Y.H., Yoon, S., Sung, R.J. (2004) Accuracy of the software genlock with digital camcorders. In: M. Lamontagne, D.G., E. Robertson, H. Sveistrup (ed) 22nd International Symposium on Biomechanics in Sports, Ottowa, Canada, p. 64

Kyröläinen, H., Belli, A., Komi, P.V., 2001, Biomechanical factors affecting running economy, medicine & science in Sports & exercice, 1330-1337.

Lafontaine, D., Lamontagne, M., Dupuis, D., Diallo, B. (1998) Analysis of the distribution of pressure under the feet of elite alpine ski instructors. In: H.J., Vieter, R.M.M. (eds) *XVI International Symposium on Biomechanics in Sports*, Konstanz, Germany, pp. 485-488

Lee, S., Wolberg, G., Shin, S.Y., 1997 Scattered data interpolation with multilevel B-splines, IEEE Transactions on Visualization and Computer Graphics 3, 228 - 244

Leite de Barros, R.M., Guedes Russomanno, T., Brenzikofer, R., Jovino Figueroa, P., 2006, A method to synchronise video cameras using the audio band, Journal of Biomechanics 39, 776-780.

LeMaster, R. The Skier's Edge 1999. Human Kinetics, Champaign, IL

Lešnik, B., Žvan, M., 2003, Comparison of centre of mass trajectories in modern giant slalom techniques, Kinesiology 35, 191-200.

Lešnik, B., Žvan, M., 2007, The best slalom competitors - kinematic analysis of tracks and velocities, Kinesiology 39, 40-48.

Lieu, D.K., C. D. Mote, J., 1980, An Electronic Ski Binding Design with Biofeedback, Journal of Mechanical Design 102, 677-682.

Lochmatter, T., 2010, Bio-inspired and probabilistic algorithms for distributed odor source localization using mobile robots, PhD Thesis, PPUR, Swiss Federal School of Technology, Lausanne

Lopez, J.G., Rodriguez-Marroyo, J.A., Juneau, C.E., Peleteiro, J., Martinez, A.C., Villa, J.G., 2008, Reference values and improvement of aerodynamic drag in professional cyclists, Journal of sport science 26, 277-286.

Louie, J.K., Kuo, C.Y., Gutierrez, M.D., Mote Jr, C.D., 1984, Surface EMG and torsion measurements during snow skiing: Laboratory and field tests, Journal of Biomechanics 17, 713-724.

Luethi, S., Denoth, J., 1987, The Influence of Aerodynamic and Anthropometric Factors on Speed in Skiing, International journal of sport biomechanics 3, 345-352.

Lüthi, A., Böttinger, G., Theile, T., Rhyner, H., Ammann, W., 2006, Freestyle aerial skiing motion analysis and simulation, Journal of Biomechanics 39, S186.

Lüthi, A., Federolf, P., Fauve, M., Oberhofer, K., Rhyner, H., Ammann, W., Stricker, G., Schiefermüller, C., Eitzlmair, E., Schwameder, H., Müller, E. (2005) Determination of forces in carving using three differents methods. In: E. Müller, D.B., R. Klika, S. Lindinger, & H. Schwameder (ed) Science and Skiing III. Oxford: Meyer & Meyer Sport (Uk), Ltd, pp. 96-106

MacGregor, D., Hull, M.L., 1985, A microcomputer controlled snow ski binding system--II. Release decision theories, Journal of Biomechanics 18, 267-275.

MacGregor, D., Hull, M.L., Dorius, L.K., 1985, A microcomputer controlled snow ski binding system--I. Instrumentation and field evaluation, Journal of Biomechanics 18, 255-265.

Margane, J., Trzecinski, L., Babiel, S., Neumaier, A. (1998) A mechanical apparatus (skiing model) executing turns on carver skis. In: Vieten, H.J.R.M.M. (ed) *XVI International Symposium on Biomechanics in Sports*, Konstanz, Germany

Maxwell, S.M., Hull, M.L., 1989, Measurement of strength and loading variables on the knee during alpine skiing, Journal of Biomechanics 22, 609-611, 613-624.

Meyer, F., Bahr, A., Lochmatter, T., Borrani, F., 2011a, Wireless GPS-based phase-locked synchronization system for outdoor environment, Journal of Biomechanics, In Press.

Meyer, F., Borrani, F. (2010) 3D model reconstruction and analysis of athletes performing giant slalom. Abstract book of the 5th International Congress on Science and Skiing, St-Christoph am Arlberg, Austria, p. 64

Meyer, F., Le Pelley, D., Borrani, F. (2010a) Aerodynamic drag modelling of alpine skiers performing giant slalom turns. 15th European Congress on Sport Science, Antalya, Turkey, p. 56

Meyer, F., Le Pelley, D., Borrani, F., In press, Aerodynamic drag modelling of alpine skiers performing giant slalom turns, medicine & science in Sports & exercice,

Meyer, F., Lochmatter, T., Bahr, A., Borrani, F. (2010b) GPS-based system for multiple devices synchronization in an outdoor environment. 5th International Congress on Science and Skiing, St-Christoph, Austria

Miller, P., Hytjan, A., Weber, M., Wheeler, M., Zable, J., Walshe, A., Ashley, A., Moritz, E.F., Haake, S. (2006) Development of a Prototype that Measures the Coefficient of Friction Between Skis and Snow. The Engineering of Sport 6. Springer New York, pp. 305-310

Minetti, A.E., Saibene, F., 1992, Mechanical work rate minimization and freely chosen stride frequency of human walking: a mathematical model, Journal of Experimental Biology 170, 19-34.

Morawski, J.M., 1973, Control systems approach to a ski-turn analysis, Journal of Biomechanics 6, 267-276, IN211-IN212, 277-279.

Mössner, M., Heinrich, D., Schindelwig, K., Kaps, P., Lugner, P., Schmiedmayer, H., Schretter, H., Nachbauer, W. (2006) Modeling of the ski-snow contact for a carved turn. In: Haake, E.F.M.S. (ed) *The engineering of sport 6.* Springer Science+Business Media, LLC., New York, NY, pp. 195-200

Mote, C.D., Louie, J.K., 1983, Accelerations induced by body motions during snow skiing, Journal of Sound and Vibration 88, 107-115.

Müller, E., 1994, Analysis of the biomechanical characteristics of different swinging techniques in alpine skiing, Journal of sport sciences 12, 261-278.

Müller, E., Bartlett, R., Raschner, C., Schwameder, H., Benko-Bernwick, U., Lindinger, S., 1998, Comparison of ski turn techniques of experienced and intermediate skiers, Journal of sport science 16, 545-559.

Mündermann, L., Corazza, S., Andriacchi, T.P., 2006, Markerless human motion capture through visual hull and articulated ICP, Proceedings of NIPS Workshop,

Mungiole, M., Martin, P.E., 1990, Estimating segment inertial properties: comparison of magnetic resonance imaging with existing methods, J Biomech 23, 1039-1046.

Nachbauer, W., Kaps, P., Mössner, M., 1992, Determination of Kinetic Friction in Downhill Skiing,, 8th Meeting of the European Society of Biomechanics,

Nachbauer, W., Kaps, P., Nigg, B., Brunner, F., Lutz, A., Obkircher, G., Mössner, M., 1996, A video technique for obtaining 3-D coordinates in alpine skiing, JOURNAL OF APPLIED BIOMECHANICS 12, 104-115.

Nigg, B., Herzog, W. Biomechanics of the musculoskeletal system 1994. John Wiley & Sons, New-York

Nigg, B.M., Schwameder, H., Stefanyshyn, D., Tscharner, V. (2001) The effect of ski binding position on performance and comfort in skiing. In: E. Müller, H.S., C. Raschner, S. Lindinger, & E. Kornexl (ed) Science and Skiing II. Hambourg: Verlag Dr. Kovač, pp. 3-13

Nilsson, J., Haugen, P., 2004, Knee angular displacement and extensor muscle activity in telemark skiing and in ski-specific strength exercises, Journal of sport science 22, 357-364.

Ohgi, Y., Seo, K., Hirai, N., Murakami, M., 2007, Aerodynamic forces acting in ski jumping, Journal of Biomechanics 40 (Supplment 2), S402.

Pavol, M.J., Owings, T.M., Grabiner, M.D., 2002, Body segment inertial parameter estimation for the general population of older adults, J Biomech 35, 707-712.

Petrone, N., Marcolin, G., De Gobbi, M., Nicoli, M., Zampieri, C. (2009) Aquisition of EMG signals during slalom with different ski boots. In: E. Muller, S.L.T.S. (ed) Scince and Skiing IV. Meyer and Meyer Sport (UK), pp. pp. 399 - 409

Pourcelot, P., Audigie, F., Degueurce, C., Geiger, D., Denoix, J.M., 2000, A method to synchronise cameras using the direct linear transformation technique, Journal of Biomechanics 33, 1751-1754.

Pozzo, R., Canclini, A., Cotelli, C., Barroni, G. (2005) 3D kinematics and kinetic analysis of geant slalom in elite skiers at Val Badia world cup race in 2002. In: E. Müller, D.B., R. Klika, S. Lindinger, & H. Schwameder (ed) Science and Skiing III. Oxford: Meyer & Meyer Sport (Uk), Ltd, pp. 125-135

Pozzo, R., Canclini, A., Cotelli, C., Martinelli, L., Röckmann, A. (2001) 3-D kinematics of the start in the downhill at the Bormio world cup in 1995. In: E. Müller, H.S., C. Raschner, S. Lindinger, & E. Kornexl (ed) Science and Skiing II. Hambourg: Verlag Dr. Kovač, pp. 95-107

Quinn, T., Mote, C., 1990, Optimal design of an uncoupled six degree of freedom dynamometer, Experimental Mechanics 30, 40-48.

Quinn, T.P., Mote Jr, C.D., 1992, Prediction of the loading along the leg during snow skiing, Journal of Biomechanics 25, 609-625.

Raschner, C., Müller, E., Schwameder, H. (1997) Kinematic and kinetic analysis of slalom turns as a basis for the development of specific training methods to improve strength and endurance. In: E. Müller, H.S., E. Kornexl, & C. Raschner, C (ed) Science and Skiing. London: E & FN Spon, pp. 251-261

Raschner, C., Schiefermüller, C., Zallinger, G., Hofer, E., Müller, E., Brunner, F. (2001) Carving turn versus traditionnal parallele turn, a comparative biomechanical analysis. In: E. Müller, H.S., C. Raschner, S.

Lindinger, & E. Kornexl (ed) Science and Skiing II. Hambourg: Verlag Dr. Kovač

Read, L., Herzog, W., 1992, External loading at the knee joint for landing movements in alpine skiing, International Journal of Sports Biomechanics 8, 62-80.

Reid, R., Gilgien, M., Moger, T., Tjorhom, H., Haugen, P., Kipp, R., Smith, G. (2009) Turn characteristics and energy dissipation in slalom. In: E. Müller, S.L., & T. Stöggl (ed) Science and Skiing IV. Maidenhead: Meyer & Meyer Sport (Uk), Ltd, pp. 419-429

Reid, R.C., 2010, A kinematic and kinetic study of alpine skiing technique in slalom, PhD Thesis, Norvegian school of sport science, Oslo

Reinisch, G., 1991, A physical theory of alpine ski racing, Spectrum der Sportwissenshaften 1,

Remondet, J., Rebert, O., Fayolle, L., Stelmakh, N., Papelier, Y., *1997*, Optimisation des performances en ski alpin : intérêt et limites d'un modèle cinématique simplifié., Science and Sports, 163-173.

Richards, J.G., 1999, The measurement of human motion: A comparison of commercially available systems, Human movement Science 18, 589-602.

Rosenhahn, B., Brox, T., Kersting, U.G., Smith, A.W., Gurney, J.K., Klette, R., 2006, A system for marker-less motion capture, Künstliche Intelligenz 1,

Rosenhahn, B., Brox, T., Seidel, H.-P., 2007, Scaled Motion Dynamics for Markerless Motion Capture, ieee 1-4244-1180-7,

Sahashi, T., Ichino, S., 1998, Coefficient of friction of snow skis during turning descents, Japanese Journal of Applied Physics 37, 720-727.

Saibene, F., Cortili, G., Roi, G., Colombini, A., 1989, The energy cost of level cross-country skiing and the effect of the friction of the ski, European Journal of Applied Physiology and Occupational Physiology 58, 791-795.

Saibene, F., Minetti, A.E., 2003, Biomechanical and physiological aspects of legged locomotion in humans, Eur J Appl Physiol 88, 297-316.

Sanders, R.J. The anatomy of skiing 1976. Golden bell Press

Sands, W.A., 2008, Measurement issues with elite athletes, sports technology 1, 101-104.

Savolainen, S., 1989, Theoretical drag analysis of a skier in the downhill speed race, International journal of sport biomechanics 5, 26-39.

Sayers, A.T., Ball, D.R., 1983, Blockage corrections for rectangular flat plates mounted in an open jet wind tunnel, ARCHIVE: Proceedings of the Institution of Mechanical Engineers, Part C: Mechanical Engineering Science 1983-1988 (vols 197-202) 197, 259-263.

Schaff, P., Schattner, R., Hauser, W. (1987) Biomechanical Enquiries on ski boot and resulting practical requirements. In: C. D. Mote, R.J.J. (ed)

Skiing trauma and safety: Sixth International Symposium. ASTM, Philadelphia, PA, pp. 154-168

Schaff, P., Senner, V., Jaiser, F. (1997) Pressure distribution mesurement for alpin skier - from the biomechanical hight tech measurement to its application as swingbeep feedback system. In: E. Müller, H.S., E. Kornexl, & C. Raschner (ed) Science and Skiing. London: E & FN Spon, pp. 159-172

Schaff, P.S., Hauser, W. (1993) 3-D video motion analysis on the slope-A practical way to analyze motion patterns in alpine skiing. In: R. J. Johnson, C.D.M., & J. Zelcer (ed) Skiing Trauma and Safety: Ninth International Symposium. American Society for Testing and Materials., Philadelphia, PA, pp. 169-176

Schaff, P.S., Schattner, R., Kulot, M., Hauser, W. (1989) Influences on the foot pressure pattern in ski boot. In: R.J. Johnson, C.D.M., M. H. Binet (ed) Skiing trauma and safety: Seventh International Symposium. ASTM, Philadelphia, PA, pp. 137-145

Schattner, R., Asang, E., Hauser, W., Velho, F. (1985) A device for measuring the influence of ski boot design on the pressure distribution in the lower leg. In: R. J. Johnson, C.D.M. (ed) Skiing trauma and safety: Fifth International Symposium. ASTM, Philadelphia, PA, pp. 182-188

Scheirman, G., Porter, J., Leigh, M., Musick, D. (1998) An integrated method to obtain three-dimensional coordinates using panning and tilting video cameras. In: Viete, H.J.R.M.M. (ed) XVI International Symposium on Biomechanics in Sports Konstanz, Germany

Schiefermüller, C., Lindinger, S., Müller, E. (2005) The skier's centre of gravity as a reference point in movement analysis for different designated systems. In: E. Müller, D.B., R. Klika, S. Lindinger, & H. Schwameder (ed) Science and Skiing III. Oxford: Meyer & Meyer Sport (Uk), Ltd, pp. 172-185

Schmidt, J., Castrillon-Santana, M., 2008, Automatic initialization for body trackings,

Schmolzer, B., Muller, W., 2005, Individual flight styles in ski jumping: results obtained during olympic games competitions, Journal of Biomechanics 38, 1055 - 1065.

Schneider, K., Zernicke, R.F., 1992, Mass, center of mass, and moment of inertia estimates for infant limb segments, J Biomech 25, 145-148.

Schöllhorn, W.I., Müller, E., Lindinger, S., Raschner, C., Schwameder, H., Benko, U. (2001) Individuality and generality in ski turn techniques. In: E. Müller, H.S., C. Raschner, S. Lindinger, & E. Kornexl (ed) Science and Skiing II. Hambourg: Verlag Dr. Kovač, pp. 69-83

Schwameder, H., Müller, E., Lindenhofer, E., Monte, G.D., Potthast, W., Brüggemann, G., Virmavirta, M., Isoletho, J., Komi, P. (2005) Kinematic characteristics of the early flight phase in ski-jumping. In: E. Müller, D.B., R. Klika, S. Lindinger, & H. Schwameder (ed) Science and Skiing III. Oxford: Meyer & Meyer Sport (Uk), Ltd, pp. 381-391

Schwameder, H., Nigg, B.M., Tscharner, V., Stefanyshyn, D. (2001) The effect of binding position on kinetic variables in alpine skiing. In: E. Müller, H.S., C. Raschner, S. Lindinger, & E. Kornexl (ed) Science and Skiing II. Hambourg: Verlag Dr. Kovač, pp. 43-53

Seifriz, F., Mester, J. (2001) Measurement and computer simulation of trajectories in alpine skiing. In: E. Müller, H.S., C. Raschner, S. Lindinger, & E. Kornexl (ed) Science and Skiing II. Hambourg: Verlag Dr. Kovač, pp. 155-164

Senner, V., Schaff, P., Hauser, W. (1991) A new artificial leg for ski boot testing. In: C. D. Mote, R.J.J. (ed) Skiing trauma and safety: Eighth International Symposium. ASTM, Philadelphia, PA, pp. 200-207

Serret, J.A., 1851, Sur quelques formules relatives à la théorie des courbes à double courbure, J de Math 16,

Shanebrook, J.R., Jaszczak, R.D., 1976, Aerodynamic drag analysis of runners, Med Sci Sports 8, 43-45.

Siegman, A.E., 1969, Comments on Pumping on a Swing American Journal of Physics 37, 843.

Skaloud, J., Limpach, P., 2003, Synergy of CP DGPS, Accelerometry and magnetic sensors for precise trajectography in ski racing, ION GPS/GNSS September 9-12,

Skaloud, J., Merminod, B. (2000) DGPS-Calibrated Accelerometric System for Dynamic Sports Events. ION GPS, Salt Lake City, UT

Skaloud, J., Vallet, J., Keller, K., Veyssière, G., Kölbl, O., 2006, An eye for landscapes - Rapid Aerial Mapping with Handheld Sensors, GPS World 17, 26-32.

Slawinski, J., Billat, V., Koralsztein, J.-P., Tavernier, M., 2004, Use of Lumbar Point for the Estimation of Potential and Kinetic Mechanical Power in Running, JOURNAL OF APPLIED BIOMECHANICS 20, 324-331.

Spitzenpfeil, P., Huber, A., Waibel, K. (2009) Mechanical load and muscular expenditure in alpine ski racing and implications for safty and material considerations. In: E. Müller, S.L., & T. Stöggl (ed) Science and Skiing IV. Maidenhead: Meyer & Meyer Sport (Uk), Ltd, pp. 479-486

Spring, E., 1988, A method for testing the gliding quality of skis, Tribologia 7, 9-14.

Spring, E., Savolainen, S., Erikkila, T., Hamalainen, T., Pihkala, P., 1988, Drag area of a cross country skier., International journal of sport biomechanics 4, 103-113.

Stöggl, T., Müller, E., Lindinger, S., 2008, Biomechanical comparison of the double-push technique and the conventional skate skiing technique in cross-country sprint skiing, Journal of sport science 26, 1225-1233.

Stricker, G., Scheiber, P., Lindenhofer, E., Müller, E., 2009, Determination of forces in alpine skiing and snowboarding: Validation of a mobile data acquisition system, European Journal of Sport Science 10, 31-41.

Supej, M., 2008, Differential specific mechanical energy as a quality parameter in racing alpine skiing, J Appl Biomech 24, 121-129.

Supej, M. (2009) A step forward in 3D measurements in alpine skiing: a combination of an inertial suit and DGPS technology. In: E. Müller, S.L., & T. Stöggl (ed) Science and Skiing IV. Maidenhead: Meyer & Meyer Sport (Uk), Ltd, pp. 497-504

Supej, M., Kugovnik, Nemec, B. (2005a) Advanced analysis of alpine skiing based on the kinematic measurments. In: E. Müller, D.B., R. Klika, S. Lindinger, & H. Schwameder (ed) Science and Skiing III. Oxford: Meyer & Meyer Sport (Uk), Ltd, pp. 216-227

Supej, M., Kugovnik, O., Nemec, B., 2003, Kinematic determination of the beginning of a ski turn, Kinesiologia Slovenica, 9, 11-17.

Supej, M., Kugovnik, O., Nemec, B., 2004, Modelling and simulation of two competition slalom techniques, Kinesiology 36, 206-212.

Supej, M., Kugovnik, O., Nemec, B. (2005b) Energy principle used for estimating the quality of a racing ski turn. In: E. Müller, D.B., R. Klika, S. Lindinger, & H. Schwameder (ed) Science and Skiing III. Oxford: Meyer & Meyer Sport (Uk), Ltd, pp. 228-237

Supej, M., Nemec, B., Kugovnik, O., 2005c, Changing conditions on the slalom ski course affect competitor's performances, Kinesiology 37, 151-158.

Tada, N., Hirano, Y. (1998) Experimental determination of snow resistance forces acting on a turning snow ski. In: Haake, S. (ed) The engineering of sport: Design and development. Blackwell Science, Oxford, pp. 423-430

Takahashi, M., Yoneyama, T. (2001) Basic ski Theory and acceleration during ski turn. In: E. Müller, H.S., C. Raschner, S. Lindinger, & E. Kornexl (ed) Science and Skiing II. Hambourg: Verlag Dr. Kovač, pp. 307-321

Takahashi, M., Yoneyama, T. (2002) Instruction on the optimal ski turn motion. In: Haake, U.S.J. (ed) The Engineering of Sport 4 Blackwell Publishing, Carlton, Australia, pp. 708-715

Tea, P.L., Falk, H., 1968, Pumping on a swing, American Journal of Physic 36, 1165.

Terrier, P., Turner, V., Schutz, Y., 2005, GPS analysis of human locomotion: Further evidence for long-range correlations in stride-to-stride fluctuations of gait parameters, Human movement Science 24, 97-115.

Thompson, B.E., Friess, W.A., II, K.N.K., 2001, Aerodynamics of speed skiers, Sports Engineering 4, 103-112.

Titterton, D.H., Weston, J.L., 1997, Strapdown inertial navigation technology, Peter Peregrinus Ltd,

van Ingen Schenau, G.J., 1982, The influence of air friction in speed skating, Journal of Biomechanics 15, 449-458.

Vaughan, C.L., Davis, B.L., O'Connor, J.C. (eds) (1992) Dynamics of Human Gait. Human Kinetics, Champaign, IL

Virmavirta, M., Isolehto, J., Komi, P., Schwameder, H., Pigozzi, F., Massazza, G., 2007, Take-off analysis of the olympic ski jumping competition (HS-106 M), Journal of Biomechanics 40, S403.

Virmavirta, M., Komi, P., 1993a, Measurement of take-off forces in ski jumping, part I, Scandinavian Journal of Medicine and Science in Sports 3, 229 - 236.

Virmavirta, M., Komi, P.V., 1993b, Measurement of take-off forces in ski jumping, part II, Scandinavian Journal of Medicine & Science in Sports 3, 237-243.

Vodickova, S., Lufinka, A., Zubek, T., 2005a, Application of the dynamographic method in alpine skiing, Human Movement 6, 19-23.

Vodickova, S., Lufinka, A., Zubek, T. (2005b) The dynamographic and kinematographic method application for a short carving turn. In: E. Müller, D.B., R. Klika, S. Lindinger, & H. Schwameder (ed) Science and Skiing III. Oxford: Meyer & Meyer Sport (Uk), Ltd, pp. 247-256

von Hertzen, R., Holmlund, U., Ranta, M.A., 1997, On the velocity maximization in downhill skiing, Journal of Biomechanics 30, 525-529.

Waegli, A., Meyer, F., Ducret, S., Skaloud, J., Pesty, R. (2009) Assessment ot timing and performance based on trajectories from low-cost GPS/INS positioning. In: E. Müller, S.L., & T. Stöggl (ed) Science and Skiing IV. Maidenhead: Meyer & Meyer Sport (Uk), Ltd, pp. 556-564

Waegli, A., Skaloud, J., 2007a, Assessment of GPS/MEMS-IMU Integration Performance in Ski Racing, In: Proceedings of ENC GNSS 2007 (TimeNav'07), Geneva, Switzerland,

Waegli, A., Skaloud, J., 2007b, Turning Point - Trajectory Analysis for Skiers, InsideGNSS Spring 2007,

Waegli, A., Skaloud, J., 2009, Optimization of two GPS/MEMS-IMU integration strategies with application to sports, GPS Solutions 13, 315-326.

Waegli, A., Skaloud, J., Tomé, P., Bonnaz, J.M. (2007) Assessment of the Integration Strategy between GPS and Body-Worn MEMS Sensors with Application to Sports. ION GNSS, Fort Worth, Texas

Walton, J.S., 1970, A high speed timing unit for cinematography, Res Q 41, 213-216.

Watanabe, K., 1981, Skiing research in Japan, Medicine & Science in Sports & Exercise 13, 205-209.

Watanabe, K., Ohtsuki, T., 1977, Postural changes and aerodynamic forces in alpine skiing, Ergonomics 20, 121-131.

Watanabe, K., Ohtsuki, T., 1978, The effect of posture on the running speed of skiing, Ergonomics 21, 987-998.

Watanabe, T., Kasaya, A., Kawahara, Y., 1972, Kinematic studies on ski jumping, Proceedings of the International Congress of Winter Sports Medicine, Sapporo, 98-105.

Willems, P.A., Cavagna, G.A., Heglund, N.C., 1995, External, internal and total work in human locomotion, J Exp Biol 198, 379-393.

Wimmer, M.A., Holzner, R. (1997) Constraint forces may influence the measurement of vertical ground reaction force during slalom skiing. In: E. Müller, H.S., E. Kornexl, & C. Raschner (ed) Science and Skiing. London: E & FN Spon, pp. 208-215

Winter, D., 1979, A new definition of mecanical work done in human movement, The american Physiological Society,

Wirkus, S., Rand, R., Ruina, A., 1998, How to pump a swing, the college mathematics journal 29, 266-275.

Wunderly, G.S., Hull, M.L., Maxwell, S., 1988, A second generation microcomputer controlled binding system for alpine skiing research, Journal of Biomechanics 21, 299-318.

Yeadon, M.R., 1989, A method for obtaining three-dimensional data on ski jumping using pan and tilt cameras, International journal of sport biomechanics 5, 238-247.

Yeadon, M.R., 1990, The simulation of aerial movement--I. The determination of orientation angles from film data, J Biomech 23, 59-66.

Yeadon, M.R., King, M.A., 1999, A method for synchronising digitised video data, Journal of Biomechanics 32, 983-986.

Yeadon, M.R., Morlock, M., 1989, The appropriate use of regression equations for the estimation of segmental inertia parameters, J Biomech 22, 683-689.

Yoneyama, T., Kagawa, H., Okamoto, A., Sawada, M. (2001) Mesurment of the joint motion in the carving versus normal ski turn. In: E. Müller, H.S., C. Raschner, S. Lindinger, & E. Kornexl (ed) Science and Skiing II. Hambourg: Verlag Dr. Kovač, pp. 218-231

Zatsiorsky, V., Seluyanov, V., 1983, The mass and inertia characteristics of the main segments of the human body, Biomechanics VIII-B, Human Kinetics, Illinois, 1152-1159.

Zatsiorsky, V.M., Seluyanov, V.N. (1985) Estimation of the mass and inertia characteristics of the human body by mean of the best predictive regression equations. In: Winter, D.A.e.a. (ed) Biomechanics IX-B. Human Kinetics, Champaign, IL, pp. 233-239

Žvan, M., Lešnik, B., 2007, Correlation between the length of the ski track and the velocity of top slalom skiers, Acta Univ Palacki Olomuc Gymn 37, 37-44.